CANADIAN THESES ON MICROFICHE

THÈSES CANADIENNES SUR MICROFICHE

National Library of Canada
Collections Development Branch

Canadian Theses on
Microfiche Service

Ottawa, Canada
K1A 0N4

Bibliothèque nationale du Canada
Direction du développement des collections

Service des thèses canadiennes
sur microfiche

NOTICE

The quality of this microfiche is heavily dependent upon the quality of the original thesis submitted for microfilming. Every effort has been made to ensure the highest quality of reproduction possible.

If pages are missing, contact the university which granted the degree.

Some pages may have indistinct print especially if the original pages were typed with a poor typewriter ribbon or if the university sent us an inferior photocopy.

Previously copyrighted materials (journal articles, published tests, etc.) are not filmed.

Reproduction in full or in part of this film is governed by the Canadian Copyright Act, R.S.C. 1970, c. C-30. Please read the authorization forms which accompany this thesis.

AVIS

La qualité de cette microfiche dépend grandement de la qualité de la thèse soumise au microfilmage. Nous avons tout fait pour assurer une qualité supérieure de reproduction.

S'il manque des pages, veuillez communiquer avec l'université qui a conféré le grade.

La qualité d'impression de certaines pages peut laisser à désirer, surtout si les pages originales ont été dactylographiées à l'aide d'un ruban usé ou si l'université nous a fait parvenir une photocopie de qualité inférieure.

Les documents qui font déjà l'objet d'un droit d'auteur (articles de revue, examens publiés, etc.) ne sont pas microfilmés.

La reproduction, même partielle, de ce microfilm est soumise à la Loi canadienne sur le droit d'auteur, SRC 1970, c. C-30. Veuillez prendre connaissance des formules d'autorisation qui accompagnent cette thèse.

THIS DISSERTATION
HAS BEEN MICROFILMED
EXACTLY AS RECEIVED

LA THÈSE A ÉTÉ
MICROFILMÉE TELLE QUE
NOUS L'AVONS REÇUE

Canada

NL 339 (r. 86/09)

Textural and Chemical Variations in a Diabase Dike, St-Pierre de Wakefield, Québec.

by

J.J.P. Gilles Reny

A thesis submitted to the School of Graduate Studies in the partial fulfilment of the requirements for the degree of M.Sc. in Geology

UNIVERSITY OF OTTAWA

OTTAWA, CANADA, 1984

UNIVERSITÉ D'OTTAWA
UNIVERSITY OF OTTAWA

To the memory of

Joseph Hormidas Marcel Reny

1911-1983

ABSTRACT

Chemical and textural variations across a 25 to 32 m wide diabase dike from St-Pierre de Wakefield, Quebec, were investigated in detail in relation to the mode of emplacement, crystallization history and differentiation. An increase was found, from dike margin to centre, in Fe, K, Ti, Zr, Sr, Rb, Y and Zn, a decrease in Al, Mg, Ca, Ba and a general decrease in total rare earth elements from the start to the end of the magma emplacements. Large K, Ba, Sr and Rb peaks were recorded at a distance of 7.5 m from the southern contact. Most of the chemical variations are attributed to differentiation in the source chamber, coupled with in situ fractional crystallization. Feldspar lath orientations at the southern contact indicate a magma flow upward and toward the west. Across-dike textural variations, notably the appearance and disappearance of pyroxene phenocrysts and the abrupt changes in feldspar lath sizes indicate a three pulse mode of emplacement. In addition, chemical data, while supporting these three initial pulses also indicate the occurence of a fourth and last pulse.

A rapid and inexpensive method for the determination of rare earth elements which combines the use of ion exchange columns and Direct Current Plasma spectroscopy was developed.

RESUME

Les variations texturales et chimiques enregistrées selon un profil perpendiculaire à la direction d'un filon diabasique de la région de St-Pierre de Wakefield, Québec, sont présentées en détail. L'information est examinée en relation avec le mode d'emplacement, l'histoire cristallographique et la différentiation magmatique du filon de diabase.

On note des augmentations en Fe, K, Ti, Zr, Sr, Rb, Y et Zn, et des diminutions en Al, Mg, Ca et Ba, du contact vers le centre de l'intrusion. Ces variations, accompagnées de pics de K, Ba, Sr et Rb sont attribuées à la différentiation lente de la source magmatique suivie de la fractionnation sur place du magma.

Au contact l'orientation tri-dimensionnelle des feldspaths indique une direction d'écoulement vers le haut et l'ouest. Les variations perpendiculaires à la direction de la caisse fillonique telles que les apparitions et les disparitions de phénocristaux de pyroxène, les changements abrupts de dimensions cristallines et les variations chimiques, indiquent un mode d'emplacement selon quatre impulsions magmatiques. Cette conclusion est soutenue par les diagrammes de variation et les teneurs en terres rares de certains échantillons.

Une recherche axée sur le développement d'une méthode rapide et peu coûteuse d'analyse des terres rares, combinant l'utilisation de colonnes d'échange ionique et la spectroscopie par Courant Direct de Plasma (D.C.P.) est présentée en détail.

TABLE OF CONTENTS

LIST OF TABLES

LIST OF ILLUSTRATIONS

FIGURES

LIST OF ILLUSTRATIONS

PLATES

INTRODUCTION

Studies such as that of Steele and Ragland (1976), depicting chemical variations across strike, have raised considerable interest in wide diabase dikes since they generally display good chemical trends related to flow differentiation or other processes active during emplacement, and textural variations related to the mode of emplacement. On the other hand, smaller diabase dikes have received little attention since they were once thought to be both mineralogically and compositionally uniform because of their rapid cooling after emplacement.

The present report deals with petrographical and petrological variations recorded for a 25 m to 32 m wide diabase dike located near the village of St-Pierre de Wakefield, Québec.

ACKNOWLEDGEMENT

The author wishes to thank Dr. R. Kretz, Dr. D.D. Hogarth and Dr. C. Pride for their guidance and helpful advice and criticism, J.S. Loop of the University of Ottawa for his indispensable help in the preparation of the rare-earth separation method, and Claudette Galipeau, without whom this work could not have been realised. The author would also like to acknowledge the financial aid received through Grant A6895, awarded to Dr. R. Kretz.

REGIONAL GEOLOGY

The study area is located about 25 km north of Ottawa, near the village of St-Pierre de Wakefield, Québec (see Fig.1). It is underlain by marble, quartzite and gneisses of the Grenville Supergroup, cut by pegmatite and diabase dikes. Following are brief descriptions of the country rocks and dikes based on field observations and on previous works by Martignole (1975) and Wilson (1920).

Marble, mostly calcitic, is common in the area of study especially around St-Pierre Lake (see Fig.1). Generally massive in appearance, it displays no foliation and little to no layering. Graphite is the main accessory mineral although phlogopite and apatite are locally present.

The quartzites are of two types; the first contains thin layers (1 cm) of pyroxene-rich gneiss and the second, layers of feldspar gneiss up to 1 m thick.

The gneisses which underlie 70% of the area are subdivided into four main types: quartz-feldspar gneiss, biotite gneiss, biotite-garnet gneiss and hornblende gneiss. Quartz-feldspar gneiss is the most abundant. It displays strong to weak foliation and locally a faint lineation. When the foliation is well developed, it is generally accompanied by a gneissosity where the biotite is concentrated in layers reaching a maximum thickness of a few centimetres. The biotite gneiss is scattered throughout the area in the form of small outcrops or thin intercalation in other types of gneiss. In general, the biotite gneiss displays a pronounced planar alignment of biotite (foliation) parallel to a well defined gneissosity. Biotite-garnet gneiss is also dispersed throughout the area but, unlike biotite gneiss, it displays only faint foliation.

Where a gneissosity is present, the rock shows alternations of coarse-graine quartz-feldspathic and dark fine-grained beds. Hornblend gneiss is less abundant and is concentrated in the S-SW portion of the study area. It is generally medium-grained and displays a well developed parallel foliation and gneissosity. Quartz and plagioclase are commonly observed forming "eyes" that do not exceed a few millimetres in length.

Two types of intrusive rocks, granite pegmatite and diabase cut rocks of the Grenville Supergroup. Pegmatitic intrusions occur as dikes or isolated, irregularly-shaped bodies, the latter being the most common. In general, the pegmatites are pink, showing graphitic textures accompanied by large feldspar crystals ranging up to over 5 by 10 cms. One interesting feature of some pegmatites is that they often form contact material for the diabase intrusions. Unfortunately, these pegmatites cannot be traced for more than a few metres on either sides of the dikes due to lack of outcrop. The pegmatites can have two origins. The first would have them formed by an extensive contact metamorphism of quartz-feldspar gneiss, related to the emplacement of the diabase dikes. This is most unlikely since it implies melting of the gneiss which in itself necessitates heat transfer impossible to reach with a 25 m to 32 m wide diabase dike. The second origin for these pegmatites would have them genetically related to the Wakefield Batholith and thus the result of partial melting during regional metamorphism. This is the most likely origin. The pegmatites would have intruded the regional rocks along existing fractures which would have been reactivated afterward to serve as passageways for the diabasic magma.

Three equally spaced diabase dikes, out of which the most northerly dike named "St-Pierre" was chosen for investigation, cross the area of study. Originally described by Wilson (1920, 1925), these diabase dikes, part of the Grenville Dike Swarm, are strictly aligned in an E-W direction, a prominent fault direction possibly controlled by the E-W fracturing in the Ottawa Bonnechere Graben. In a paleomagnetic study of the Grenville diabases, Murthy (1971) indicated that the similarity between the poles of the Franklin diabase, dated at 675 m.y., and the Grenville dikes suggests coeval emplacement for the two groups of rock. K-Ar dating, performed on various dikes of the Grenville Swarm, gave ages ranging from 408 to 488 m.y. (Wanless et al. 1972). Regardless of their true age, they obviously postdate the regional metamorphism.

Outcrops showing both northern and southern contacts of the studied dike are rare. In general, the contact rocks are extremely fractured and often covered. In one instance, the dike was completely covered with the exception of a few contact diabase fragments fused to a vertical fault wall parallel to the dike contacts. This evidence suggests that the faults along which the diabasic magma intruded were reactivated after solidification.

The St-Pierre dike was initially sampled at 5 m. intervals across it's width at 500 m. intervals along it's length and these samples are designated as A1-letc. The study dike was further sampled at a natural cross-section indicated by X11 on figure 1. All the samples collected at this location are designated by the X11 prefix.

GENERAL PETROGRAPHY

Mineralogy

Individual descriptions of thin-sections of the St-Pierre dike are presented in Appendix 1. Five main minerals were observed; plagioclase, augite, pigeonite, magnetite and ilmenite. These are accompanied by minor minerals such as chlorite, calcite, quartz, potassium feldspar and titanite. From Appendix 1, it is clear that there are no determinable modal variations for the above minerals.

Plagioclase is the most abundant mineral. Taking the form of subhedral to euhedral lath-shaped crystals, plagioclase displays both albite and Carlsbad twins. It also displays normal zoning (see Plate 1), the zones decreasing in thickness toward the rims of the grains. In the contact zones of the dike, the plagioclase crystals have irregularly rounded outlines, indicating a reaction relation with the magma (see Plate 2). The anorthite content of plagioclase crystals, evaluated by the Michel-Lévy method (Kerr, 1977), gave labradorite compositions. The plagioclase crystals increase gradually in mean size from the contact, where they average 0.4 mm by 0.1 mm, inward to reach a maximum of 1.0 mm by 0.4 mm in the centre of the dike (see Fig.2).

Although augite is by far the most abundant pyroxene, both augite and pigeonite are observed throughout the dike. Near and at the contacts, the pyroxenes form oval phenocrysts of aggregate nature into which poikilitically enclosed plagioclase crystals wedge out (see Plate 3).

In places, especially in the coarse-grained regions of the dike, augite and pigeonite are found in association forming intergrowths of two

Plate 1. Photo-micrograph of zoned plagioclase crystals.

Photo-micrograph is approximately 0.4 mm in length.

Plate 2. Photo-micrograph showing the corroded outline of a plagioclase feldspar crystals.

Photo-micrograph is approximately 0.2 mm in length.

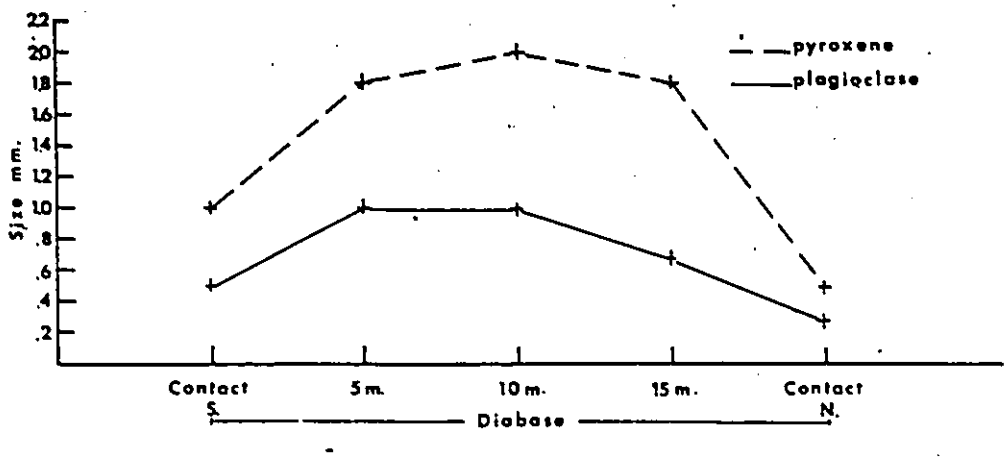

Figure 2. Variation in mean grain size across the St-Pierre dike at A1. Each value is the mean of twenty grains per sample. See figure 1 for sample location.

Plate 3. Photo-micrograph of a composite pyroxene phenocryst into which feldspars wedge out.
Photo-micrograph is approximately 0.2 mm in length.

Plate 4. Photo-micrograph of a zoned pyroxene crystal, pigeonite forming the inner core and augite the outer rim.
Photo-micrograph is approximately 0.4 mm in length.

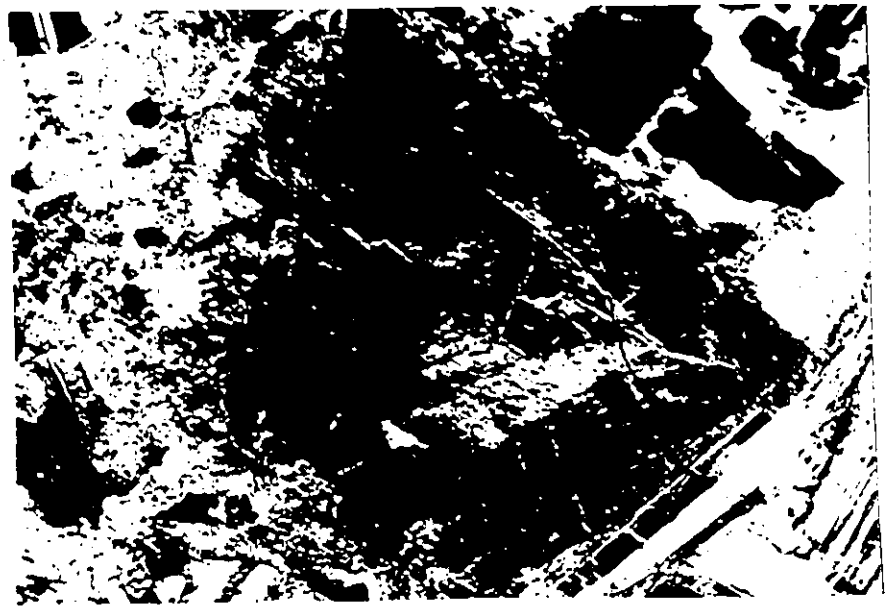

different kinds. The most common type consists of an irregular patch of pigeonite surrounded by augite (see Plate 4), both pyroxenes distinguishable by their different 2V angle. Often the pigeonite portion has been replaced by chlorite leaving an augite grain with a chloritic centre (see Plate 5). The least common but by far the most spectacular intergrowth takes the form of an augite hourglass within pigeonite.

The opaque minerals present are magnetite (possibly titanomagnetite) and ilmenite. The magnetite varies both in content and shape from the contact where it is inconspicuous in the groundmass, to the central portions of the dike where it occurs as dendritic 2 mm. by 2 mm. crystals often showing polygonal outlines (see Plate 6). The appearance and geometry of similar magnetite crystals have been described by Kretz (in press). Rarely, magnetite grains are totally or partially enclosed by titanite or sphene. Baragar (1960) observed such an association in gabbro dikes and attributed the presence of titanite or sphene as the result of magnetite alteration. Similar observations were reported by Buddington et al. (1955).

Ilmenite is also present throughout the dike but in smaller concentration and size. It occurs as minute (0.01 mm) euhedral crystals associated with both chlorite and magnetite (see Plate 7). Kretz (in press) attributed the presence of ilmenite and chlorite to the breakdown of magnetite accompanied by a reaction involving silication. One piece of evidence supporting this replacement is the polygonal outline, usually displayed by magnetite crystals, adopted by the masses of ilmenite grains.

Distributed throughout the dike, chlorite occurs as anhedral 1.5 mm by 1.5 mm grains usually associated with magnetite and ilmenite. In

Plate 5. Photo-micrograph of a zoned pyroxene crystal where the inner pigeonite core is partially replaced by chlorite.
Photo-micrograph is approximately 0.4 mm in length.

Plate 6. Photo-micrograph of magnetite crystals showing polyhedral outlines.
Photo-micrograph is approximately 0.4 mm in length.

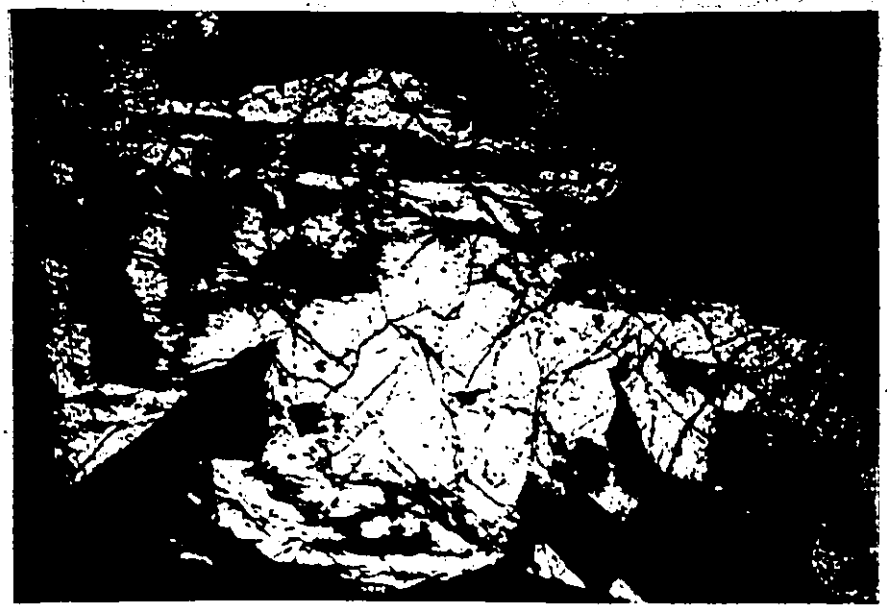

Plate 7. Photo-micrograph of minute ilmenite crystals associated with chlorite. Note the outline of the mass of ilmenite crystals which can indicate the replacement of magnetite by ilmenite. Photo-micrograph is approximately 0.2 mm in length.

Plate 8. Photo-micrograph of quartz and K-feldspar micro-pegmatite. Photo-micrograph is approximately 0.2 mm in length.

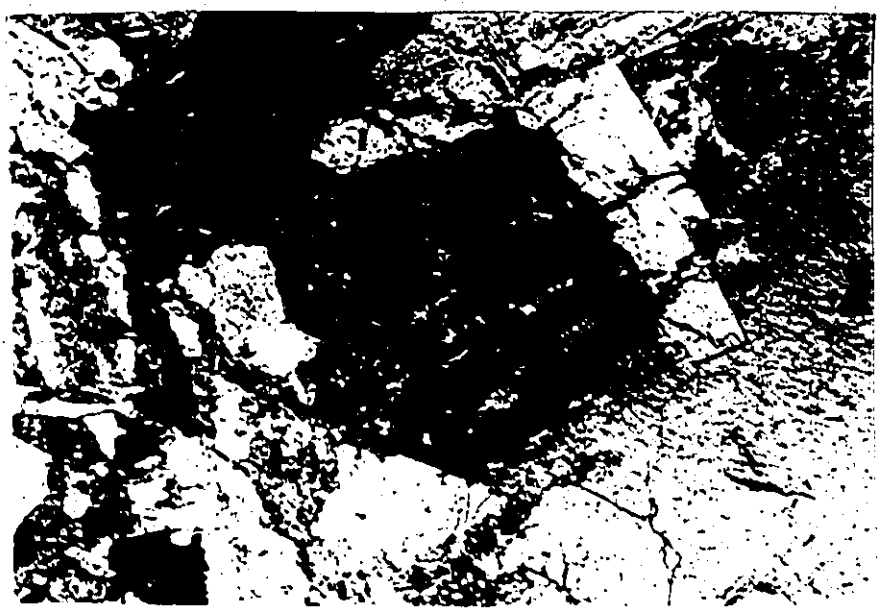

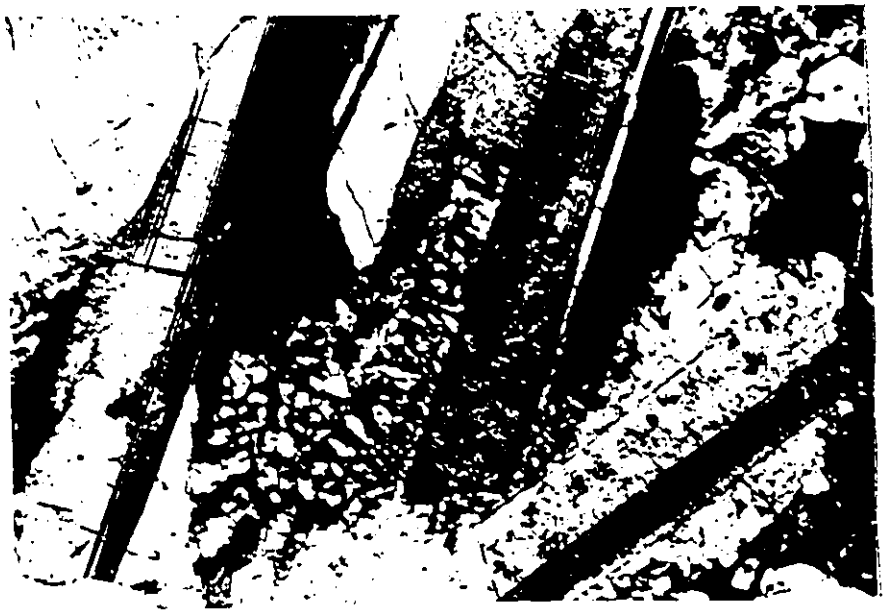

general, the chlorite grains are light green displaying faint pleochroism but brilliant yellow grains may be found.

Calcite, described in very few thin-sections, constitutes an extremely small portion of the total rock (1%). Kretz (in press) indicates that the calcite locally appears to be pseudomorphous after olivine. Since the observed calcite grains are extremely small (0.1 mm), no textural features pointing toward pseudomorphism could be recorded.

Quartz and K-feldspar are also minor constituents of the diabase. Usually occuring as minute grains (0.1 mm), they are observed together forming interstitial graphic intergrowths. In general, these intergrowths are small (0.1 mm) and thus more readily observed in the coarse-grained portions of the dike (see Plate 8).

Least in abundance, titanite or sphene is generally found in close association with the opaque minerals. It occurs as anhedral grains partially or totally enclosing magnetite.

Textures and Structures

Although a variety of textures have been described in the previous section, feldspar lath orientations and large scale textural variations will be presented and discussed here.

The contact between the wallrock and the diabase dike is marked by a discrete, devitrified glassy seam, 1.0 mm thick (see Plate 9). In hand specimen it is evident that the seam runs parallel to the contact but also bifurcates into the wallrock, isolating small xenoliths of pegmatite in the diabase (see Plate 9).

Plate 9. Photograph of a contact specimen showing the small seam, the first and second pulse and the location of Samples A, B, C and D. Scale in cm.

This is a portion of sample X11-9 from the southern contact.

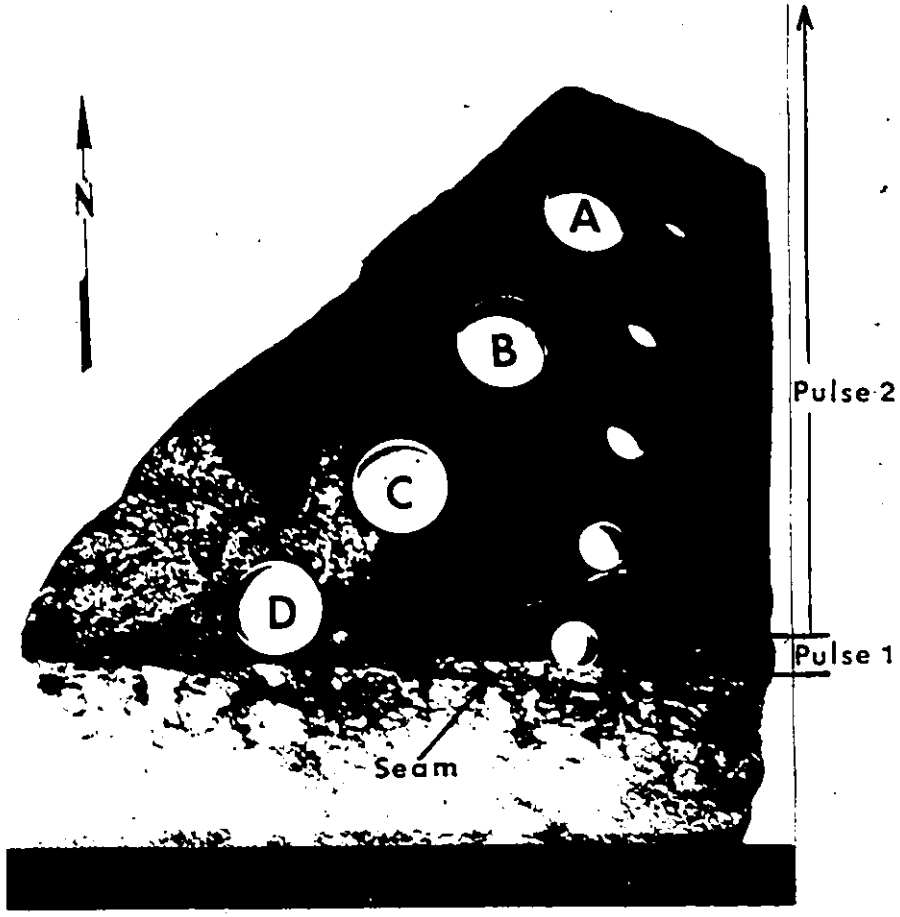
N
A
B
C
D
Pulse 2
Pulse 1
Seam

The general smoothness of the contacts is interrupted by small protuberances of pegmatite, 1.0 cm by 1.5 cm, into the diabase. The examination of contact thin-sections leaves no doubt as to their origin. They are integral parts of the regional rocks and not xenoliths. They generally display a wedge-shaped appearance with the gentle slope of the wedge facing east (see Plate 10).

Composite pyroxene phenocrysts mark the first 0.5 cm of diabase at the contacts. These are generally rounded and range from 0.6 mm to 1.0 mm in diameter. Imbedded with plagioclase phenocrysts in an extremely fine-grained, black matrix, the pyroxenes, when in contact with the regional rock extensions, have been deposited in a similar fashion as would sediments in a river (see Plate 10). On the eastern side of the protuberances, where the slope is gentle, the pyroxene phenocrysts were deposited one beside the other. Toward the top of the protuberances they gradually disappear to reappear on the western side of the extension where they are deposited one on top of the other. This indicates a higher energy level on the eastern side of the wedge-shaped extensions as compared to the western side.

At the southern contact, three oriented thin-sections were examined for plagioclase lath directions. Two sections S1 and S2 were cut perpendicular to each other and the contact, and the third, S3 , was cut at a distance of 2 mm from and parallel to the contact. The orientation and location of these sections are represented in Figure 3a. From 130 to 160 feldspar long axis orientations and size measurements were performed per thin-section along five traverses spaced at 2 mm distances. The measured orientations were then plotted on rose diagrams (see Fig.4, 5

and 6).

Blanchard et al. (1979) indicated that for a Newtonian flow, platy minerals would align themselves parallel to the flow configuration (see Fig.3b). This alignment is due to the rotation of particles at the contact, itself related to flow shear and relative magma velocities. This arrangement seems relatively simple but in fact a Newtonian flow configuration, viewed in three dimensions, would look much like a bullet head. In fact, the feldspars at the contact would obtain a three-dimensional orientation. This orientation is displayed in both rose diagrams and Figure 7. On the vertical (S1), long axis orientations show a definite concentration from 0° to 10° while on the horizontal (S2), the concentration is from 0° to 25°, both inclinations being away from the southern contact toward the north. Section S3, parallel to the contact, confirms this three- dimensional orientation of the feldspars with a discrete concentration at 45° away from the top (vertical) and toward the east.

The feldspar orientation can only be explained by a Newtonian flow originating in the lower east and moving toward the top west (see Fig.7). This is in direct agreement with both the protuberances morphology and the mode of pyroxene phenocryts deposition at the contact.

As distance from the contact increases, a series of textural changes appear. At 0.5 cm from the contact, there is an abrupt loss of all pyroxene phenocrysts and the rock becomes an extremely fine-grained contact diabase (see Plate 9). The pyroxene phenocrysts then gradually reappear at 3 cm from the contacts, where they are generally 0.5 mm in diameter and imbedded in the fine-grained matrix. They gradually

increase in size to reach a maximum of 2 mm in diameter at about 19 cm away from the contact. Again at 22 cm, the pyroxene phenocrysts disappear and the feldspar laths abruptly decrease in size by half (0.1 mm by 0.2 mm by 0.5 mm) (see Plate 11). Finally the pyroxenes reappear at about 25 cm from the contact and remain throughout. It is evident that these textural variations cannot be generated by flow differentiation and must be the result of a multi-pulse mode of emplacement of the diabase dike. The first 0.5 cm of diabase would then represent the first pulse, the material between 0.5 cm and 22 cm the second pulse, and 22 cm inward the third pulse. What comes to light is that the textural changes recorded at the beginning of each pulse become harder to distinguish as distance increases away from the contacts. It is then possible that the studied diabase dike was emplaced via more than three pulses although visible textural variations indicate only three.

Plate 10. Photograph of a hand specimen showing a quartz-feldspar pegmatite protuberance and small composite pyroxenes at the contact. Note the shape of the protuberance and the location of pyroxene phenocrysts. This is a portion of sample X11-9 taken from the soutern contact. Scale in cm .

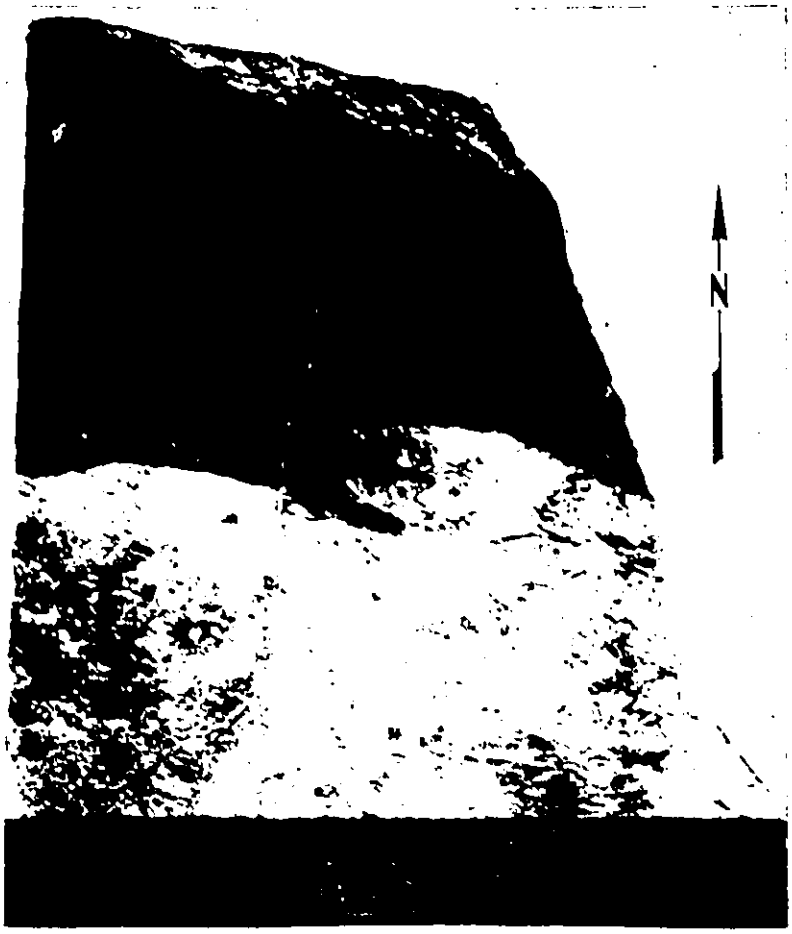
N

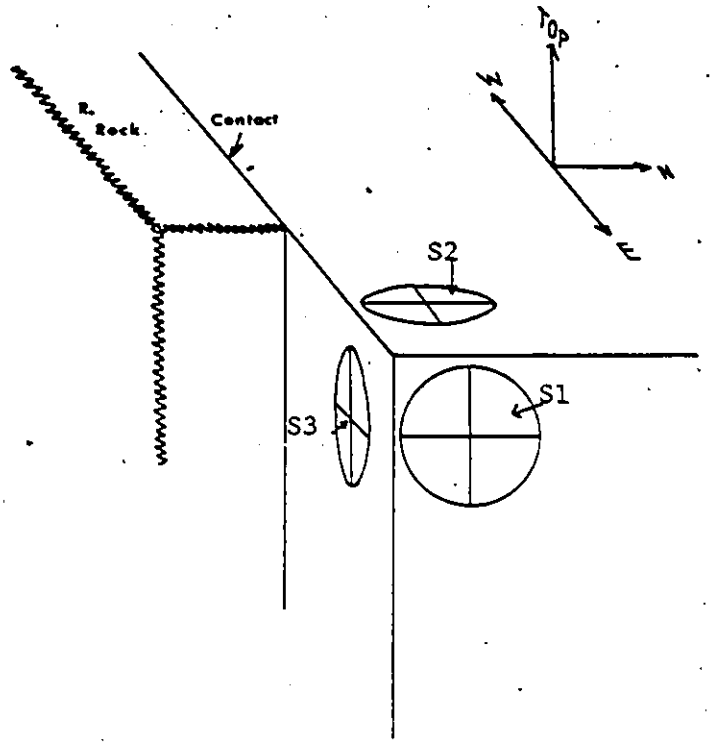

Figure 3a. Location and orientation of sections S1, S2 and S3 with respect to the southern contact of the St-Pierre dike.

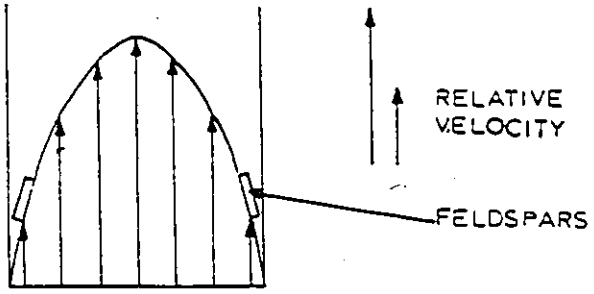

Figure 3b. Orientation of feldspar laths parallel to a Newtonian flow configuration.

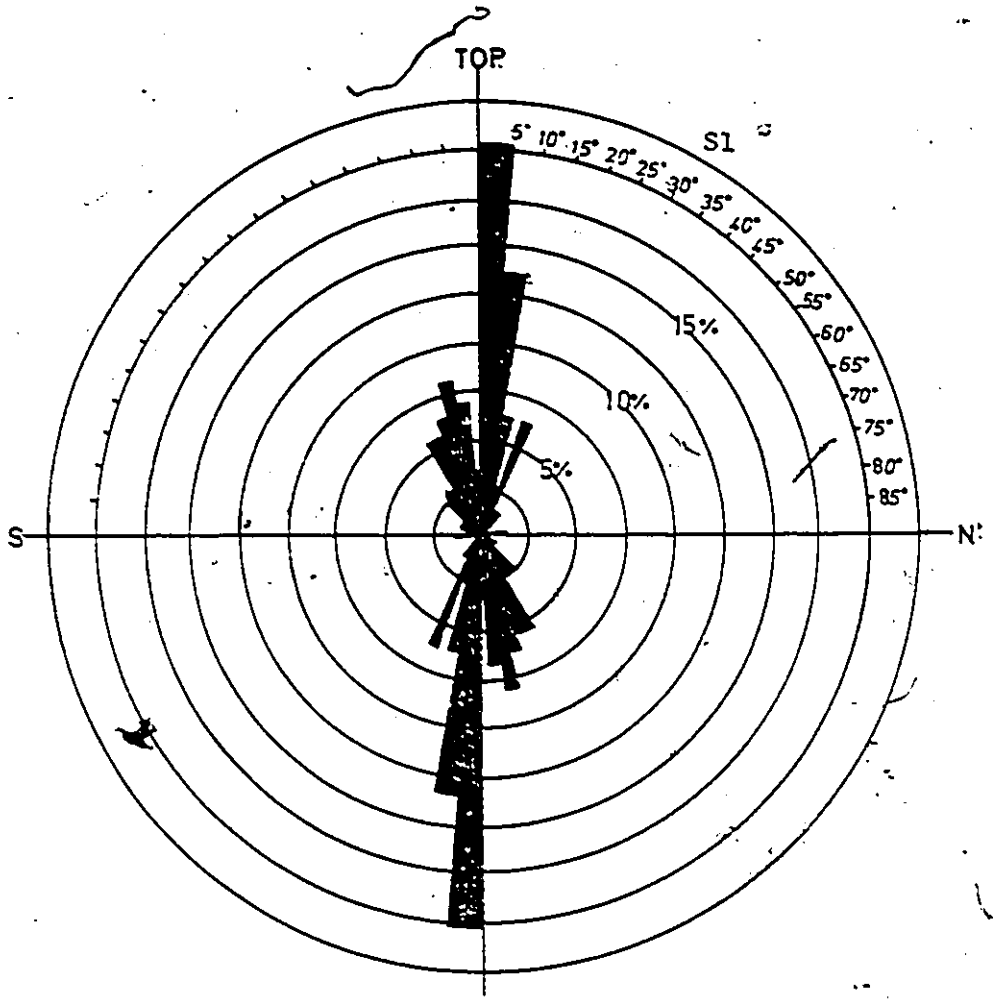

Figure 4. Rose diagram of feldspar long axis orientations for S1, relative to the southern contact which is vertical.

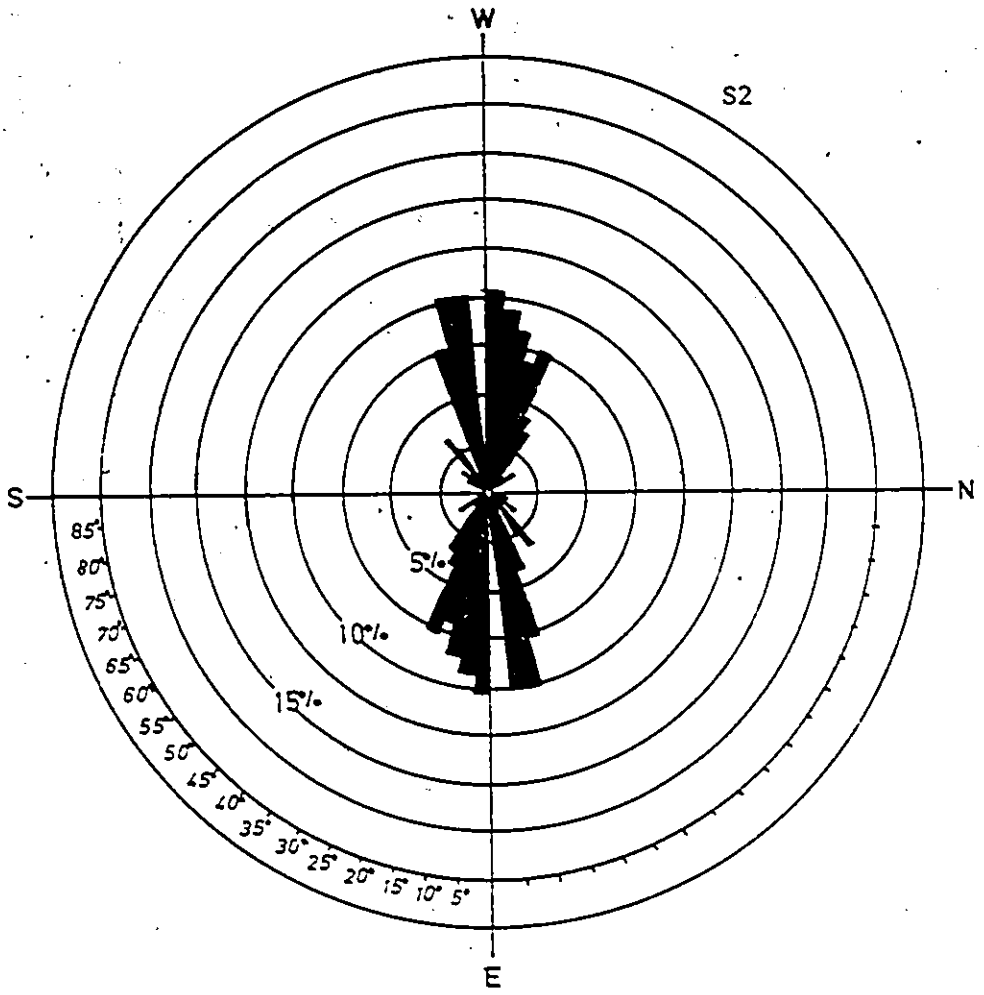

Figure 5. Rose diagram of feldspar long axis orientations for S2, relative to the southern contact which is vertical

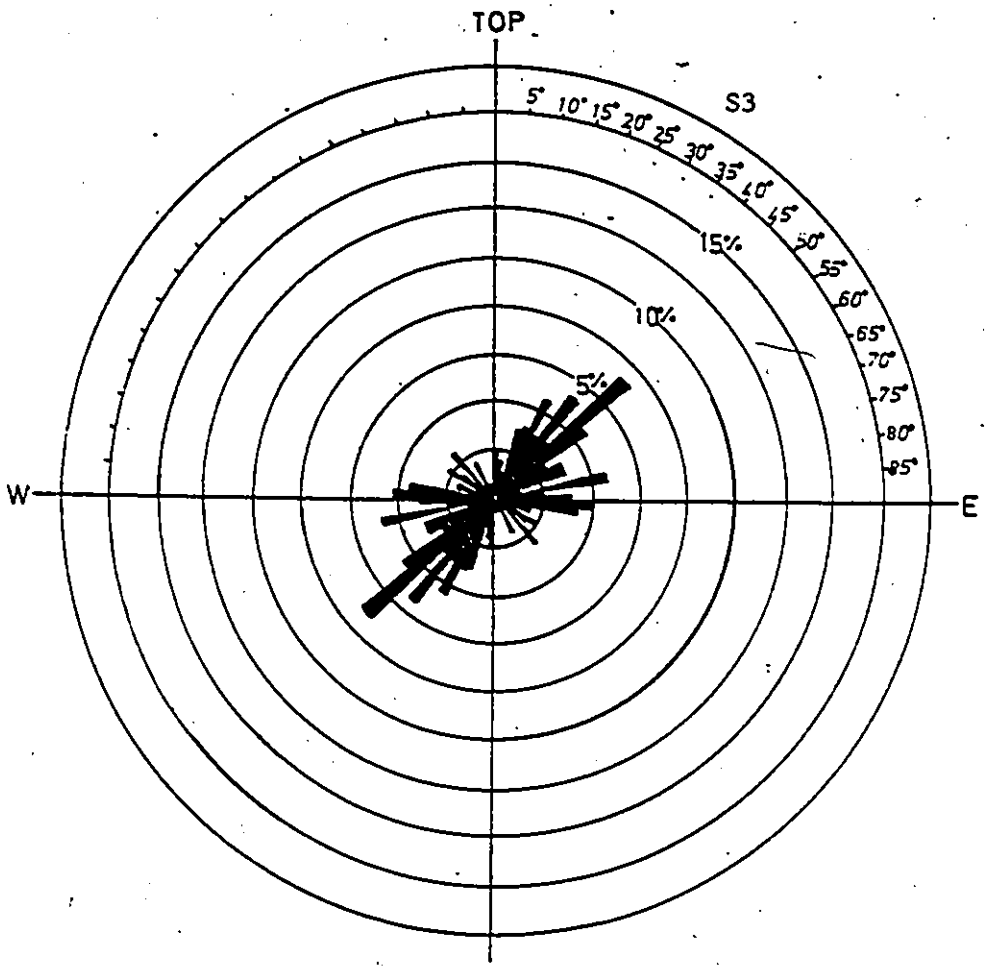

Figure 6. Rose diagram of feldspar long axis orientations for S3, relative to the vertical and the east.

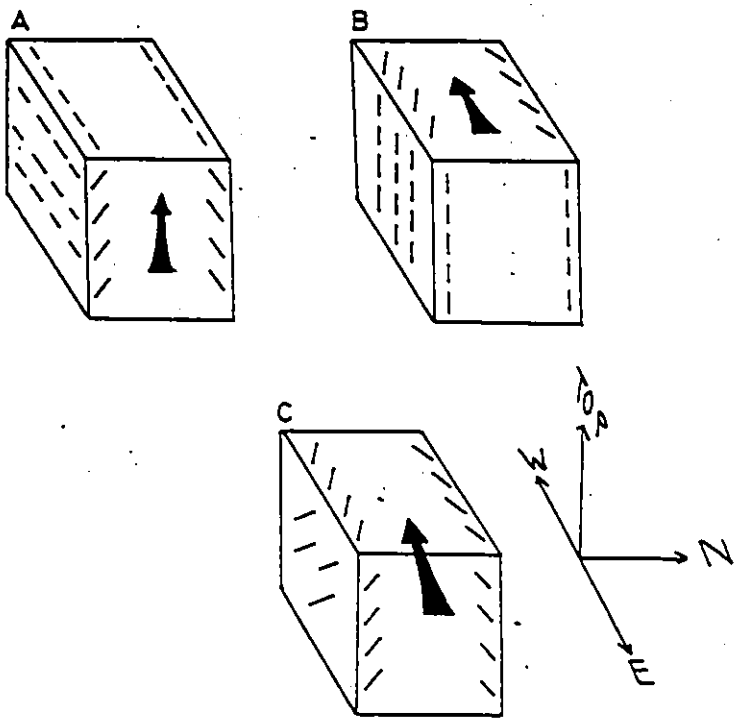

Figure 7. Feldspar lath orientations relative to magma flow directions.
A: vertical flow
B: horizontal flow
C: inclined flow

Plate 11. Photograph of a hand specimen showing the inner contact emphasised by the abrupt loss of pyroxenes (light grey) and the decrease in feldspar size. Scale in cm.

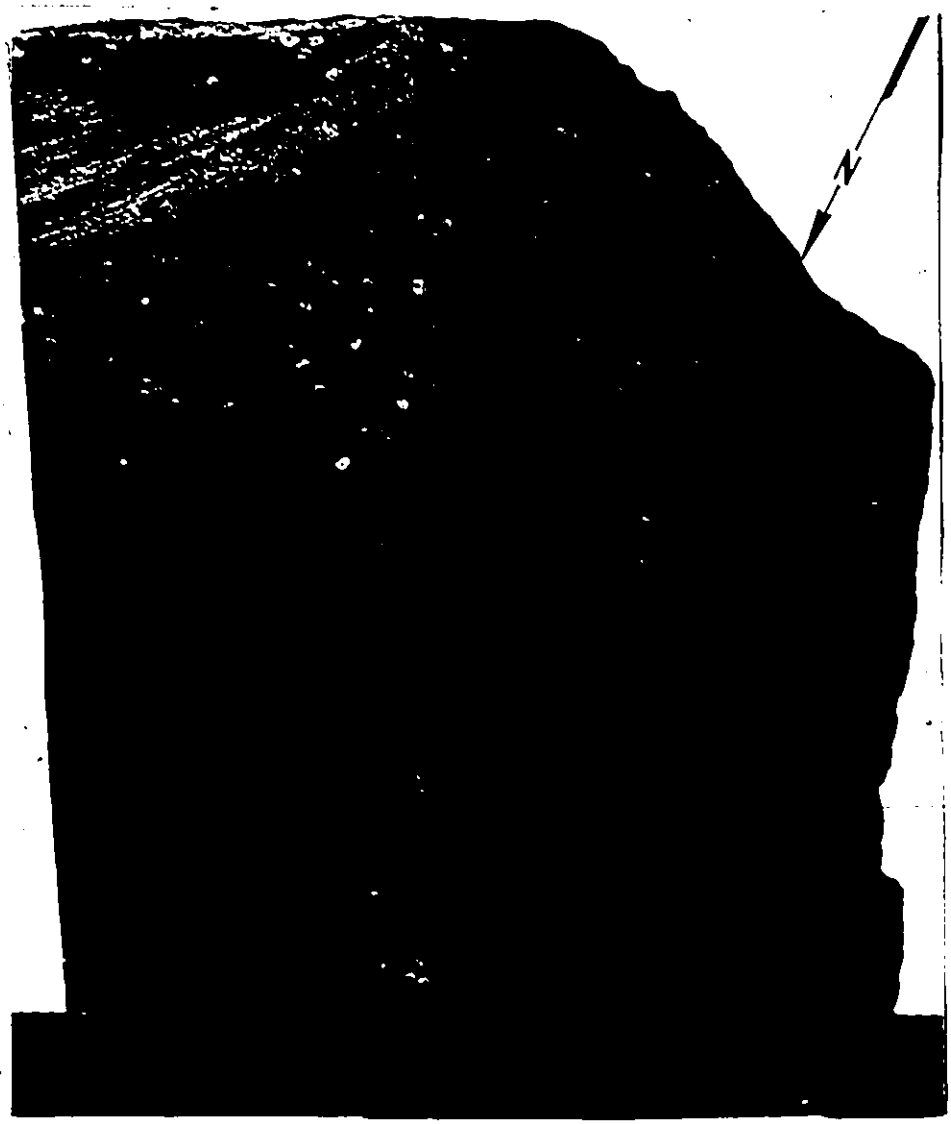
N

PETROLOGY

Out of three diabase dikes that cross the area of study, the most northerly dike was chosen for investigation because of its accessibility, the quality of its contacts and its good natural cross-section. The studied dike is in general 32 m wide although the width can vary considerably depending on location. The dike displays an E-W trend and vertical contacts.

At the natural section (marked X11 in Fig.1) where the dike is approximately 28.5 m wide, seventy samples, out of which eight were regional rock, were collected at intervals of approximately 30 cm along a line extending from wall to wall.

Diabase Sample X11-9 was taken at the southern contact and Sample X11-71c at the northern contact. Other diabase samples, from X11-9 to X11-71c, were taken in between at progressively larger distances from the southern contact.

All samples were powdered as described in Appendix 3. Major and trace element analyses were performed on a "Philips" PW 140 X-Ray Spectrometer and rare earth elements (REE) on a SpectraSpan 5 Direct Current Plasma (D.C.P.) Spectrometer. Results are presented in Appendix 2 along with CIPW norms. The REE separation method, along with its accuracy and precision is presented in Appendix 4.

General Composition

Chemical analyses of the diabase samples were plotted on an Alkalies-Silica diagram (see Fig.8) and plot well into the sub-alkalic field.

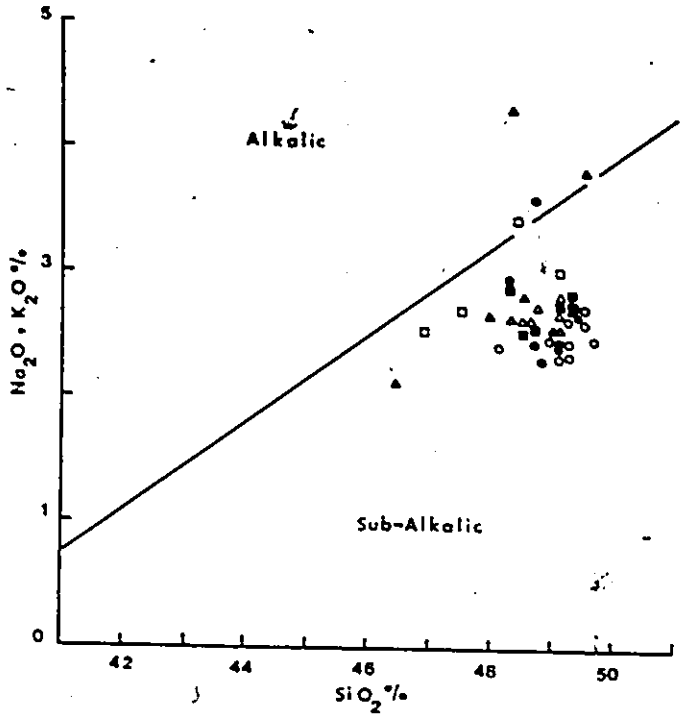

Figure 8. Alkalies versus Silica diagram showing concentrations of St-Pierre diabase samples in the sub-alkalic field. Only forty-five diabase samples are plotted for clarity (dividing line by Scoates et al. 1978)

- ● Samples from the southern contact zone.
- ○ Samples from the northern contact zone.
- ▲ Samples from the intermediate zone, southern half.
- △ Samples from the intermediate zone, northern half.
- ■ Samples from the central zone, southern half.
- □ Samples from the central zone, northern half.

For zone boundaries refer to Figure 25.

When comparing chemical analyses for Grenville diabase dikes, that is, the St-Pierre dike along with values reported by Kretz (in-press) and Nixon (1977) to other diabase dikes such as those of the Pageland and the Pennsylvania dikes, one marked difference is noted. The Grenville dikes display higher Ti values (see Table 1). This feature may imply that these Grenville diabase dikes originated from similar sources, rich in Ti.

Chemical Variations

Samples D, C, B and A (plate 9), collected at 0, 1.5, 3.6 and 5.7 cm respectively from the southern contact of the St-Pierre dike, were analysed for chemical changes. The results are given in Appendix 2 and plotted on Figures 9 to 24. Although no definite conclusions may be drawn from only four samples, a few general observations can be made. The majority of the elements display saw-tooth variation patterns either of general increase or decrease away from the contact. Chemical analysis of Sample D, which is presumed to be the first pulse is relatively poor in Si, Mn and Zn, and richer in Mg, Cr and Fe, as expected for a diabasic rock containing pyroxene phenocrysts (possibly primocrysts). The first portion of the second pulse, represented by Sample C, contained more Si, Ca, Mn, Zn, Rb, Sr and Y. As pyroxene phenocrysts gradually reappear (Sample B), the Si, Mn, Zn, Sr and Y values again decrease only to gradually reincrease at Sample A. The marked difference in some element contents between each pulse may reflect changes which occured at the source area during and in between the emplacement of the magmas.

Chemical variations across strike in the remainder and major portion

TABLE 1

	1	2	3	4	5	6	7
SiO_2	47.8	51.4	48.3	49.6	48.6	48.4	47.8
Al_2O_3	14.2	17.1	14.6	14.0	15.4	15.0	14.2
Fe_2O_3T	13.8	10.2	16.3	15.0	11.5	13.4	13.9
MgO	6.2	6.5	4.3	4.6	10.0	5.2	5.8
CaO	10.6	11.5	10.0	9.3	10.6	11.7	11.5
Na_2O	2.5	2.4	2.6	2.6	2.2	2.3	2.2.
K_2O	0.4	0.6	0.4	0.9	0.4	0.3	0.3
TiO_2	1.7	0.6	2.3	2.9	0.5	1.6	1.6
P_2O_5	-	-	0.1	0.2	-	-	-
MnO	0.3	0.2	0.2	0.2	0.2	0.1	0.1
Ba	86	-	24	116	-	-	-
Cr	160	301	82	90	807	-	-
Zr	81	66	115	182	43	-	-
Sr	174	135	221	278	78	-	-
Rb	14	16	8	15	13	-	-
Y	28	-	31	38	-	-	-
Zn	93	72	122	116	82	-	-
Ni	68	83	31	102	352	-	-

Chemical comparison of various diabase dikes.

Note: SiO_2 to MnO in %, Ba to Ni in ppm

1: Average St-Pierre dike, contact(4 samples)

2: Average Mesozoic Pageland dike, contact (Steele and Ragland, 1976)

3: Average St-Pierre dike, central zone (10 samples)

4: Average Kretz (in-press), cental zone (15 dikes)

5: Average Mesozoic Pennsylvania, central zone (Ragland,1979)

6: Average Gatineau, central zone (Nixon,1977)

7: Average Gatineau, contact zone (Nixon,1977)

Figures 9 to 24. Chemical variations displayed by diabase Samples D, C, B and A (see Plate 9).
■ Regional rock sample collected 30 cm away from the contact.
--- Regression line.
I Error bars, 95% confidence limits.

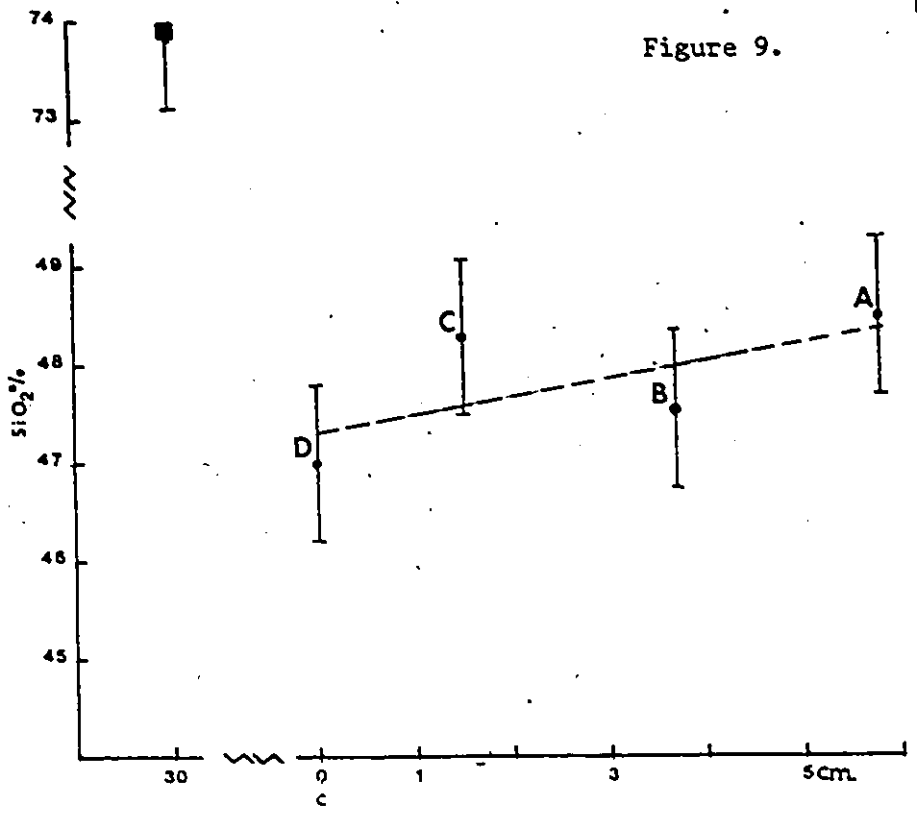

Figure 9.

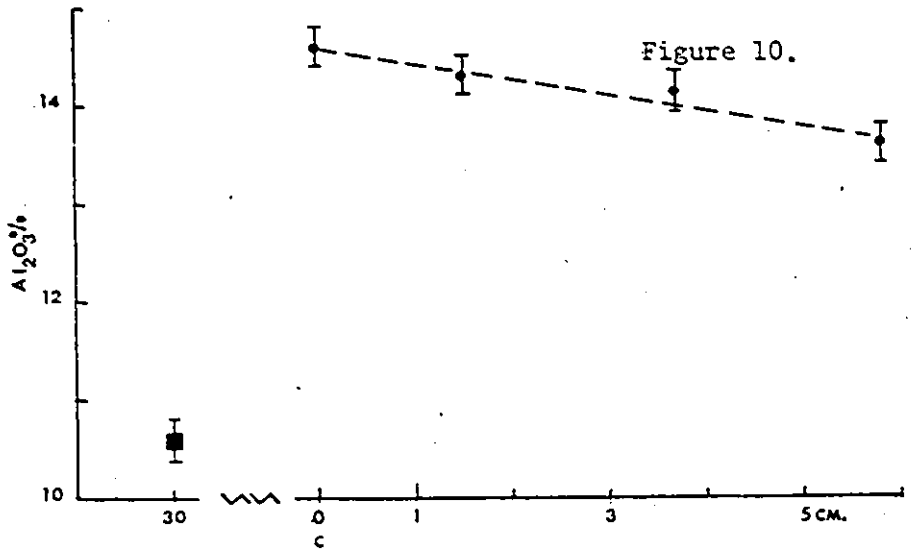

Figure 10.

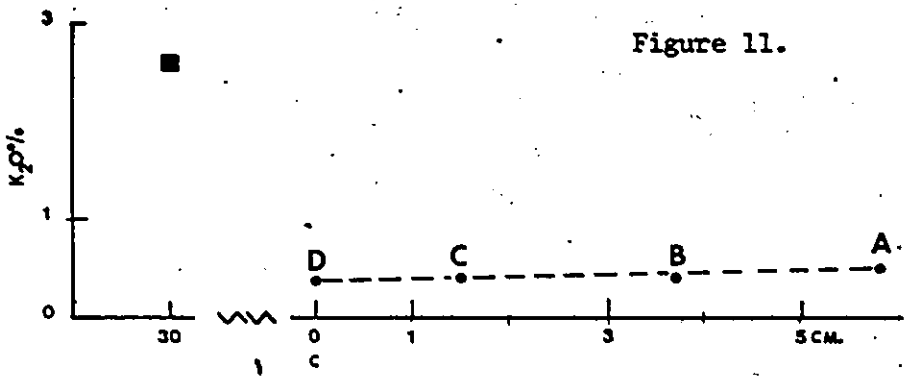

Figure 11.

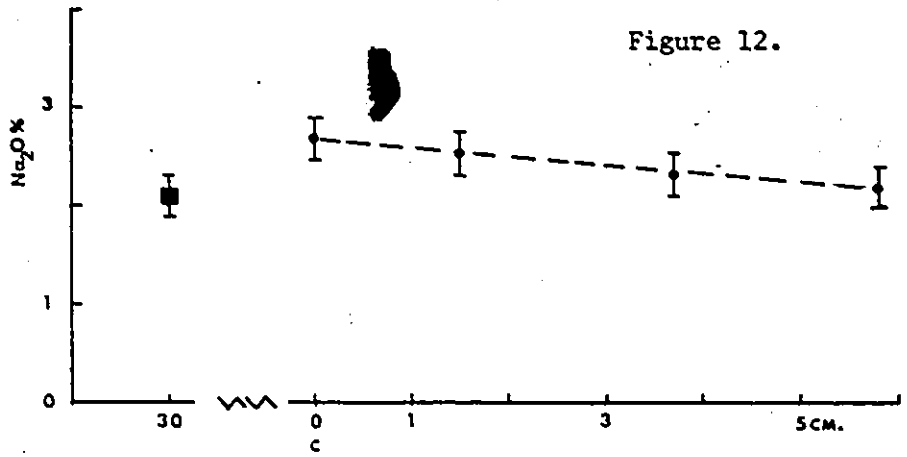

Figure 12.

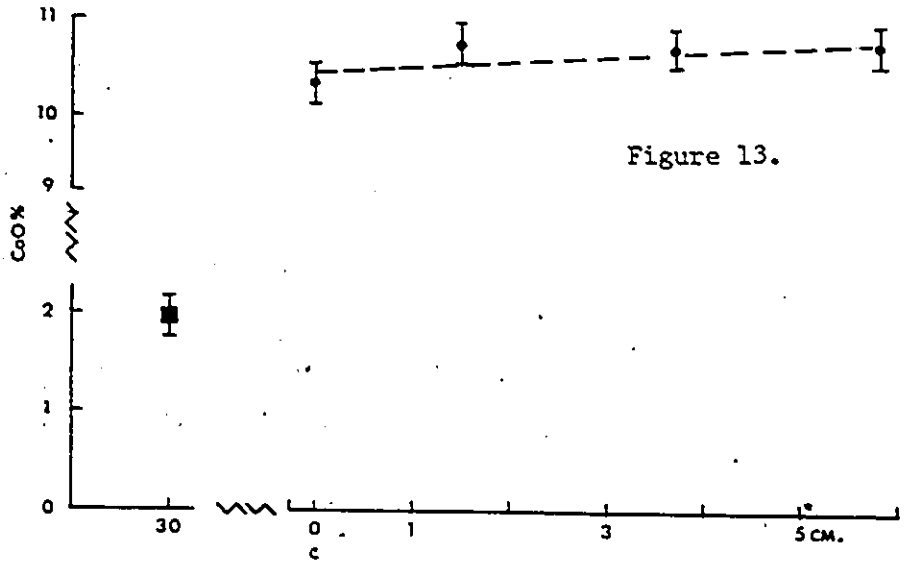

Figure 13.

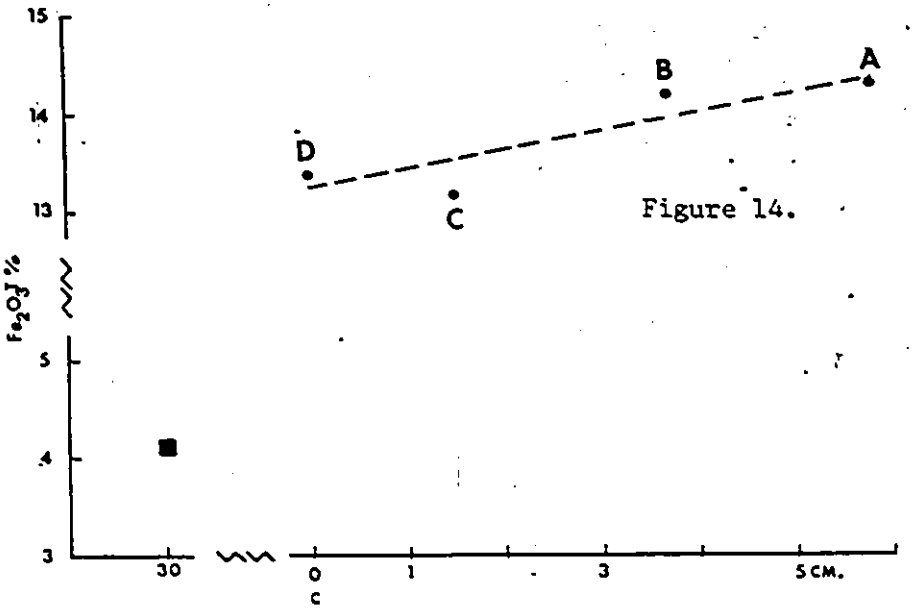

Figure 14.

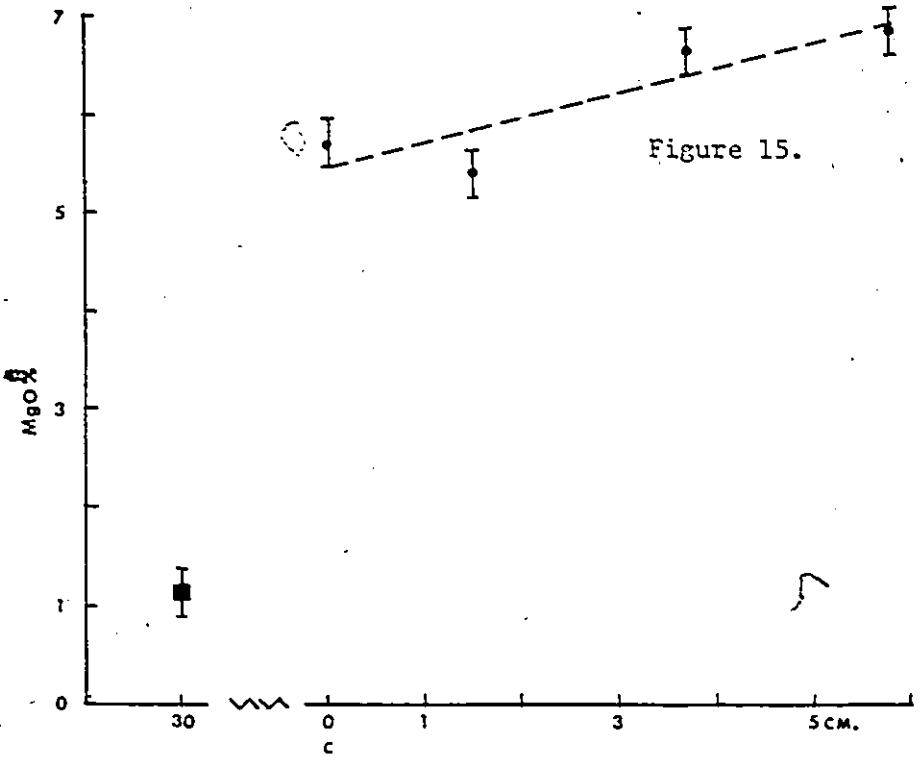

Figure 15.

Figure 16.

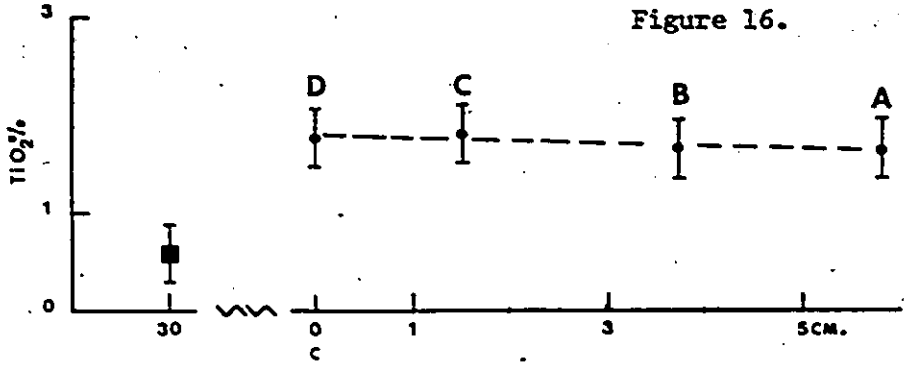

Figure 17.

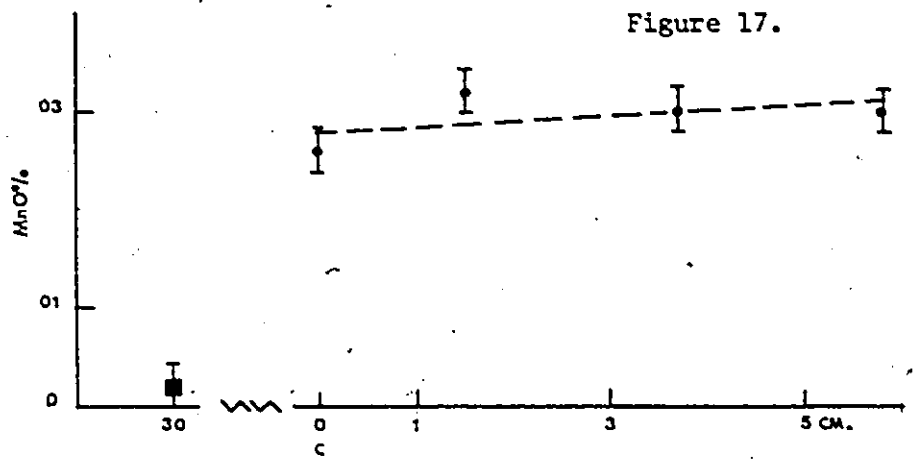

Figure 18.

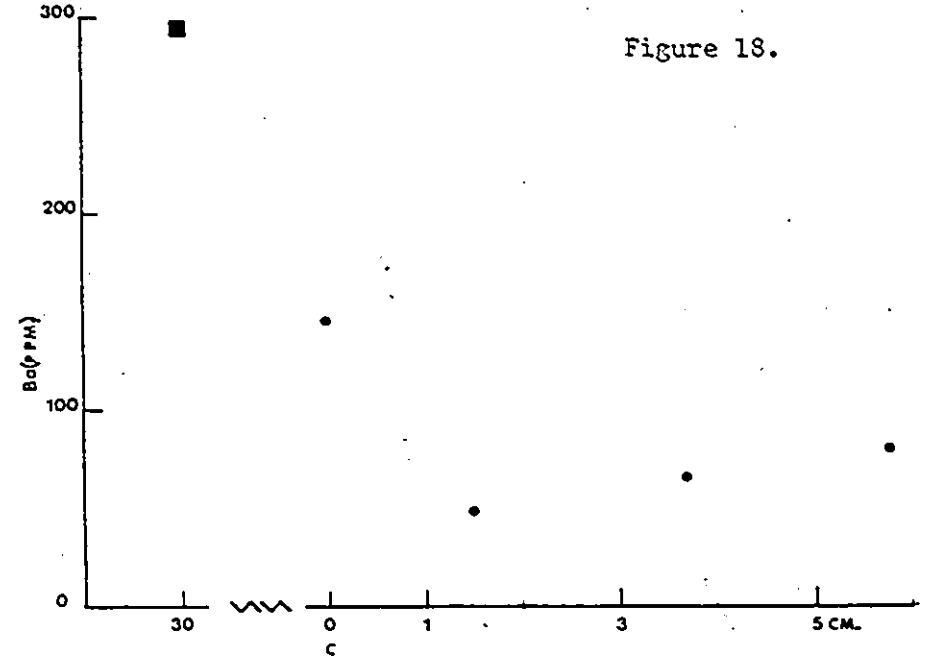

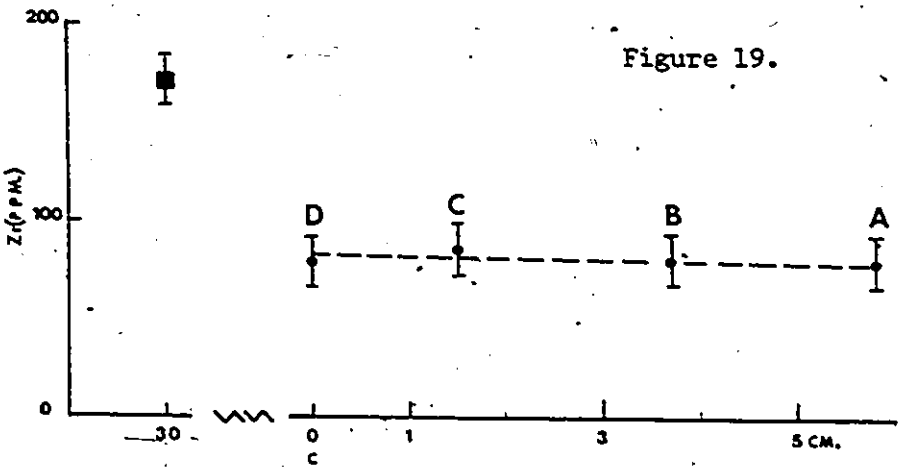

Figure 19.

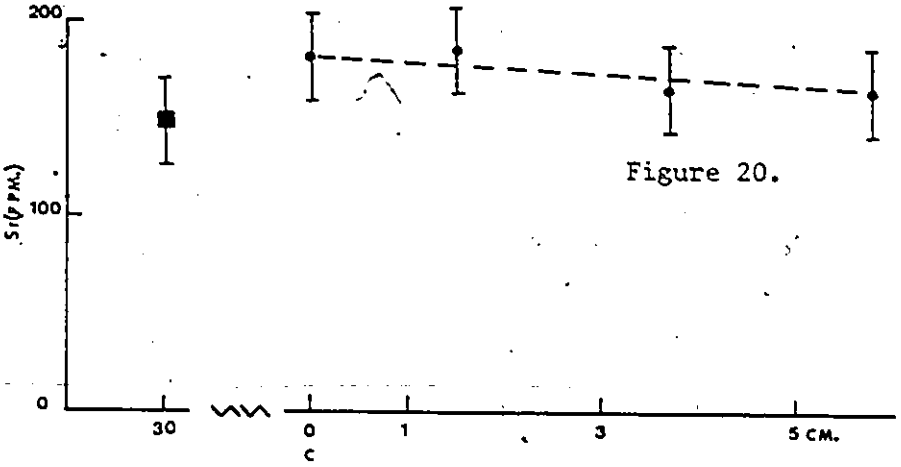

Figure 20.

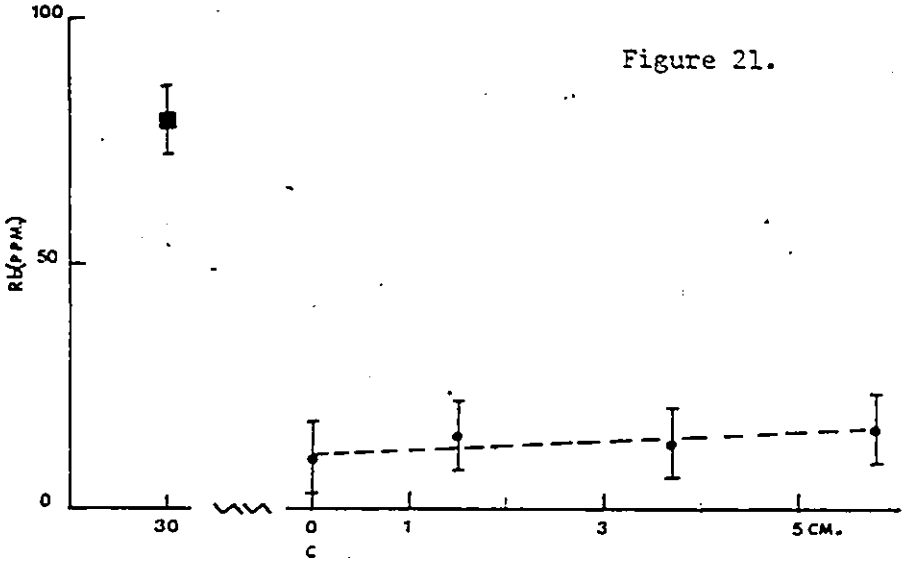

Figure 21.

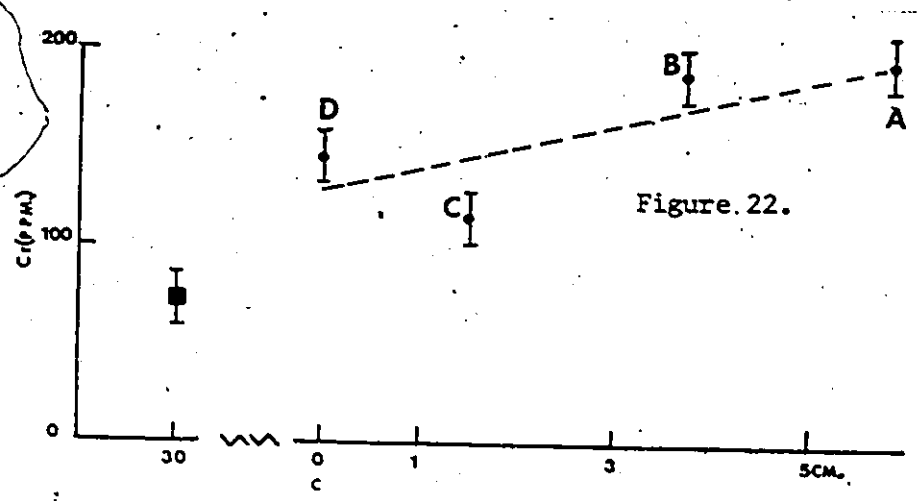

Figure 22.

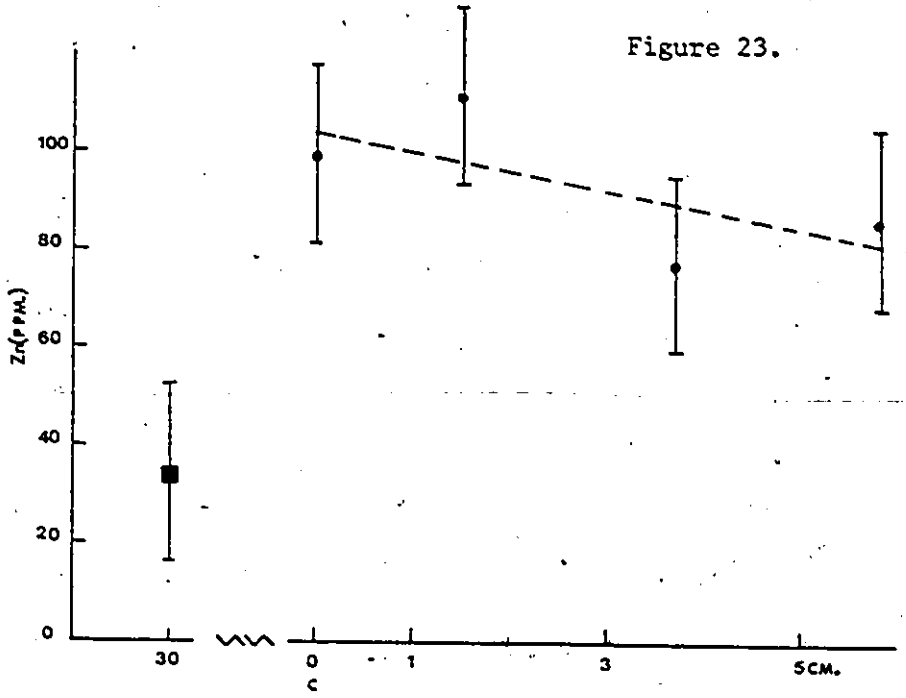

Figure 23.

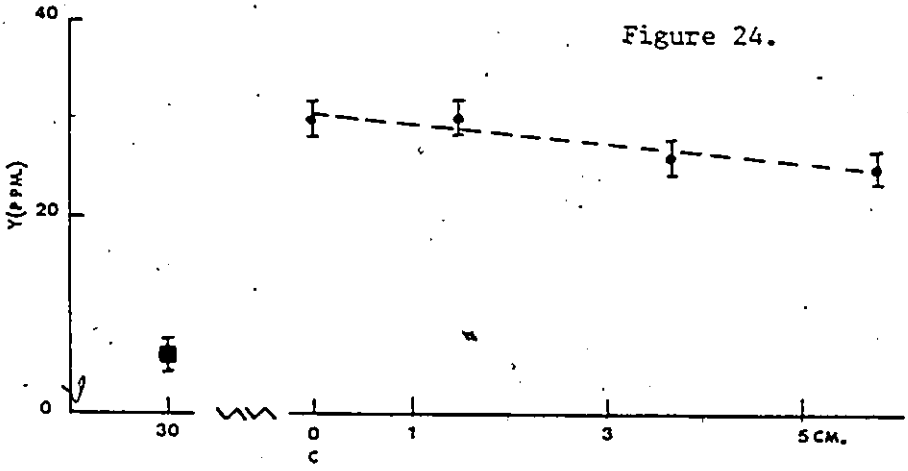

Figure 24.

of the St-Pierre dike are shown in Figures 25 to 42. The analyses are listed in Appendix 2. Analyses of the adjacent country rock, composed of quartz-feldspar pegmatite, are also shown.

The first features that are observed in Figures 25 to 42 are the general trends displayed by most elements. Fe, K, Ti, Zr, Sr, Rb, Y and Zn appear to increase from the contact inward while Al, Mg, Ca and Ba appear to decrease, Na and Mn seem to remain stable throughout while Sr, Cr and Ni contents vary erratically.

Other important features observed, apart from the general trends, occur as large K, Ba, Sr and Rb peaks at the 10.5 m station (see Figs 32 to 39). The possibility of these peaks being the result of analytical contamination is improbable since the samples were not analysed in order of occurrence. The peaks correspond to more than one sample and petrographic studies of samples X11-25 and X11-26 showed marked increases in K-feldspar. The peaks could represent abrupt changes in the magma composition brought about by a possible fourth pulse. The new magma would have crystallized K-feldspar incorporating Ba and Rb and Sr-rich plagioclase. Analyses of samples 7.5 m south of the northern contact are not available due to lack of exposure, but chemical analyses of adjacent samples show a tendency toward the formation of similar and possibly larger peaks. A second possibility would call for samples X11-25 and X11-26 to have crystallized out of a residual magma that collected in a small pocket during the crystallization of pulse 3. This is most unlikely since such a pocket would have been visible in the field and most important of all, residual liquids are usually pushed toward the central portion of the dike, that is the last portion to crystallize.

Figures 25 to 42. Chemical profiles of the St-Pierre diabase dike and adjacent rocks. Sample X11-9 marks the location of the southern contact and X11-71c the northern contact.

I Error bars, 95 % confidence limits.

C Location of contact.

■ Regional rock samples.

Note: 1. The regression lines are not to be taken quantitatively but are incorporated as a visual aid.

2. Contact, intermediate and central zones were determined by dividing the total number of samples by a total of 6 zones.

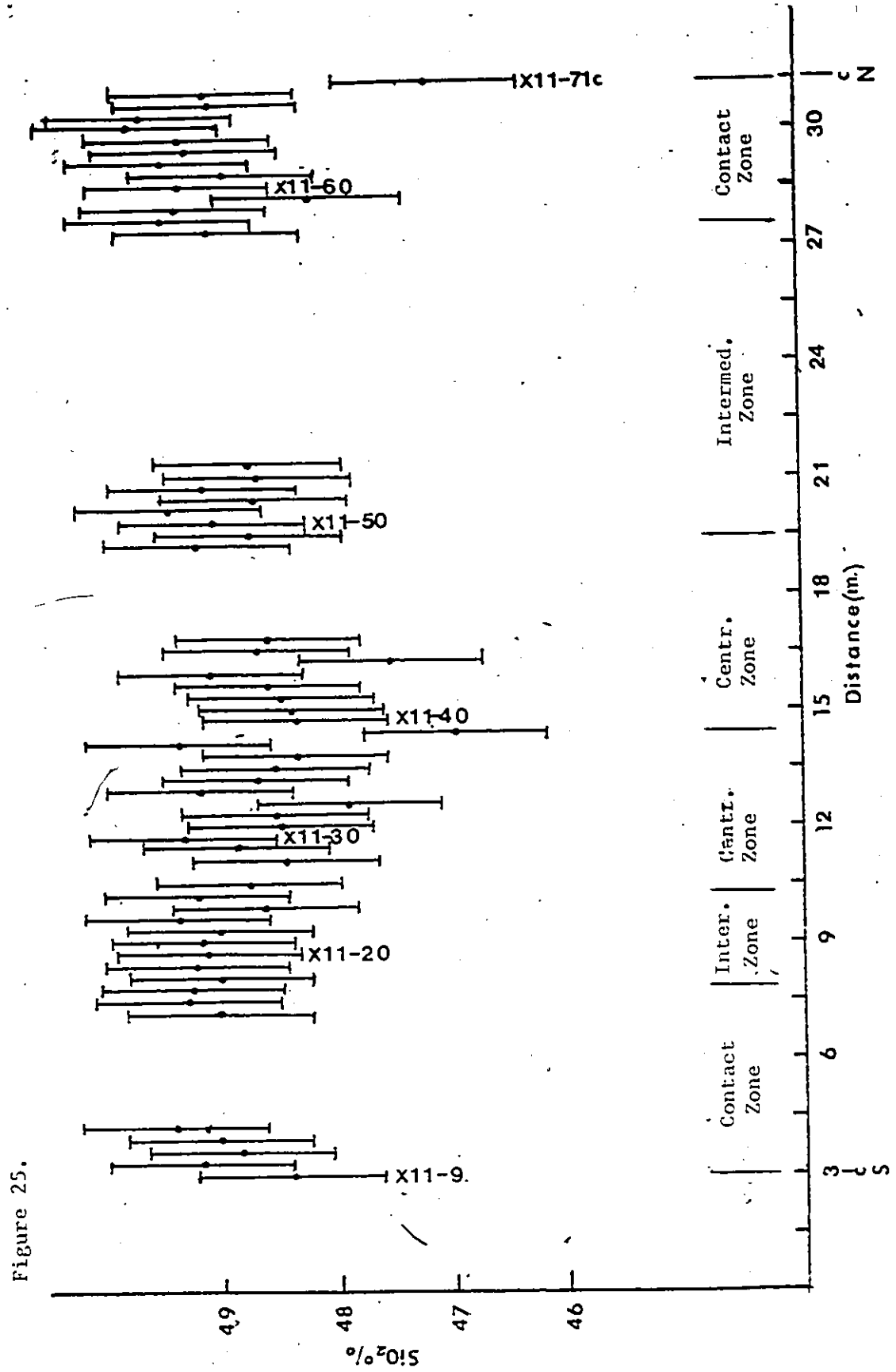
X11-71c
X11-60
X11-50
X11-40
X11-30
X11-20
X11-9
Contact Zone
Inter. Zone
Centr. Zone
Intermed. Zone
Contact Zone
S
N
3
6
9
12
15
18
21
24
27
30
Distance(m.)
46
47
48
49
SiO2 %

Figure 25.

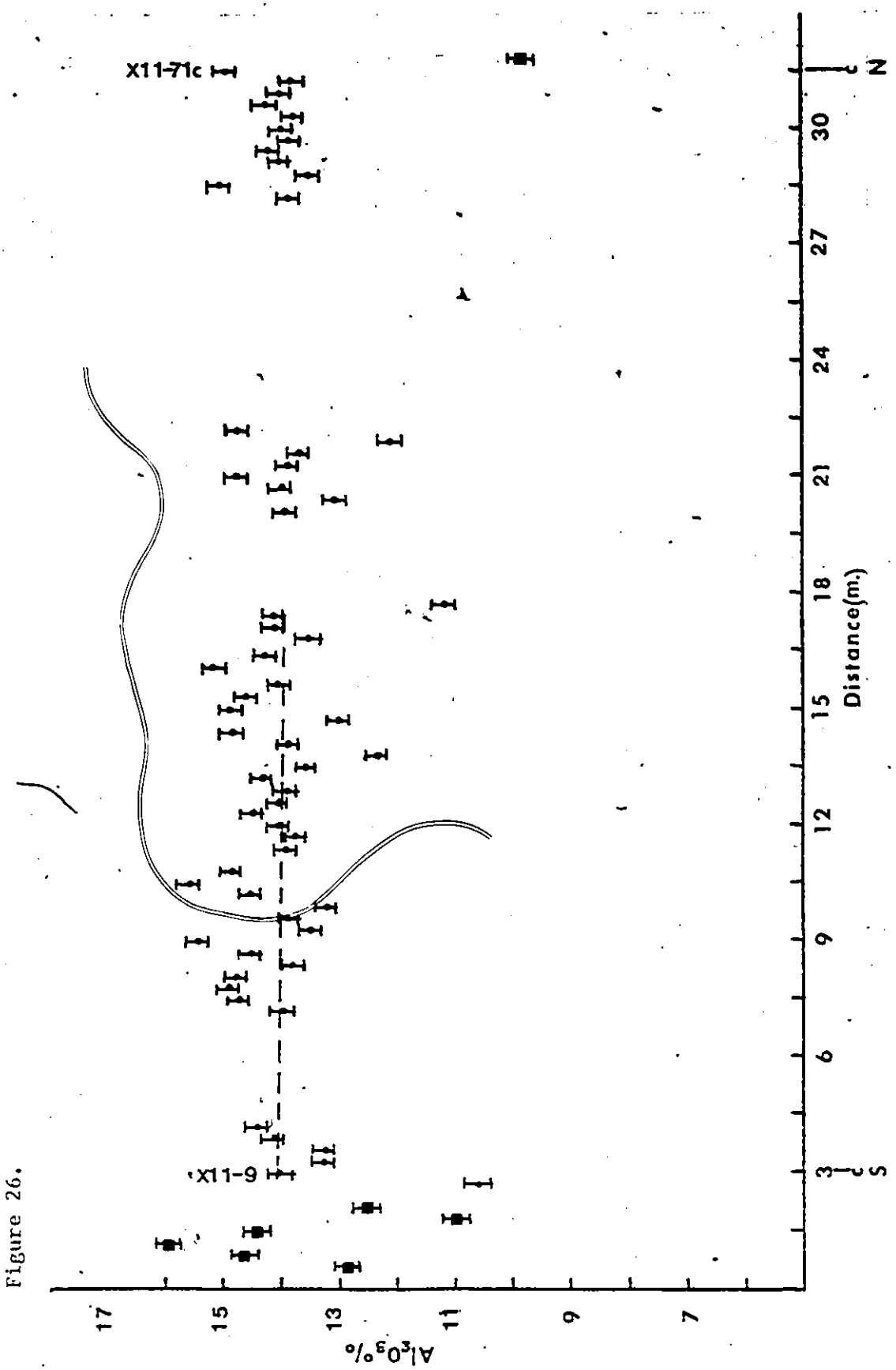
X11-71c
X11-9
S
N
3
6
9
12
15
18
21
24
27
30
Distance(m.)
Al_2O_3%
17
15
13
11
9
7

Figure 26.

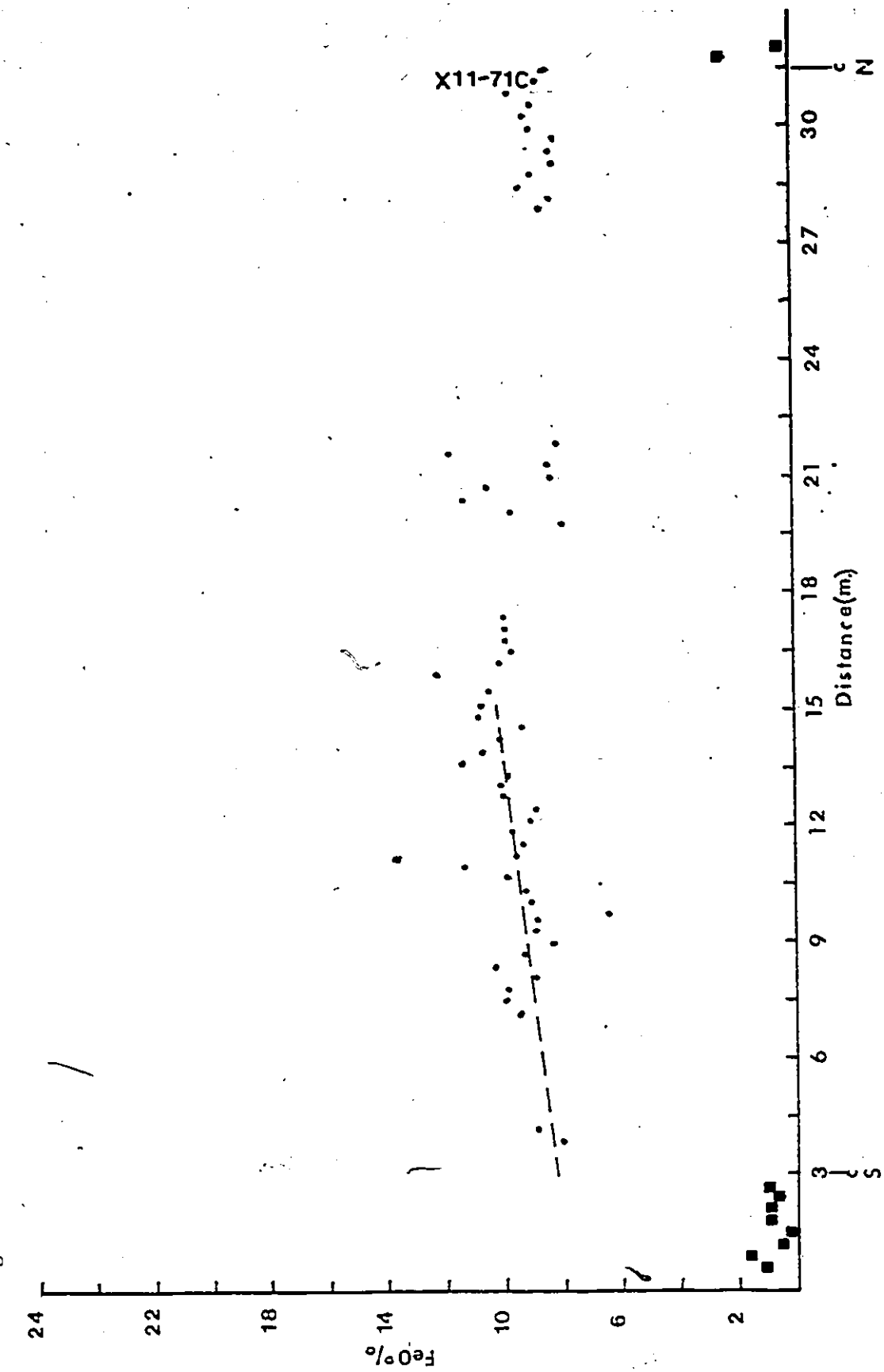

Figure 27.

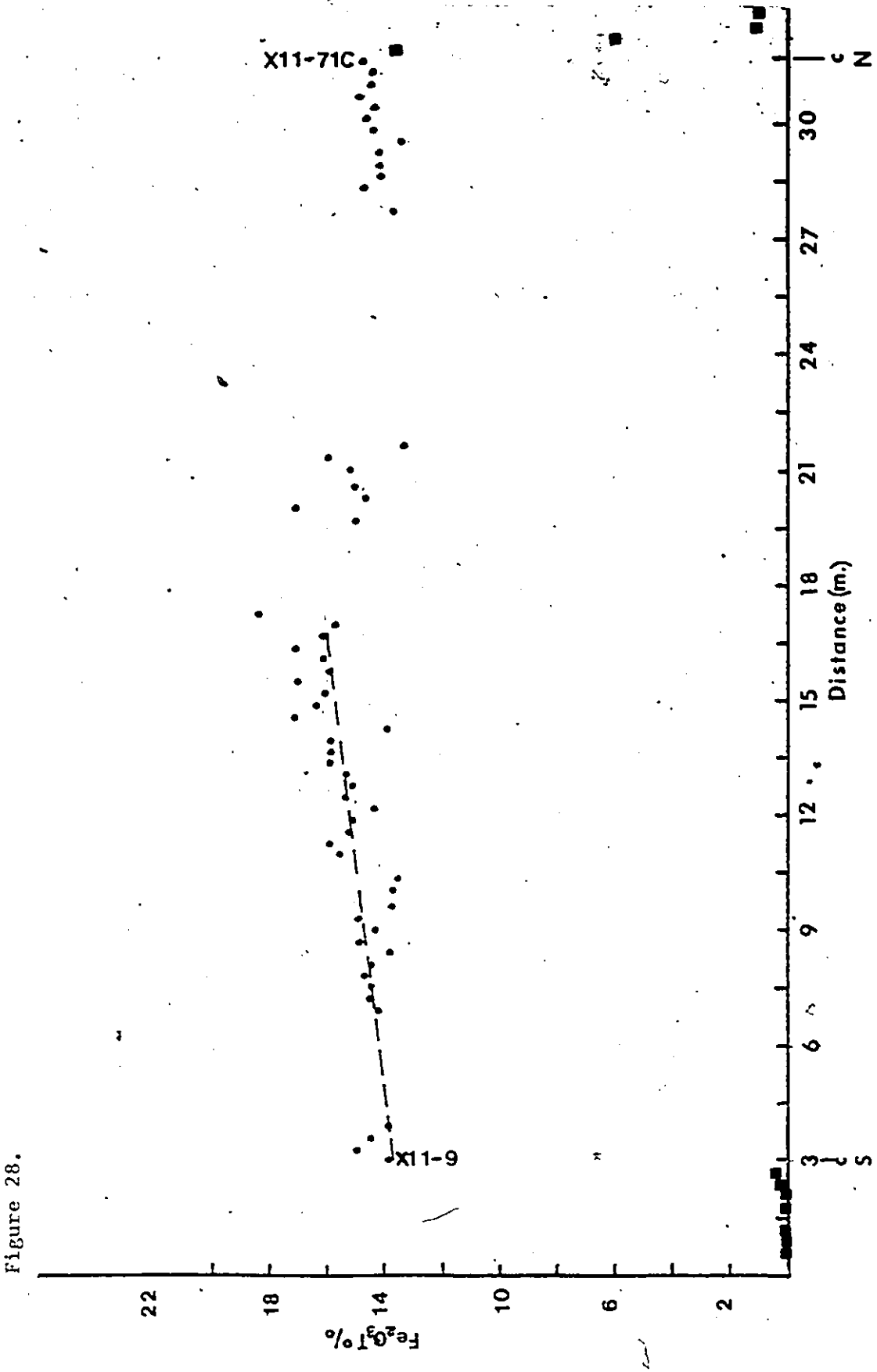
X11-71C
X11-9
S
N
3
6
9
12
15
18
21
24
27
30
Distance (m.)
2
6
10
14
18
22
Fe_2O_3T %

Figure 28.

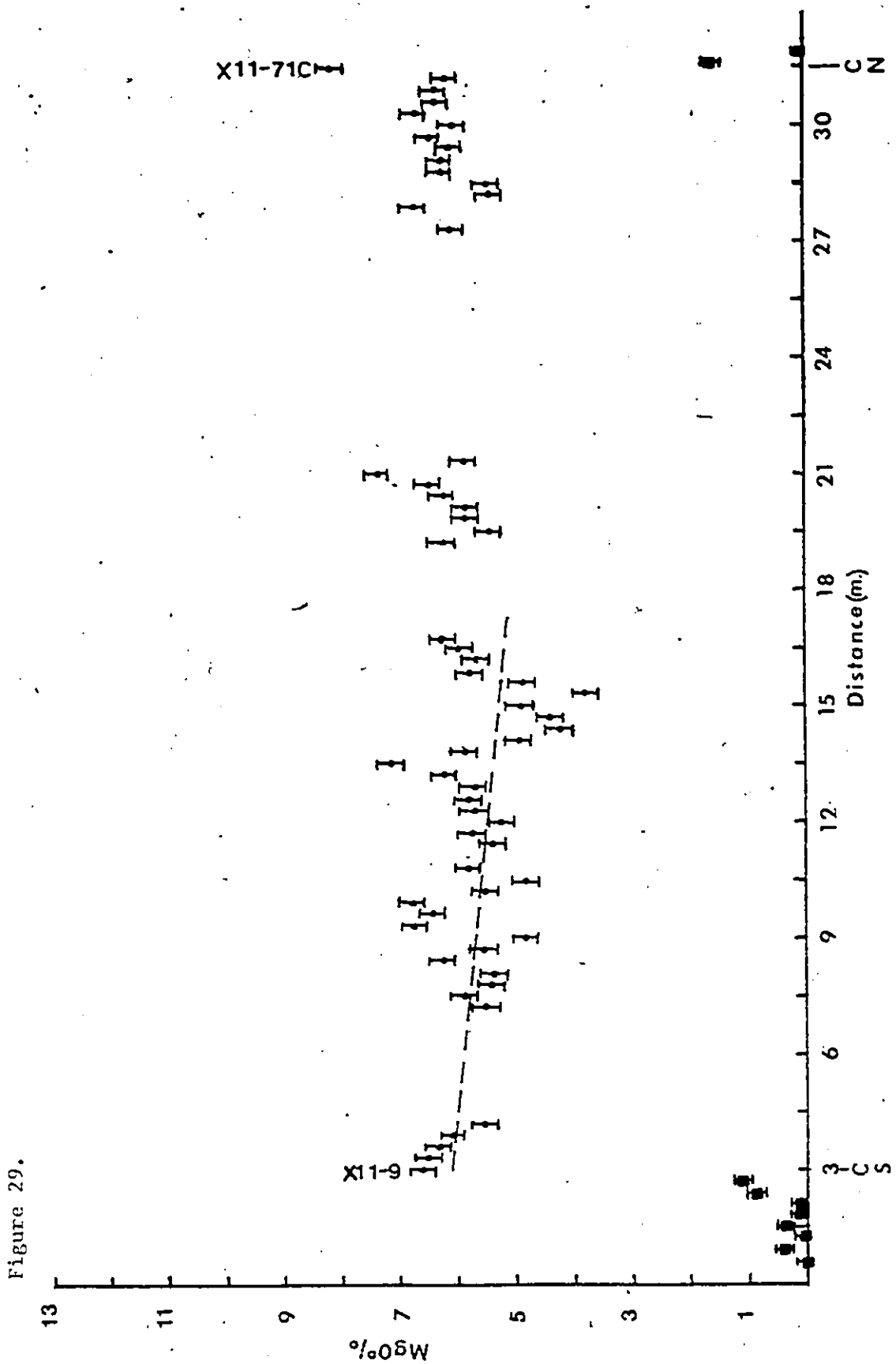
X11-71C
X11-9
Mg0%
13
11
9
7
5
3
1
3
6
9
12
15
18
21
24
27
30
Distance(m.)
C
S
C
N

Figure 29.

Figure 30.

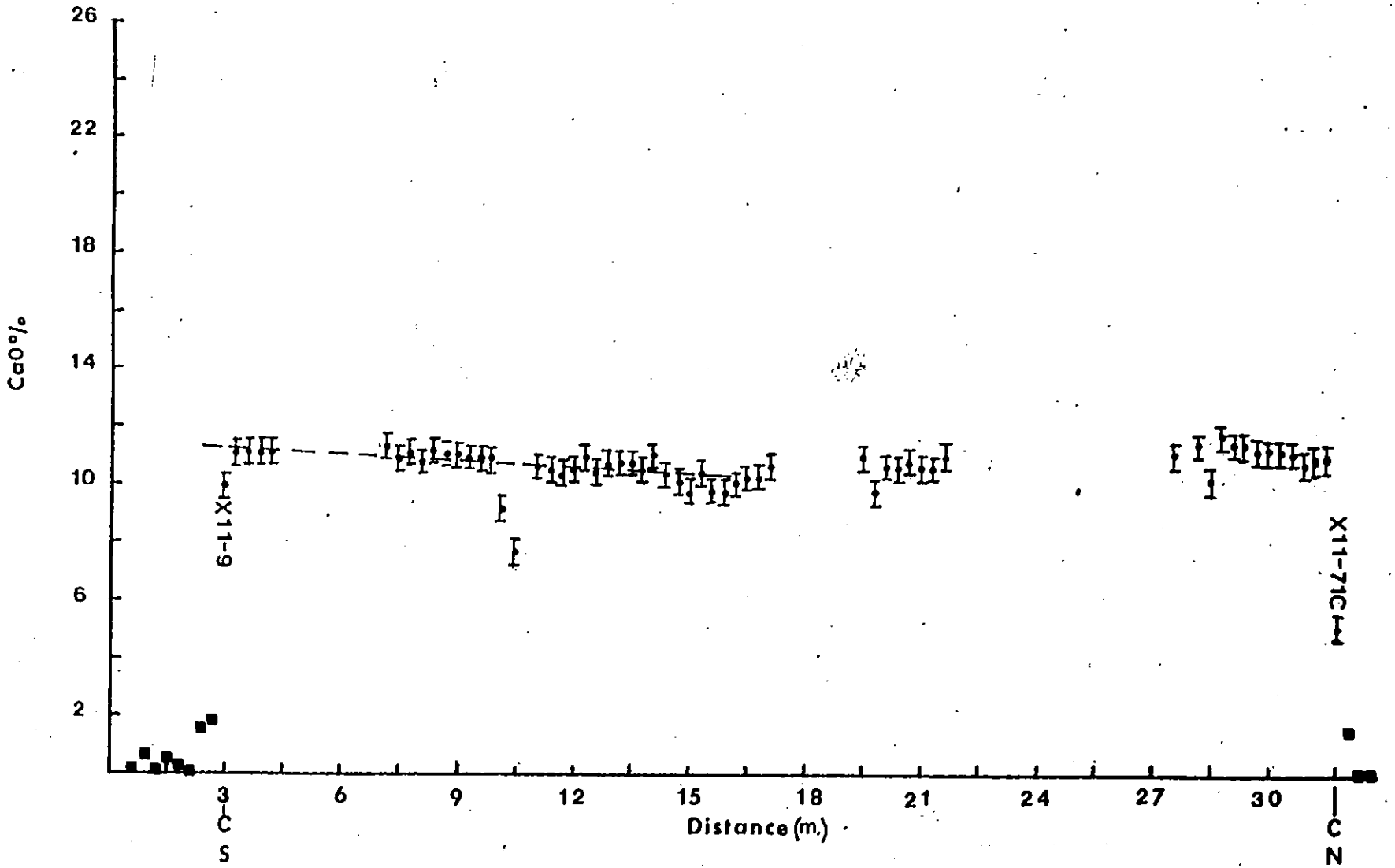
26
22
18
14
10
6
2
CaO%
X11-9
X11-71C
3
6
9
12
15
18
21
24
27
30
Distance (m.)
C
S
C
N

Figure 31.

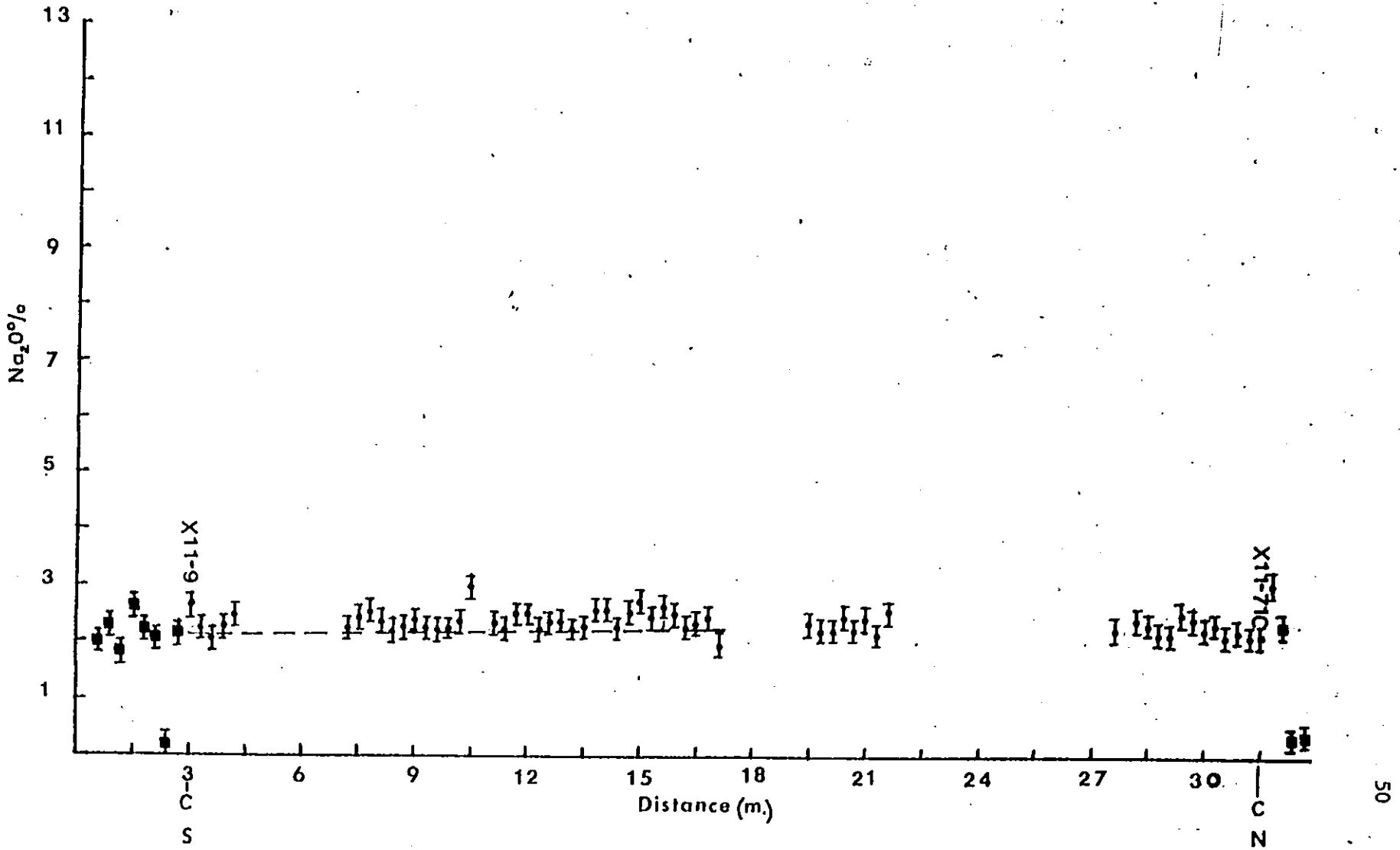
13
11
9
7
5
3
1
Na2O%
X11-9
X11-7
3
6
9
12
15
18
21
24
27
30
Distance (m.)
C
S
C
N

Figure 32.

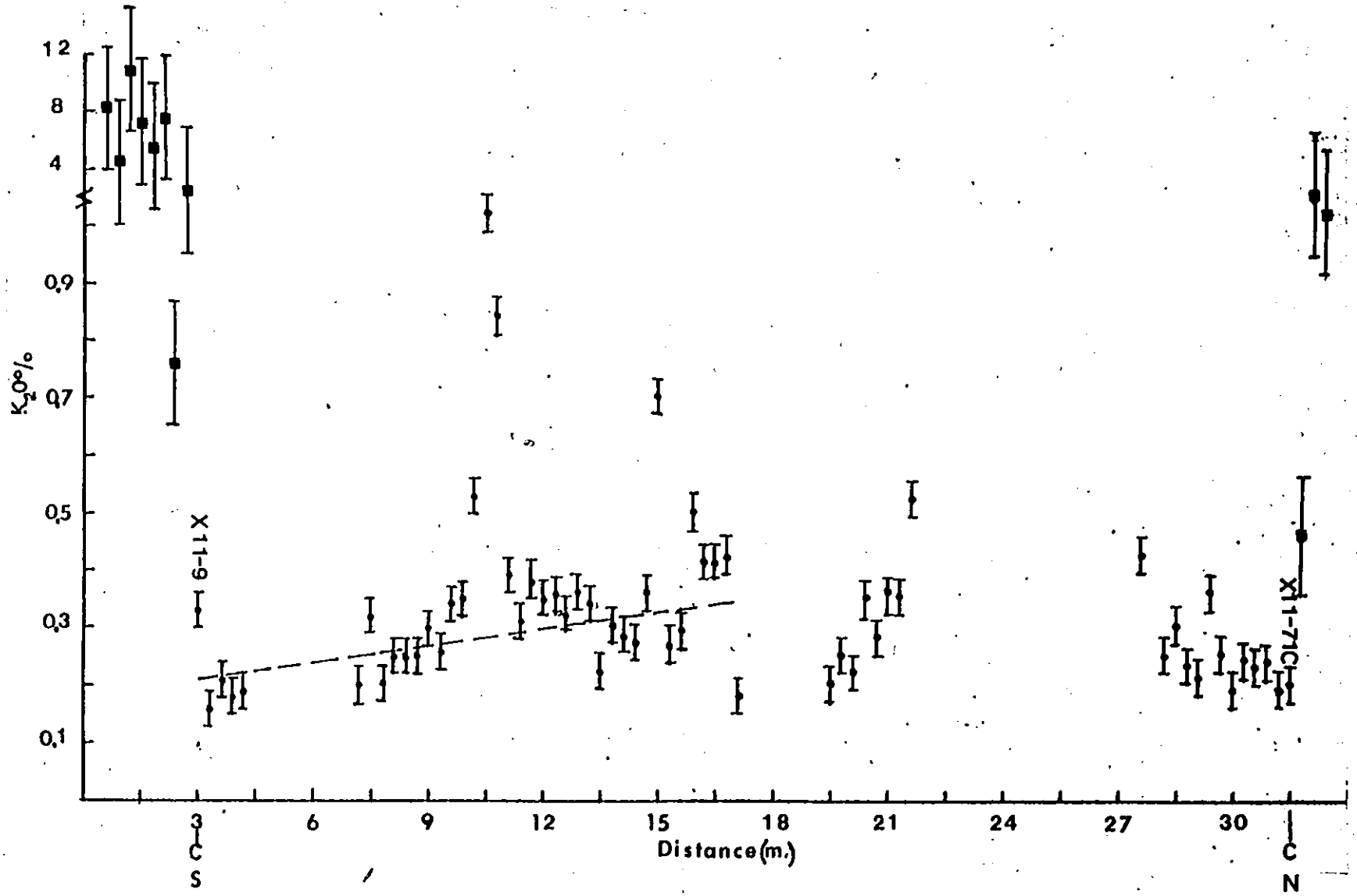
12
8
4
0,9
0,7
0,5
0,3
0,1
K2O%
X11-9
X11-71C
3
6
9
12
15
18
21
24
27
30
C
S
C
N
Distance(m.)

Figure 33.

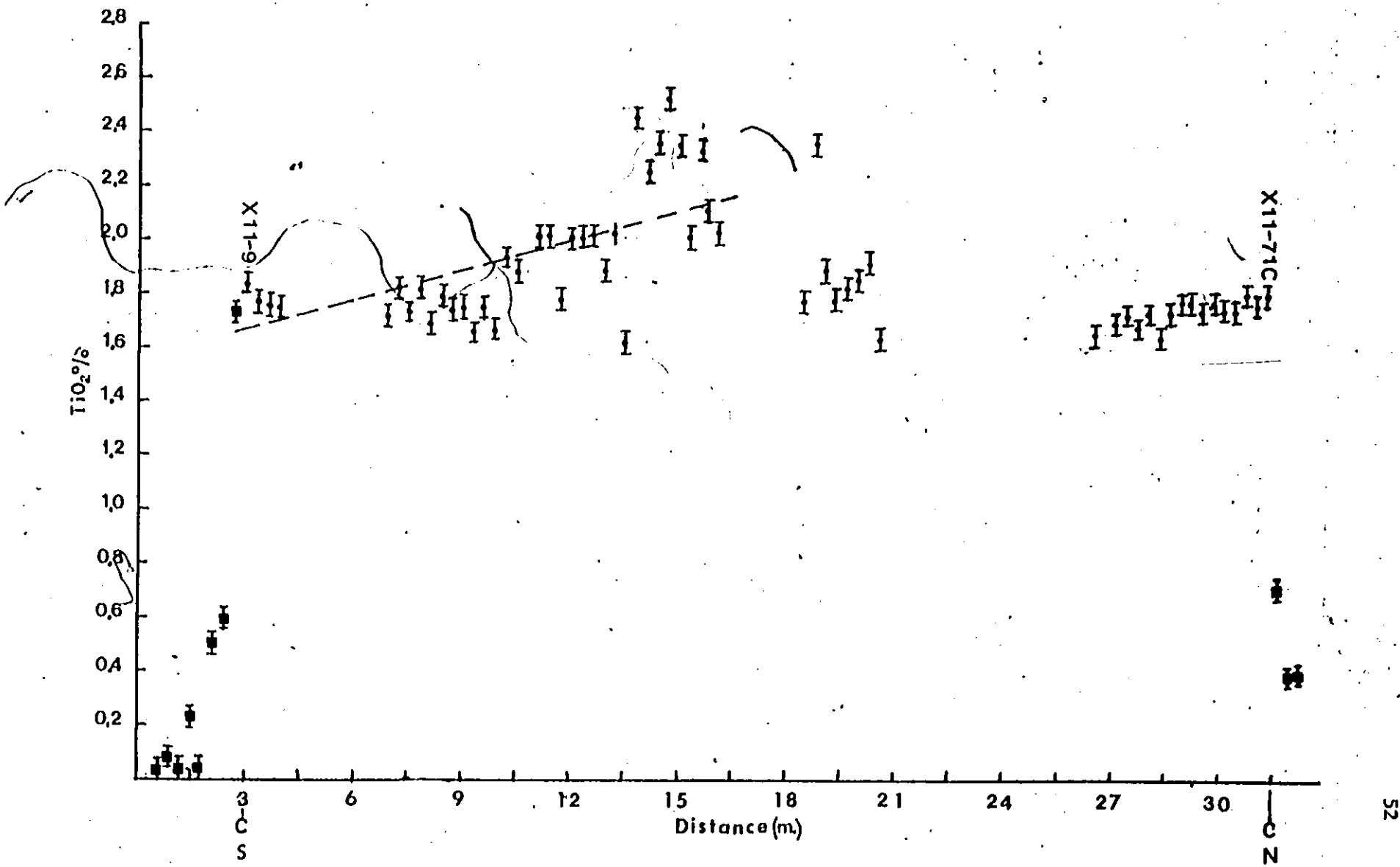
2,8
2,6
2,4
2,2
2,0
1,8
1,6
1,4
1,2
1,0
0,8
0,6
0,4
0,2
TiO2 %
X11-9
X11-71C
3
6
9
12
15
18
21
24
27
30
C
S
Distance (m)
C
N

Figure 34.

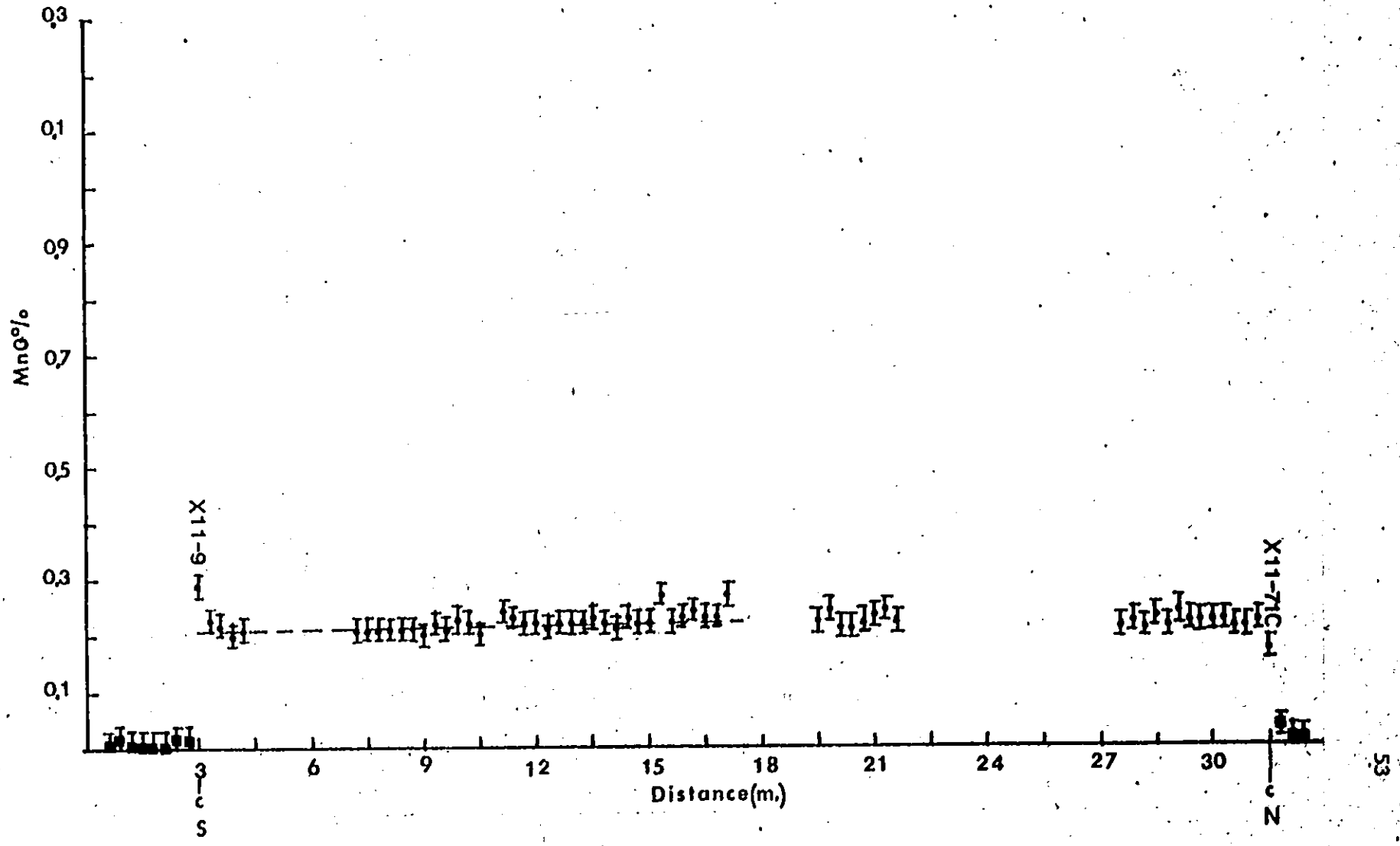
MnO%
0.3
0.1
0.9
0.7
0.5
0.3
0.1
X11-9
X11-7
3
6
9
12
15
18
21
24
27
30
Distance(m.)
S
N

Figure 35.

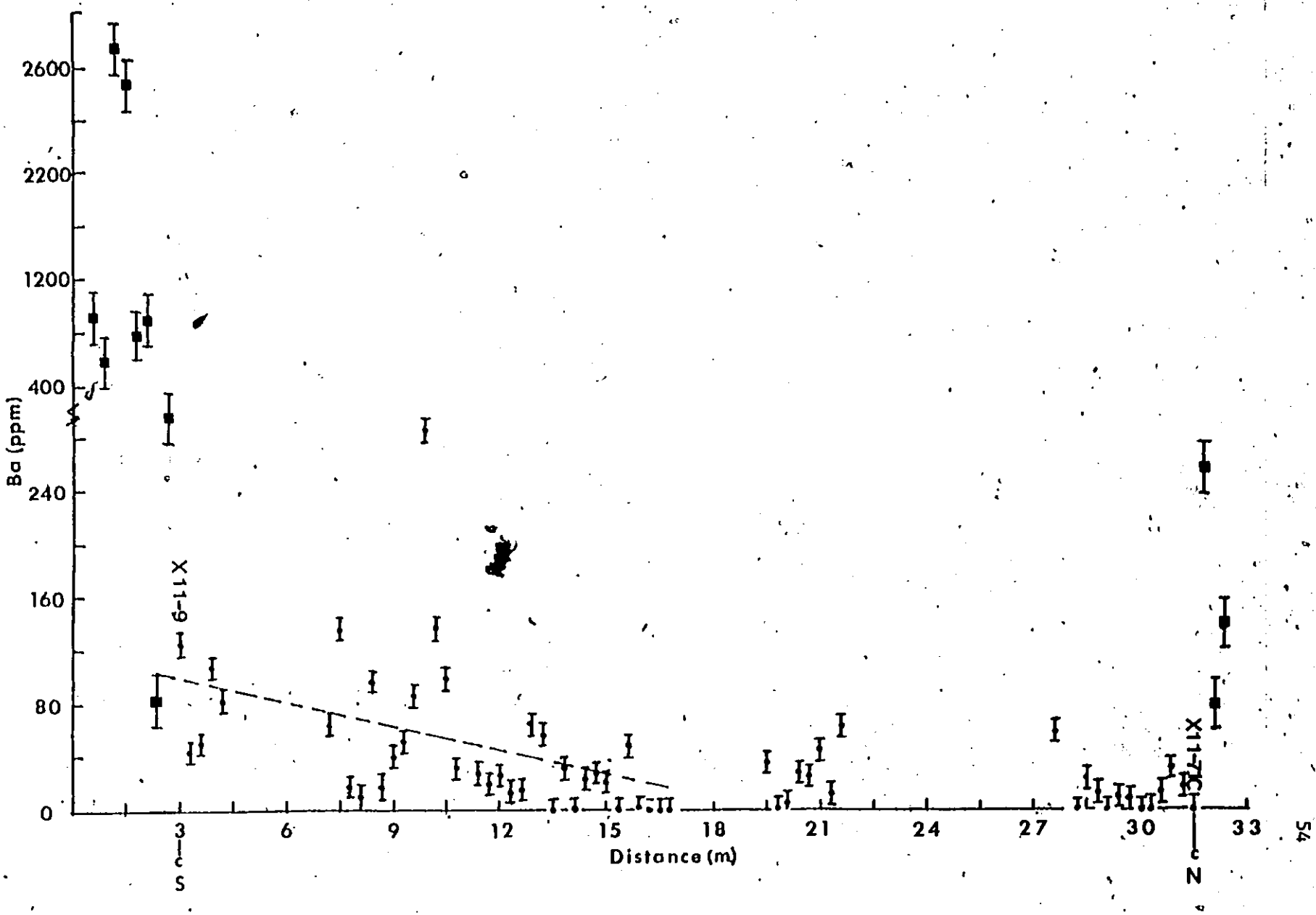
Ba (ppm)
2600
2200
1200
400
240
160
80
0
X11-9
X11-7
3
6
9
12
15
18
21
24
27
30
33
Distance (m)
S
N

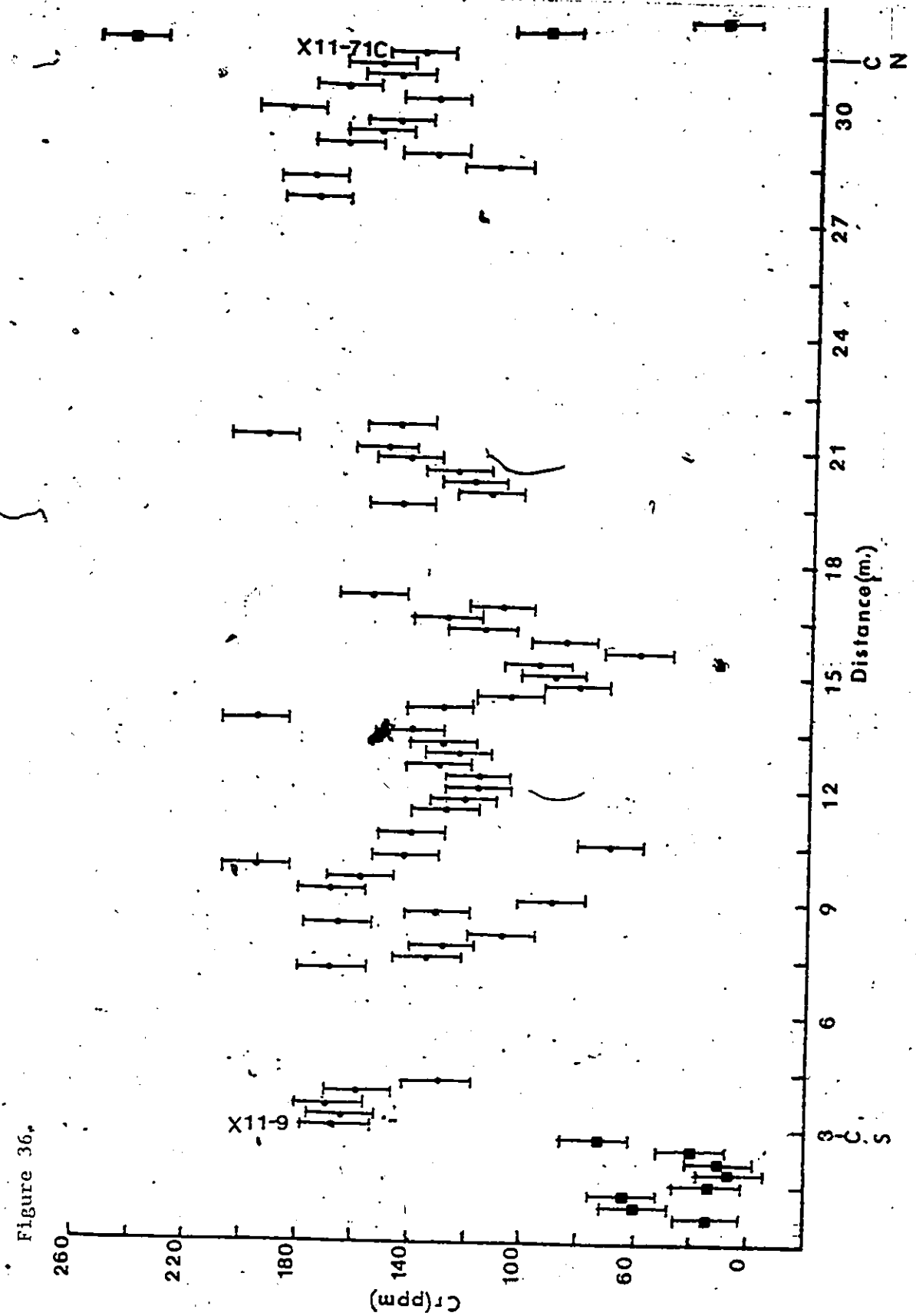
X11-71C
X11-9
C
N
S
3
6
9
12
15
18
21
24
27
30
Distance(m.)
Cr(ppm)
260
220
180
140
100
60
0

Figure 36.

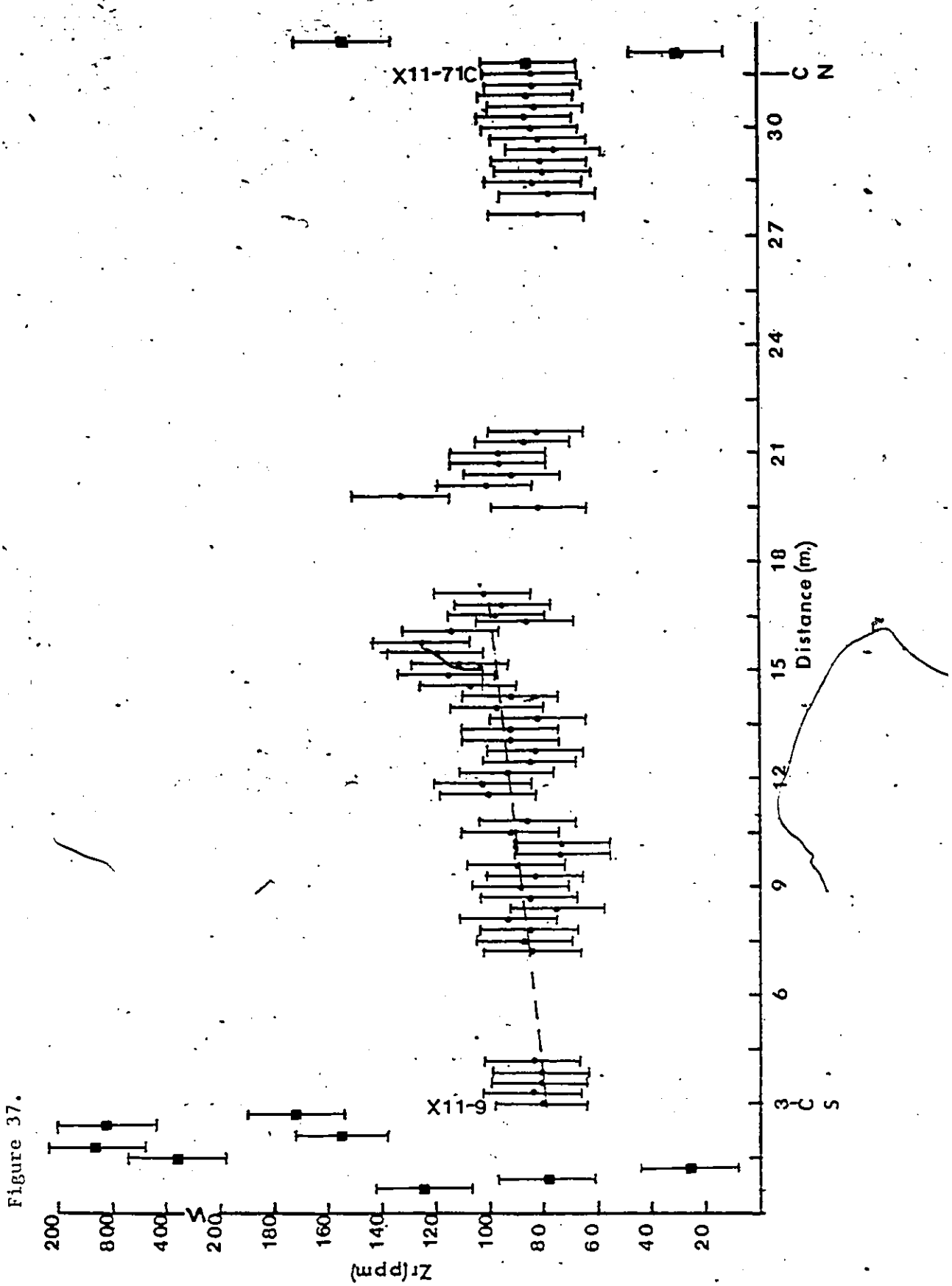
X11-71C
X11-9
C
N
S
Distance (m.)
3
6
9
12
15
18
21
24
27
30
Zr(ppm)
200
800
400
200
180
160
140
120
100
80
60
40
20

Figure 37.

Figure 38.

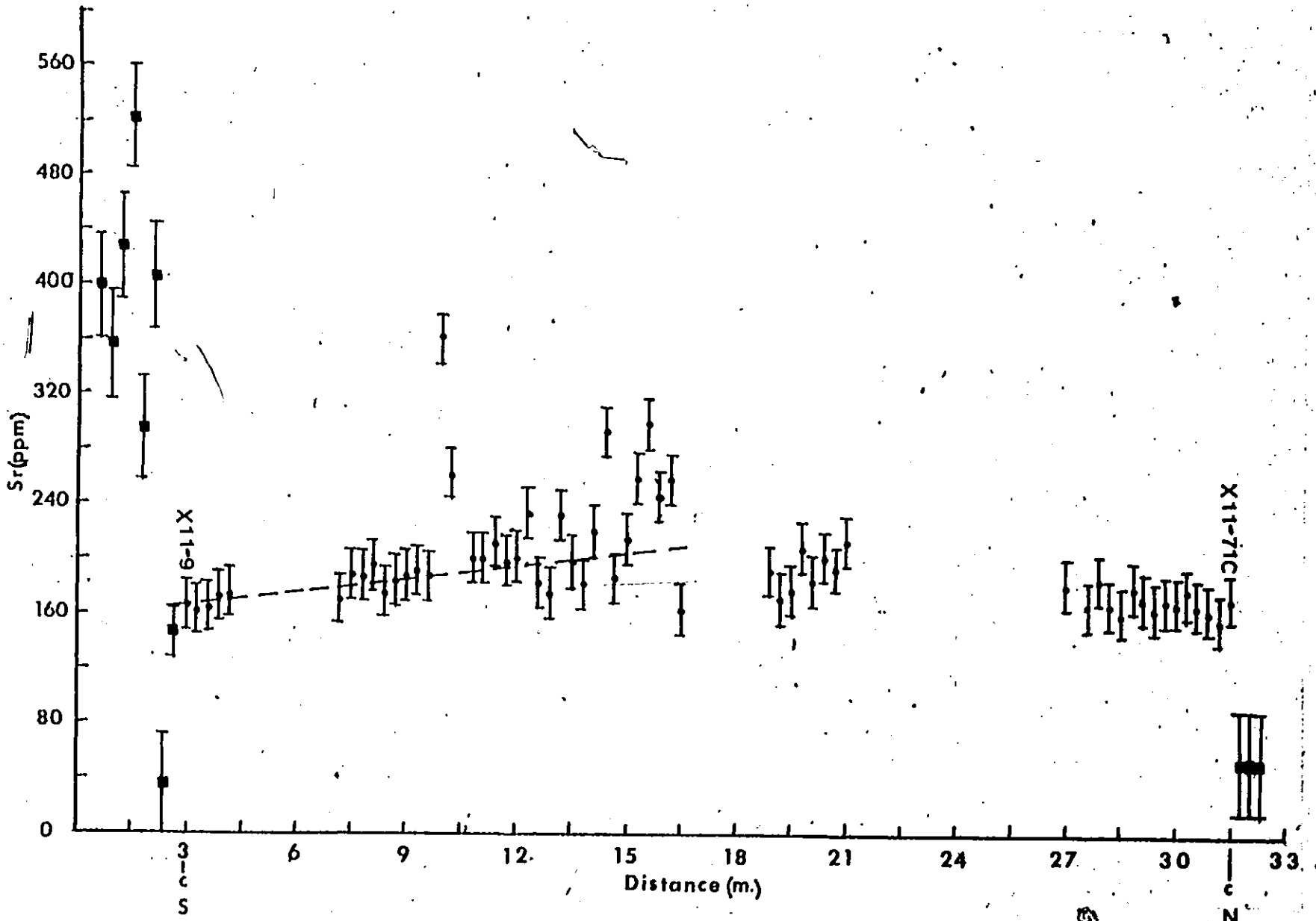
Sr(ppm)
560
480
400
320
240
160
80
0
X11-6
X11-7C
3
6
9
12
15
18
21
24
27
30
33
Distance (m.)
S
N

Figure 39.

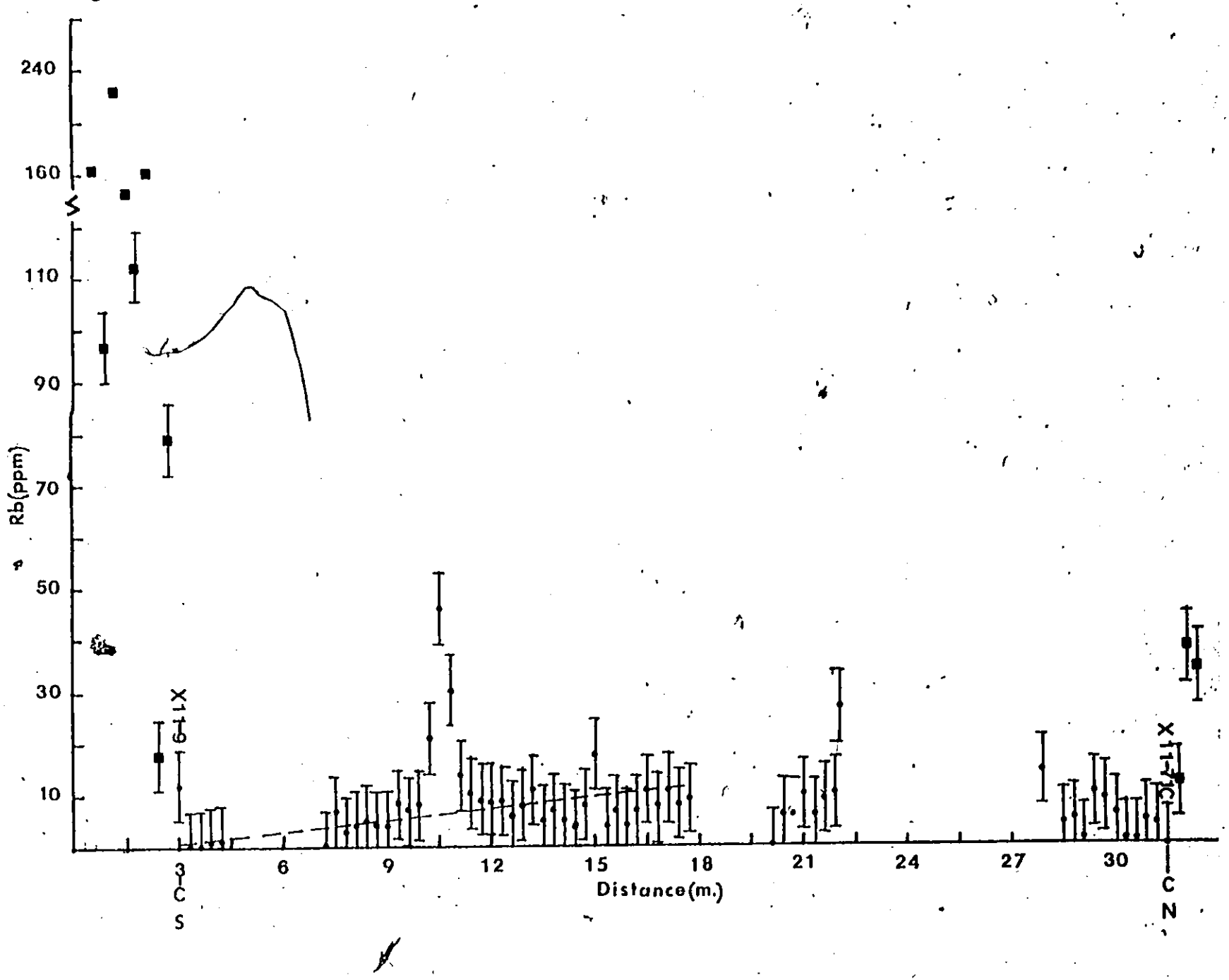
240
160
110
90
70
50
30
10
Rb(ppm)
X1-64
3
6
9
12
15
18
21
24
27
30
Distance(m.)
C
S
X1-4
C
N

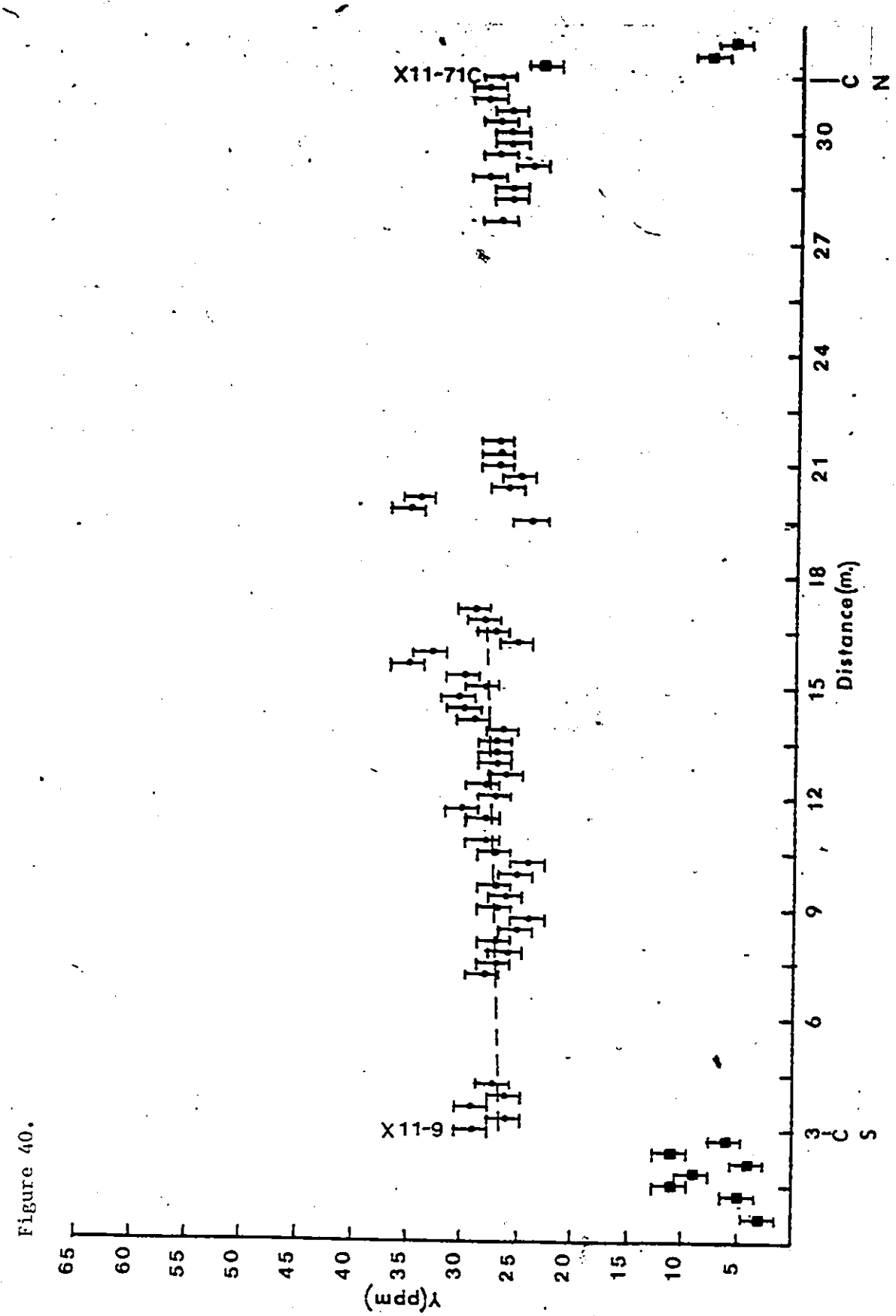

Figure 40.

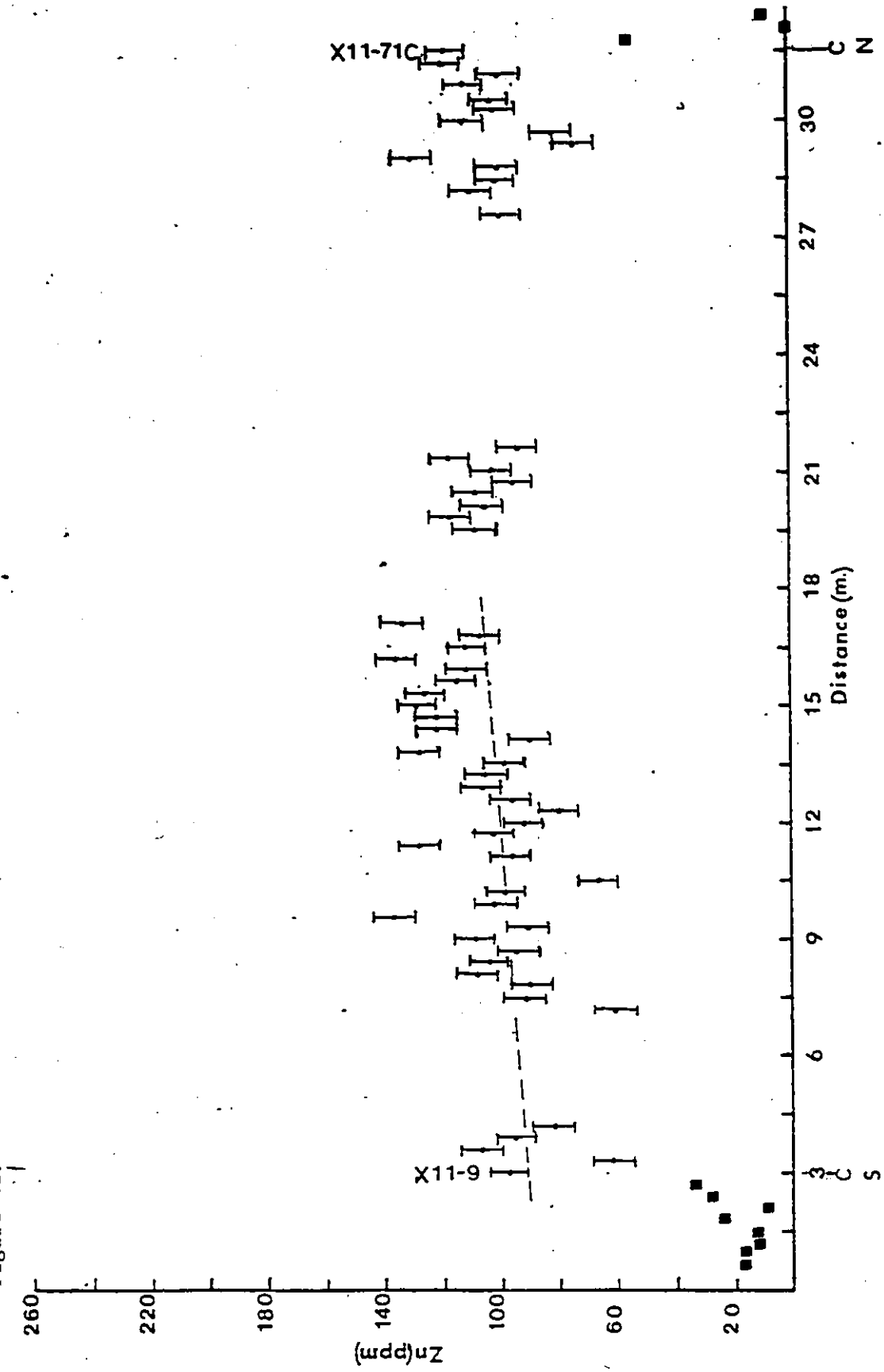
X11-71C
X11-9
Zn(ppm)
260
220
180
140
100
60
20
3
6
9
12
15
18
21
24
27
30
S
N
Distance (m.)

Figure 41.

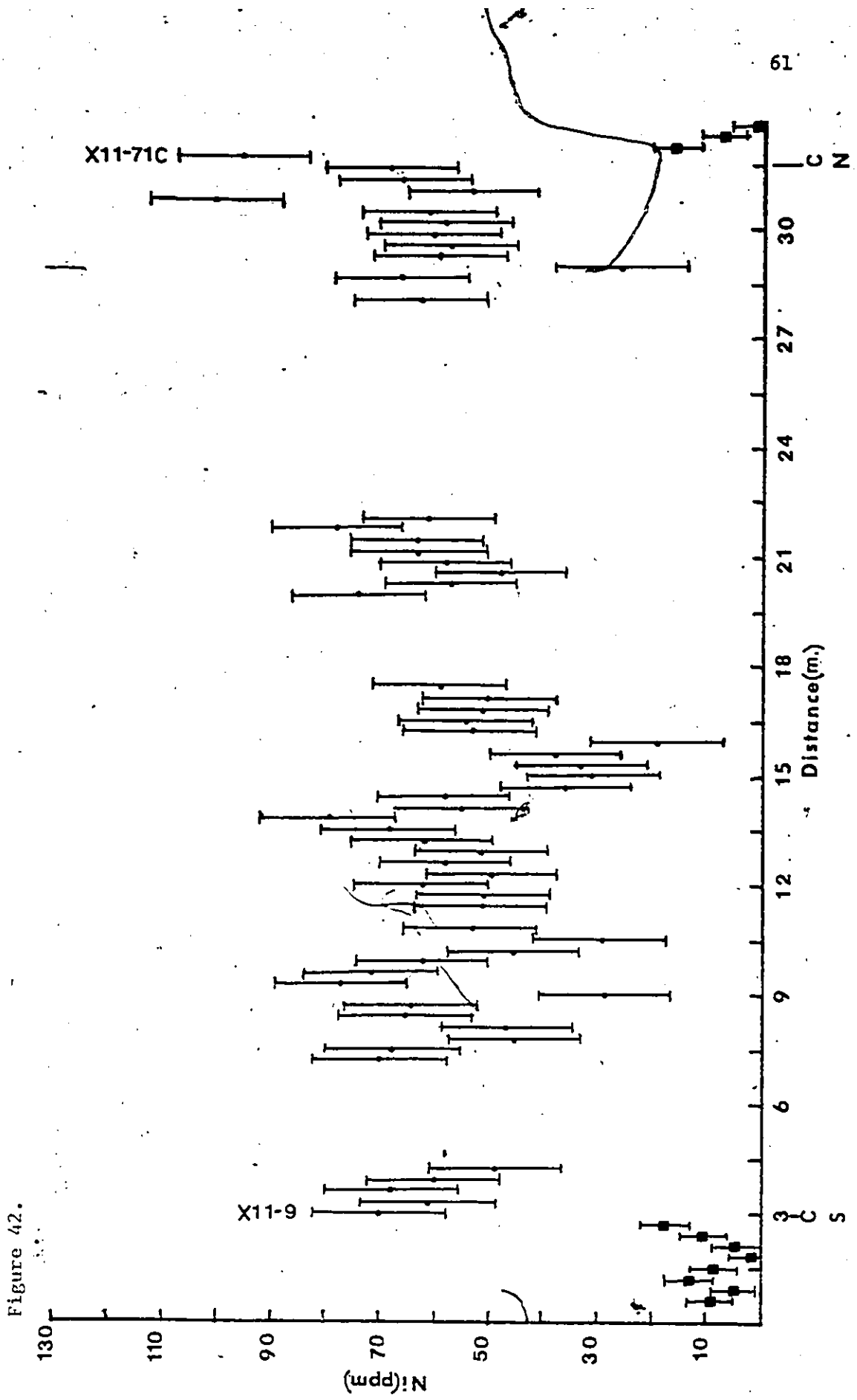
X11-71C
X11-9
C
N
C
S
3
6
9
12
15
18
21
24
27
30
Distance(m.)
10
30
50
70
90
110
130
Ni(ppm)

Figure 42.

The peaks are not recorded in the central portions of the dike, but at 7.5 m from the southern contact.

Another feature, distinguishable from these diagrams, is the scattering of some results. The scatter displayed by each element is represented in Figures 43 to 59 in which the southern half of the dike was seperated into three zones. The scatter of each element was then represented by plotting the lowest and highest recorded values for each zone with the exception of the peak samples. Some elements, such as Si, Al, Ti, K, Cr, Zr, Sr, Rb, Y and Ni, display an increase in scatter from the contact inward whereas Mn and Ba show decreasing scatter inward. In general, the elements that show increasing scatter also increase in concentration from the contact inward. This information implies that the elements which were progressively concentrated in more differentiated late magmas also show increasing scatter.

REE analysed for eight samples from the profile are plotted in Figures 60, 61 and 62 and analytical methods and data are presented in Appendix 2, 3 and 4. From these figures the following observations are made;

1. The diabase samples are from five to thirty times richer in certain REE than the chondritic values.
2. The diabase samples display a slight to moderate light REE enrichment as compared to heavy REE, the degree of light REE enrichment being smaller than that of most continental basalts. This is thought to reflect the lower degree of fractionation for the diabase when compared to most continental basalts.

Figures 43 to 59. Analytical data of the southern half of the St-Pierre dike. Samples displaying large peaks (X11-25 and X11-26) are not included. Contact, intermediate and central zones are equal in width and are represented by eight, eight and ten samples respectively. For zone boundaries refer to Figure 25.

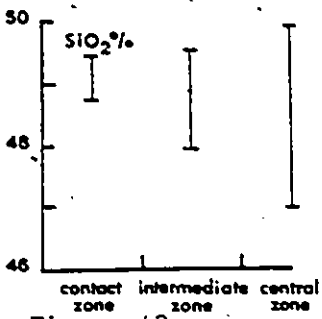

Figure 43.

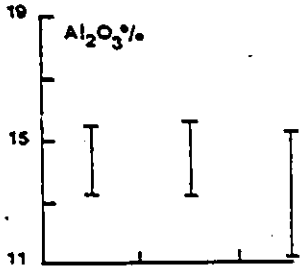

Figure 44.

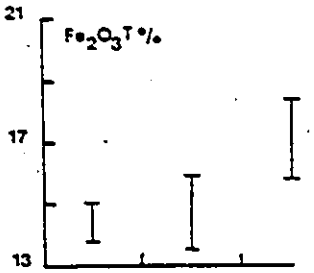

Figure 45.

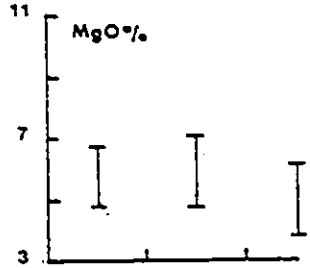

Figure 46.

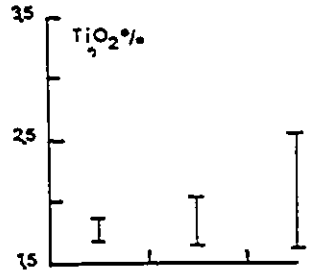

Figure 47.

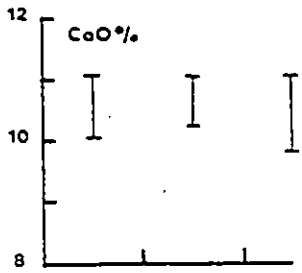

Figure 48.

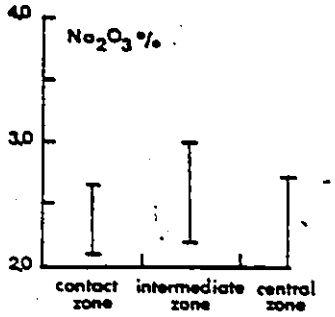

Figure 49.

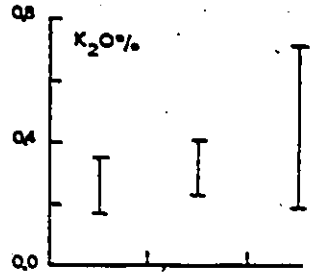

Figure 50.

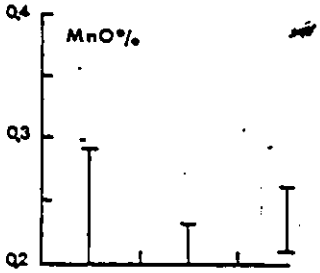

Figure 51.

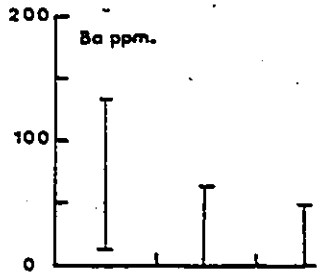

Figure 52.

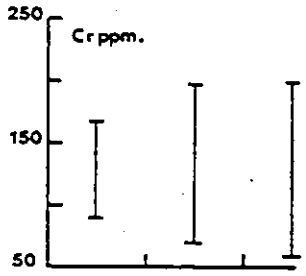

Figure 53.

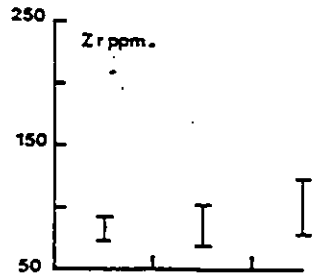

Figure 54.

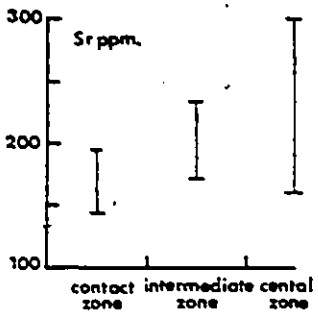

Figure 55.

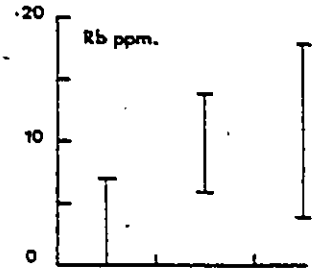

Figure 56.

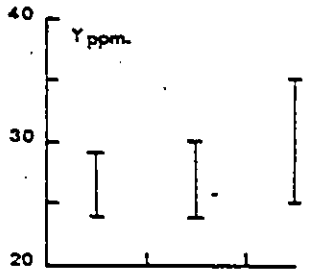

Figure 57.

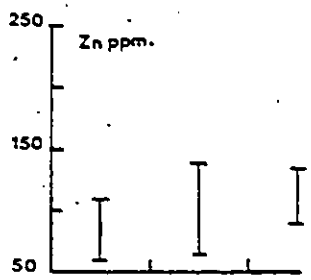

Figure 58.

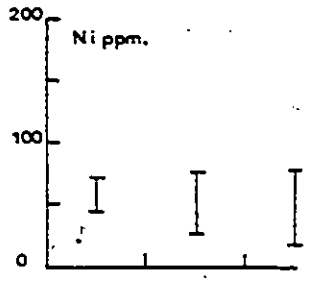

Figure 59.

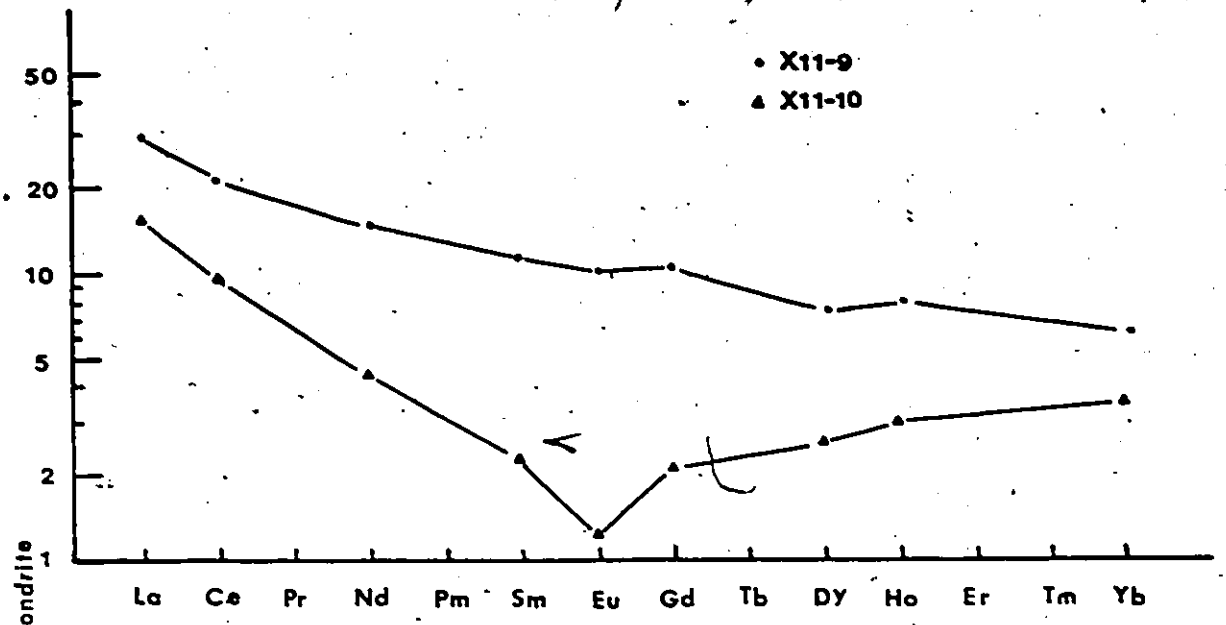

Figure 60. Whole rock REE/chondrite values (for sample location see Fig.25).

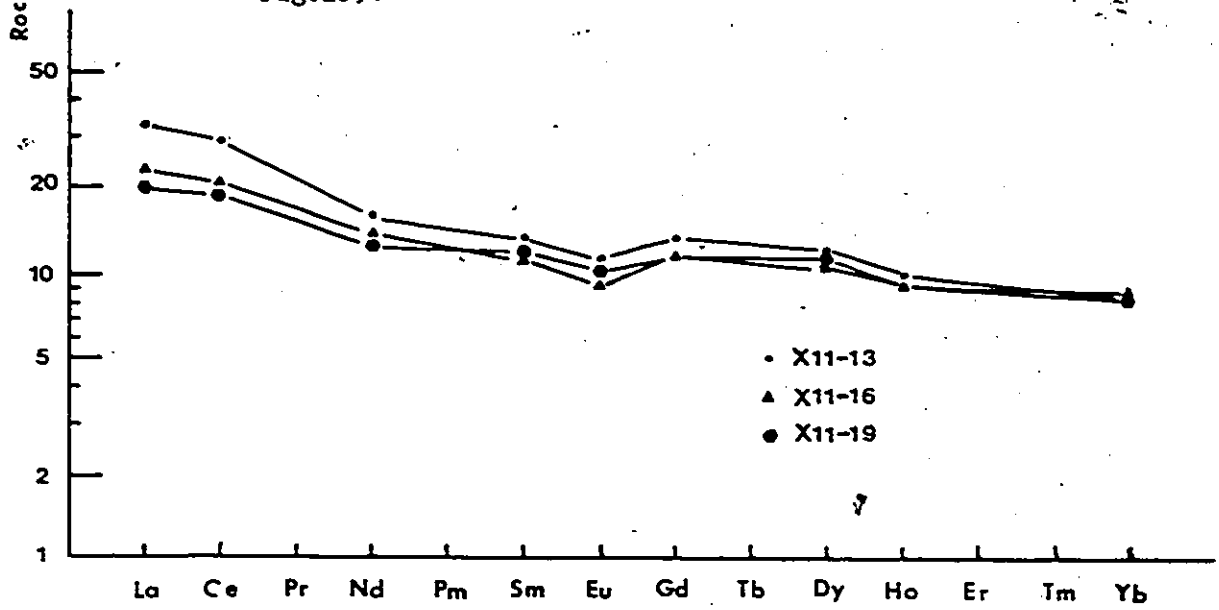

Figure 61. Whole rock REE/chondrite values (for sample location see Fig.25).
X11-9 and X11-10 1ST Pulse
X11-13, 16 and 19 2ND Pulse
X11-25, 26 and 31 3RD Pulse

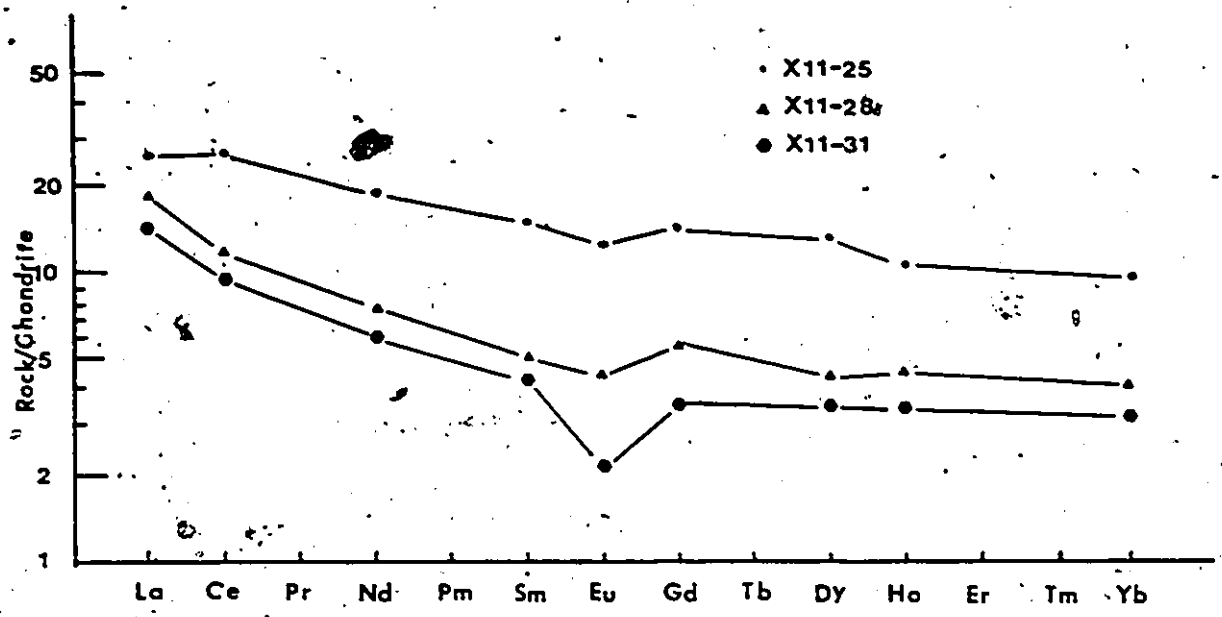

Figure 62. Whole rock REE/chondrite values (for sample location see Fig.25).

3. Slight to moderate negative anomalies are also discernable.

4. In general a slight to moderate decrease in total REE is recorded from the begining to the end of each pulse. This feature comes to light when Samples X11-9 and X11-10 are taken together as representing the second pulse, Samples X11-13, X11-16 and X11-19 as the third pulse and Samples X11-25, X11-26 and X11-31 as the fourth pulse.

The observed REE variations cannot be explained solely by the crystallization of either or all the essential mineral constituents of the diabase. Here two possibilities might have arisen; A: The distribution and the REE variations was regulated by the crystallization of apatite, which has high Kd values for middle REE. The crystallization of a small amount of apatite would cause a decrease in the REE contents (except Eu) of residual liquids since the REE Kd values of apatite are in the 100 range. The small positive Eu anomaly (in the residual liquids) could then have been countered by the crystallization of plagioclase. Although XRF and petrographic studies indicated little to no apatite, this mineral could have been concentrated at a location which was overlooked during the studies. B: The observed REE variations were caused by a fluid phase, possibly rich in REE, which accumulated in the top portion of the magma chamber. No evidence supporting the presence of this fluid phase could be recorded.

When one compares results from the St-Pierre dike and those of the Pageland dike (Steele and Ragland 1976) (see table 2) it becomes evident that both dikes show incrases from dike margin to center in Fe, K, Ti, Zr, Sr, Rb and Zn accompanied by decreases in Al, Mg and

TABLE 2

	1	2
SiO_2	↓?	↑
Al_2O_3	↓	↓
Fe_2O_3T	↑	↑
MgO	↓	↓
CaO	↓	↓
Na_2O	S	↑
K_2O	↑	↑
TiO_2	↑	↑
MnO	S	↑
Ba	↓	
Cr	V	↓
Zr	↑	↑
Sr	↑	↑
Rb	↑	↑
Y	↑	
Zn	↑	↑
Ni	V	↓

General across-strike chemical variations.
1: St-Pierre dike
2: Pageland dike (Steele and Ragland, 1976)
↑ increase from contact inwards
↓ decrease from contact inwards
? possible variation
S stable
V variable

Ca. Additional variations such as increases in Si, Na and Mn, and decreases in Cr and Ni, described for the Pageland dike, were not observed across the St-Pierre dike. Since both dikes display similar general trends, they must therefore have had similar differentiation histories. Steele and Ragland (1976) have attributed the Pageland chemical variations to in situ fractionation of the diabasic magma accompanied by a two pulse mode of emplacement.

Not all chemical variations across the St-Pierre dike can be explained solely by in situ fractionation. A second process involving a slow differentiation at the source, so as to create a poorly zoned magma chamber, may have been active.

Evidence of zoned magma chambers is rare. An example is the Shamsan caldera sequence of Aden, where the first erupted lavas originated from the upper differentiated portions of the magma chamber, whereas the last eruption represented less differentiated lower portions of the magma chamber (Cox, Bell and Pankhurst, 1979).

Chemical variations along strike of the St-Pierre dike are presented in Figures 63 to 72 together with the maximum and minimum chemical values recorded at the natural cross-section. Since the chemical changes along strike vary between these maxima and minima, any subtle variation along strike may be the result of chance and lack of samples. For this reason, only the major changes will be discussed.

In the central portion of the study area, the St-Pierre dike crosses a marble-rich zone, flanked by two gneiss-rich areas. On Figures 63 to 72, the marble area is marked by a low in the diabase Ba, K, Sr and Rb contents. Here two possibilities can be considered. The decreases may

Figures 63 to 72. Chemical variations along strike of the St-Pierre dike. Vertical bars on the right hand side of the diagrams give chemical variations recorded at the cross-section.

I Error bars (95% confidence limits)

● Samples collected 0 m to 10 m north of the southern contact

o Samples collected 10 m to 20 m north of the southern contact

△ Samples collected 20 m to 30 m north of the southern contact

□ Samples collected at more than 30 m north of the southern contact

Figure 63.

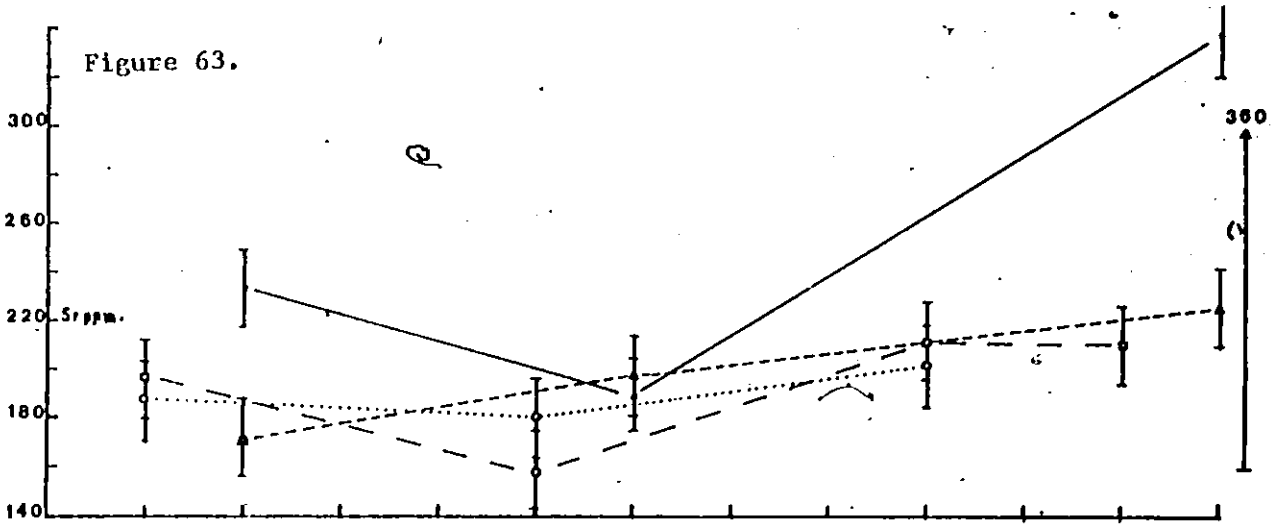

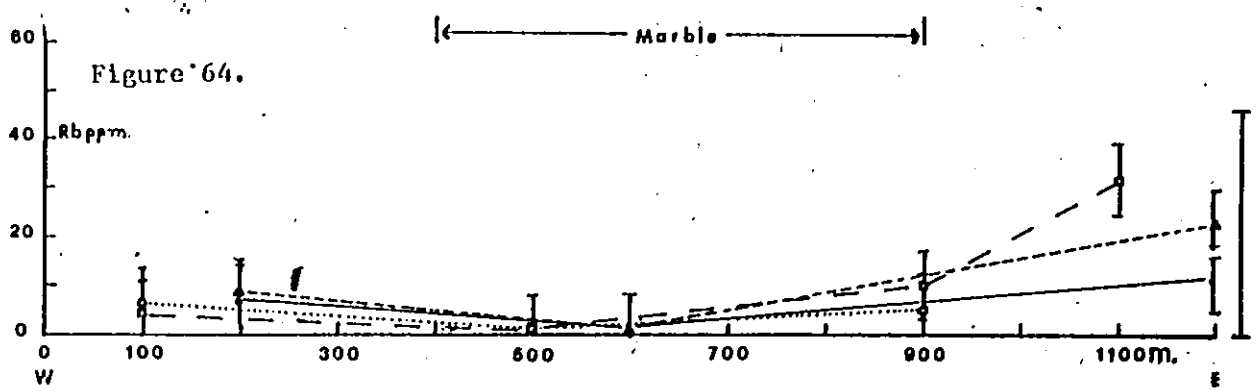

Figure 64.

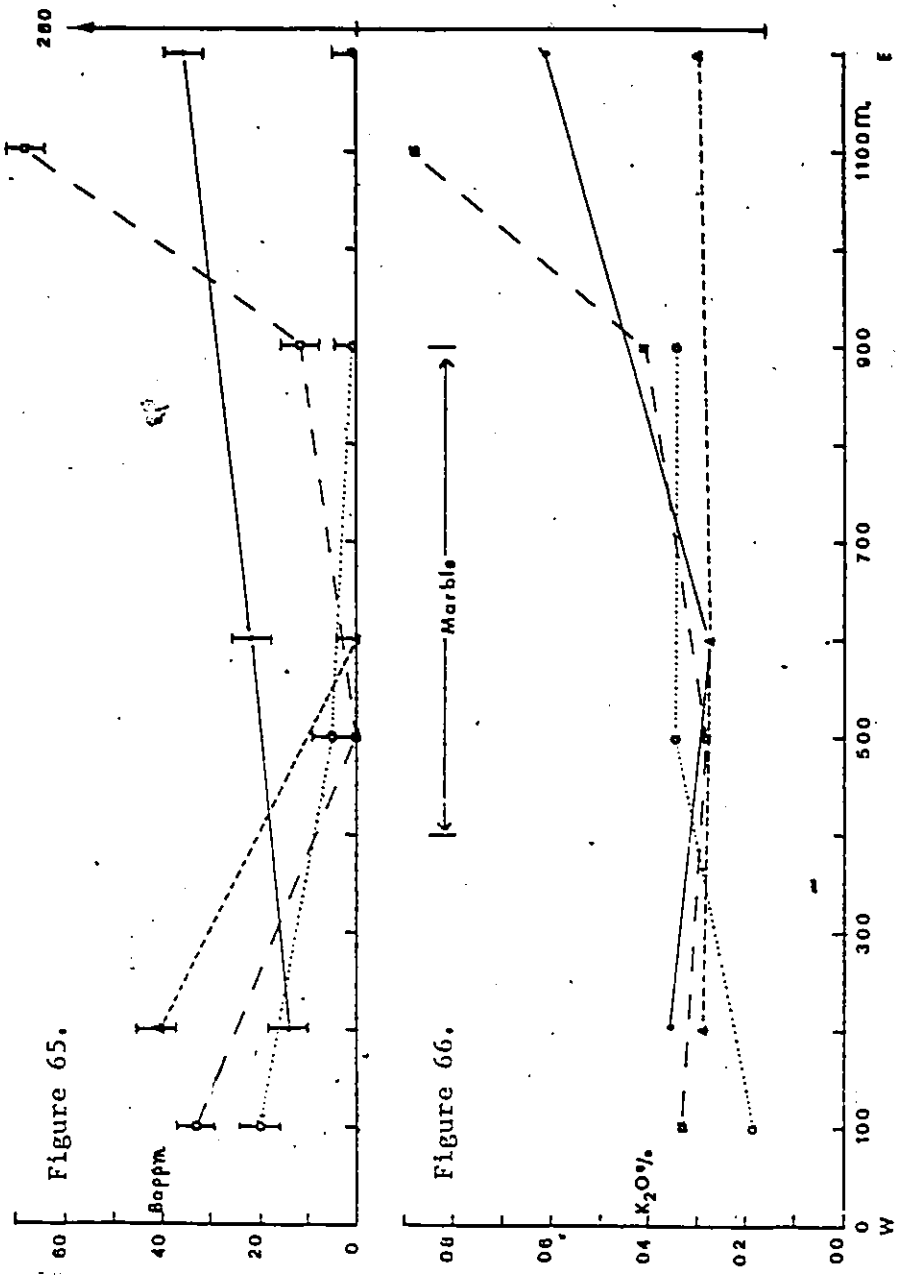
Figure 65.
Ba ppm
60
40
20
0
Figure 66.
Marble
$K_2O\%$
08
06
04
02
00
W
0
100
300
500
700
900
1100m
E

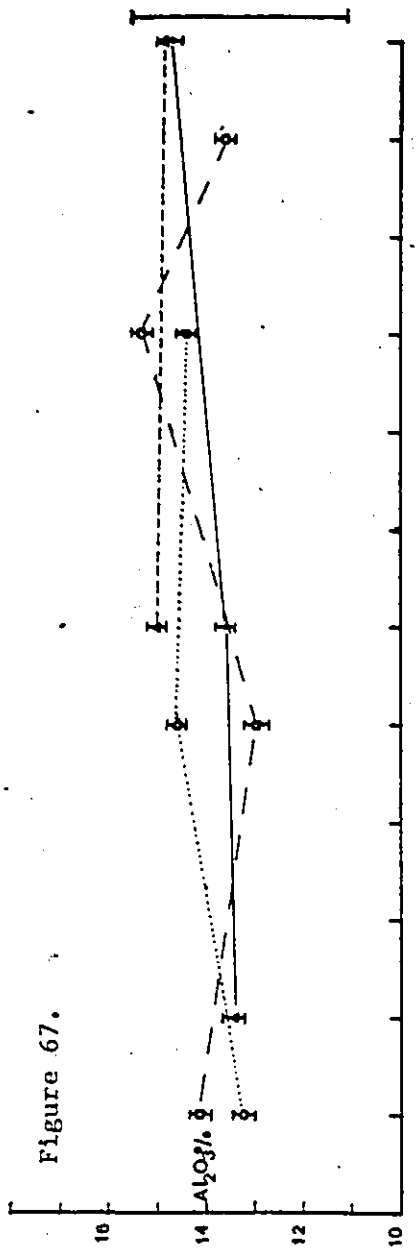

Figure 67.

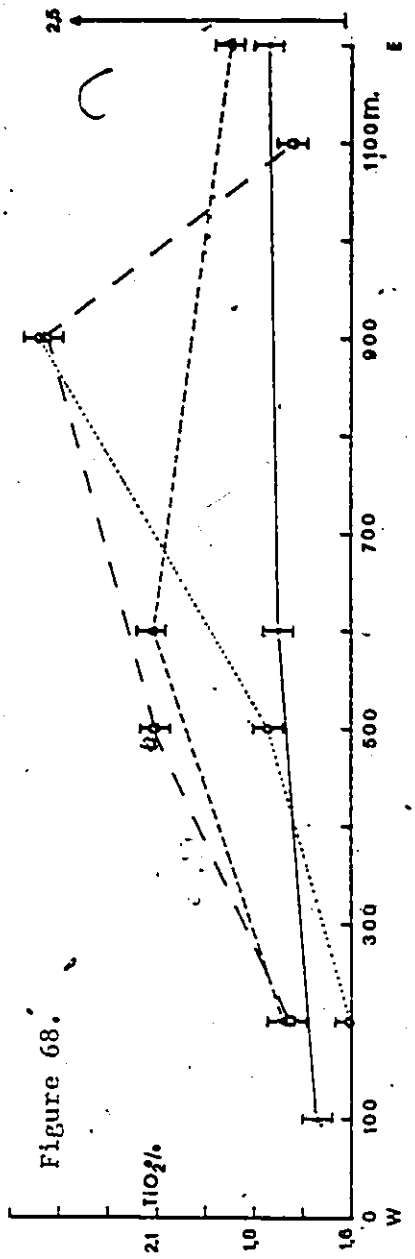

Figure 68.

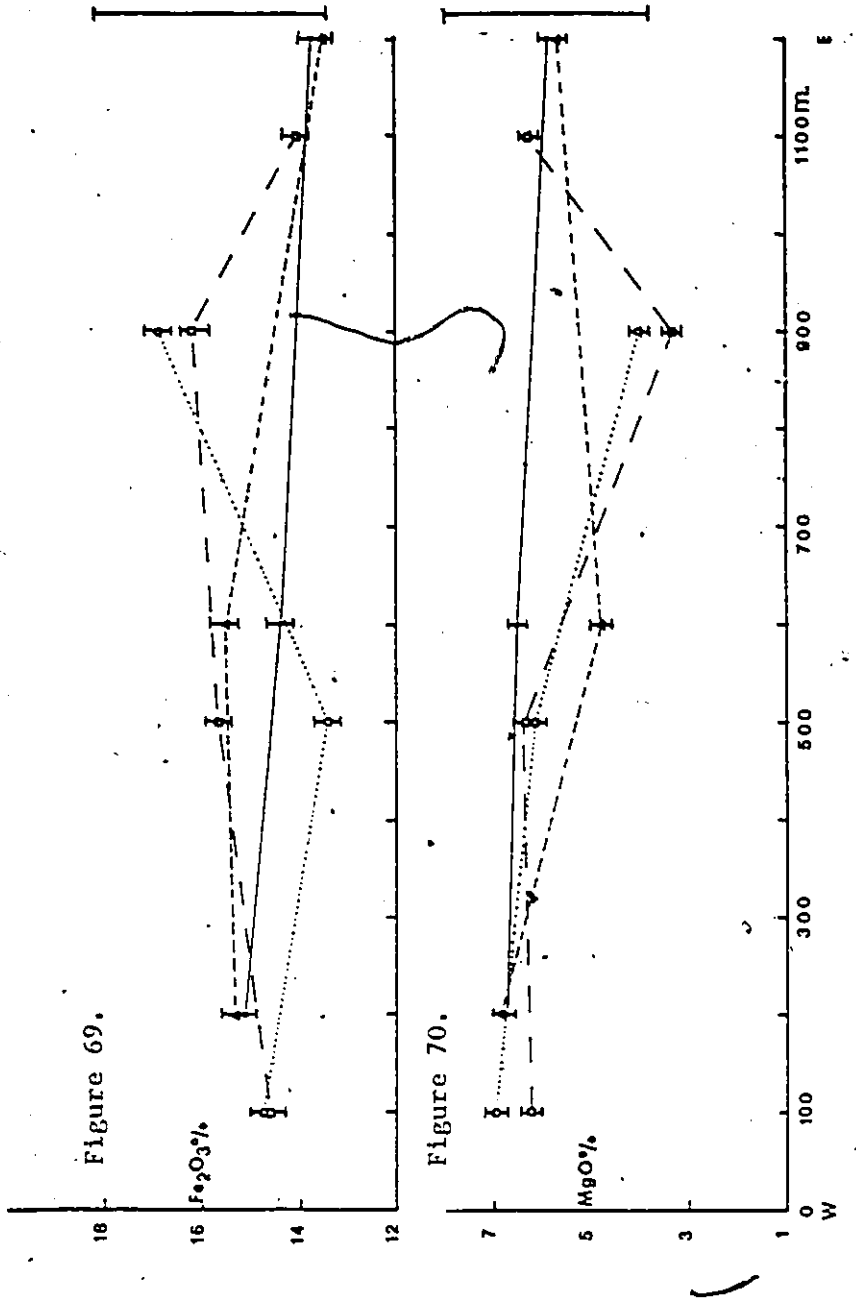

Figure 69.

Figure 70.

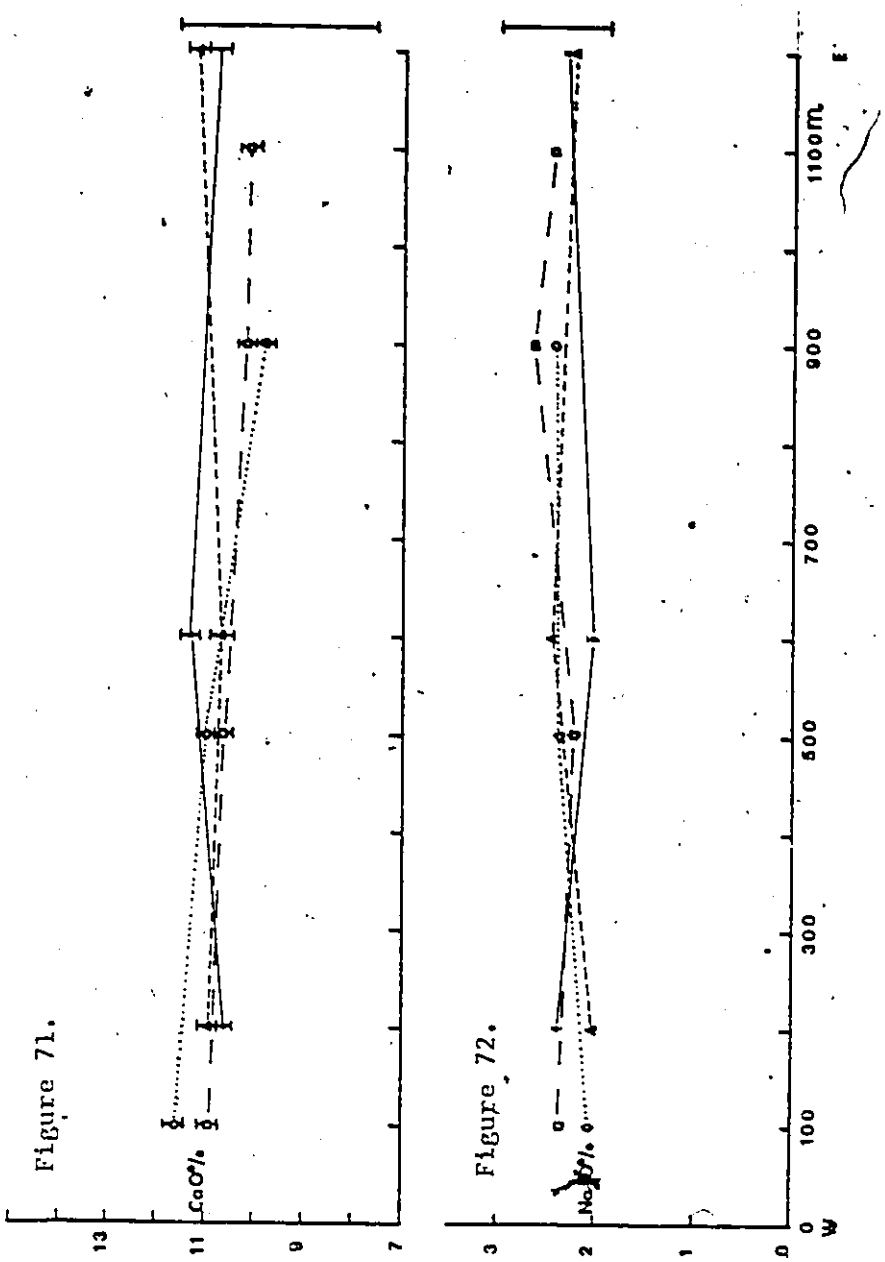

Figure 71.

Figure 72.

result from the selective removal of the elements by minerals present in the marble or be due to a lack of availability of the elements in the wallrock. Since no evidence supporting either one of these proposals could be obtained, no conclusion can be deduced to explain the chemical variations along strike.

CIPW Norm and Differentiation Index

Norm values are presented in Appendix 2. From these values, it is evident that the St-Pierre dike is quartz normative except for Samples B, D and X11-71c, from the southern and northern contact, and X11-25 from the first portion of the fourth pulse. Table 3 gives the differentiation indices of samples from the southern half of the dike. When this half is separated into three portions and the mean of differentiation indices calculated, it is then apparent that the studied dike becomes slightly more differentiated toward the center.

Element Correlations

Variation diagrams used to evaluate element-element variations are presented in Figure 73 to 85 and the corresponding correlation coefficients and regression equations are given in Table 4. From these diagrams, only a few elements such as Zr, K, Y, Sr and Rb thought to be "incompatible", show good correlation throughout the dike with no strict preference to sample location. In other words, the least differentiated samples, such as those from the contact zones, do not plot respectively at one or the other end of the regression lines but show a tendency toward a concentration at these locations. This masking of

TABLE 3

	D.I.	Mean D.I.
X11-9	25.21	
X11-10	22.45	
X11-11	22.53	
X11-12	23.41	23.87
X11-13	25.20	
X11-14	22.23	
X11-15	24.54	
X11-16	25 45	
X11-17	25.04	
X11-18	22.50	
X11-19	24.12	
X11-20	25.60	23.91
X11-21	22.20	
X11-22	23.66	
X11-23	22.10	
X11-24	25.39*	
X11-25	32.66*	
X11-26	33.29*	
X11-28	24.90	
X11-29	23.83	
X11-30	21.01	24.10
X11-31	25.75	
X11-32	24.53	
X11-33	24.16	
X11-34	24.60	
X11-35	23.68	

? D.I.values for samples collected in the southern half of the St-Pierre dike. This dike portion is separated in three segments of equal length. Mean D.I. values are given for each segment.

*: sample not taken into consideration.

Figures 73 to 85: Element-element variation diagrams.

- ● Samples from the southern contact zone
- ○ Samples from the northern contact zone
- ▲ Samples from the intermediate zone, southern half
- △ Samples from the intermediate zone, northern half
- ■ Samples from the central zone, southern half
- □ Samples from the central zone, northern half.

For zone boundaries refer to Figure 25.

Figure 73.

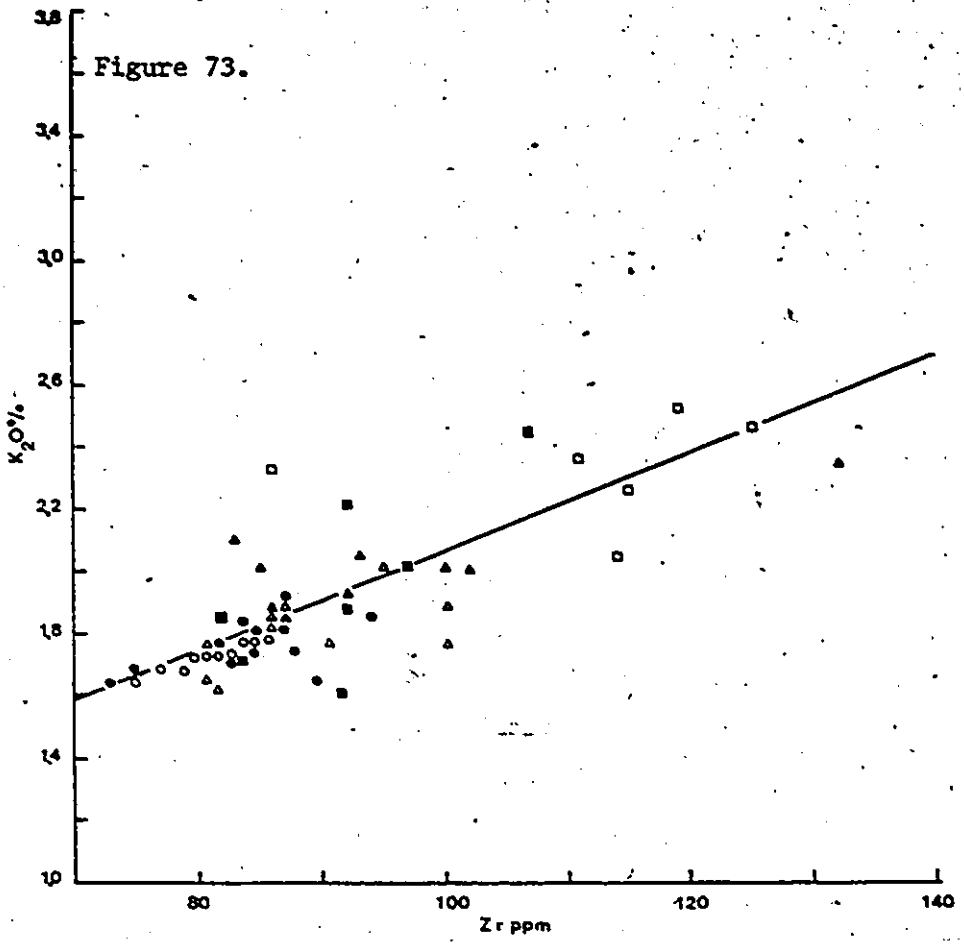

Figure 74.

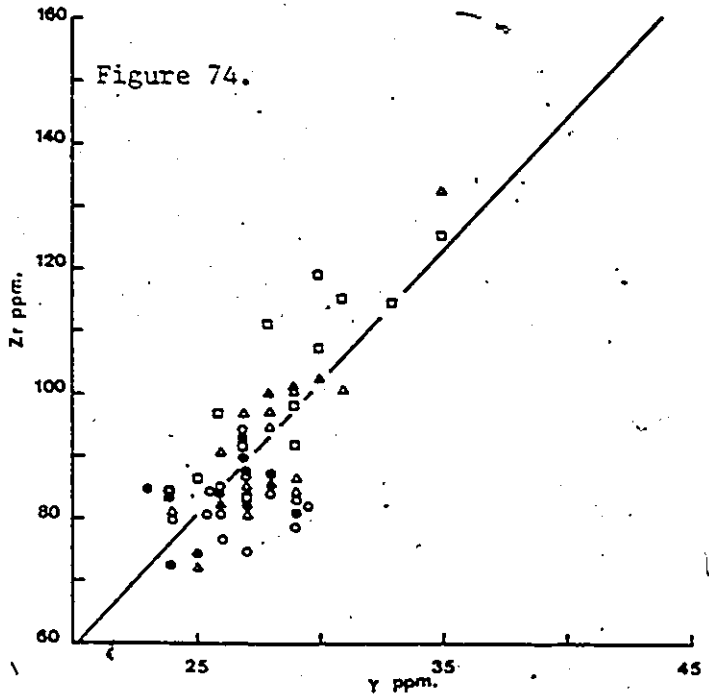

Figure 75.

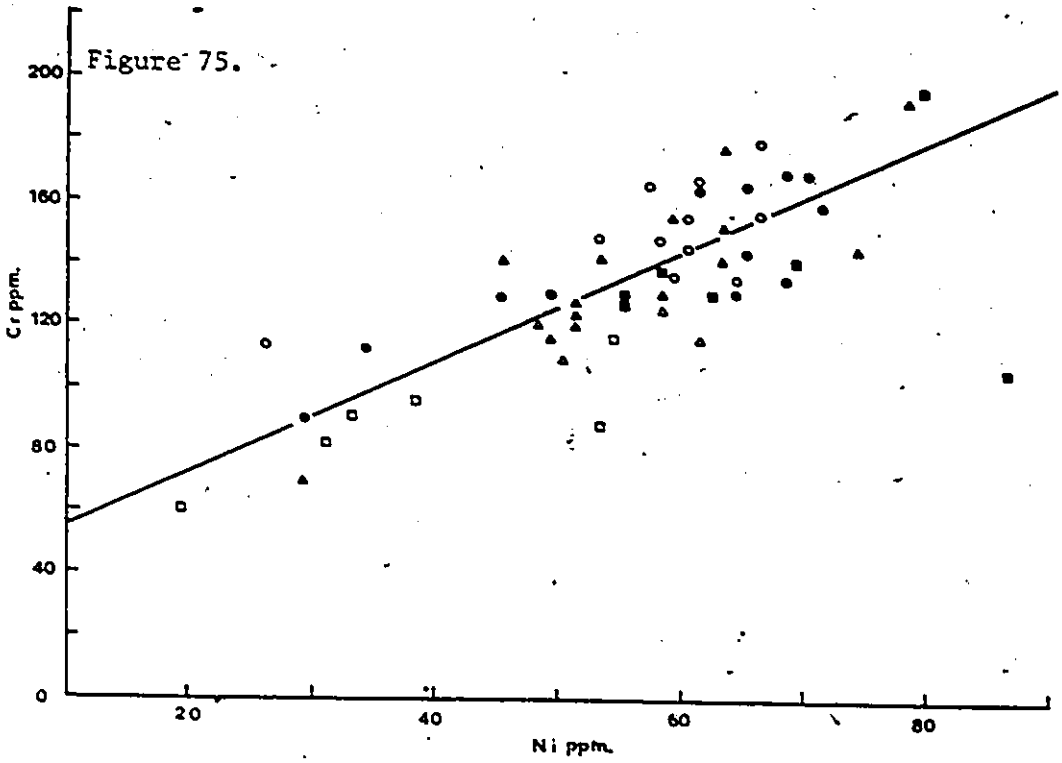

Figure 76.

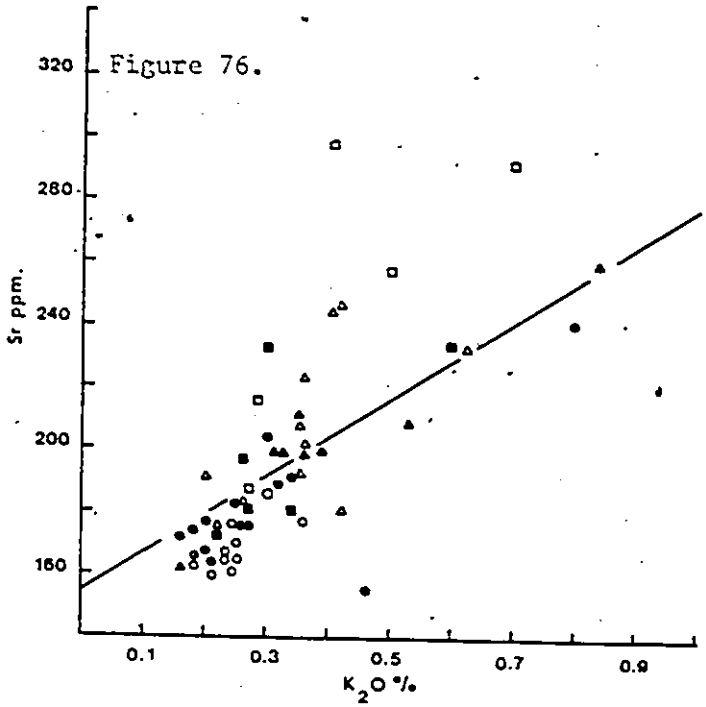

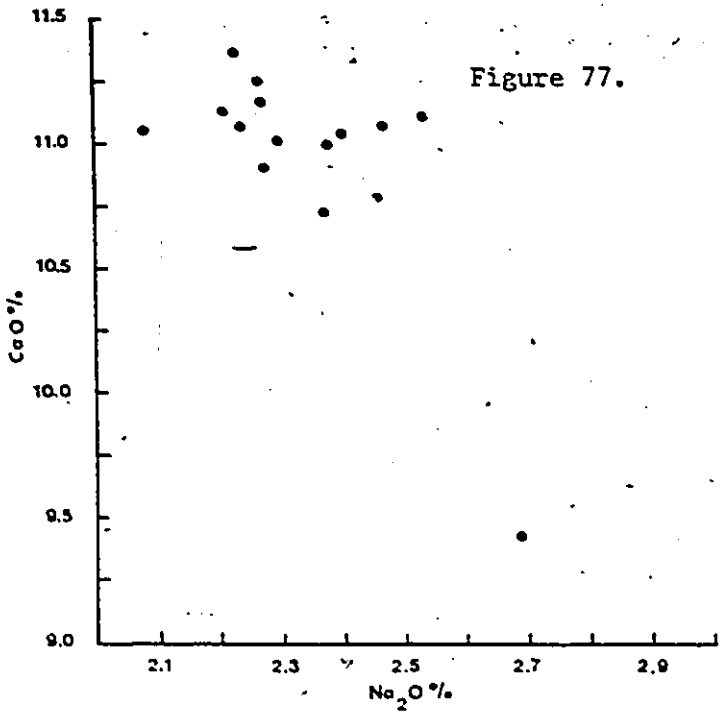

Figure 77.

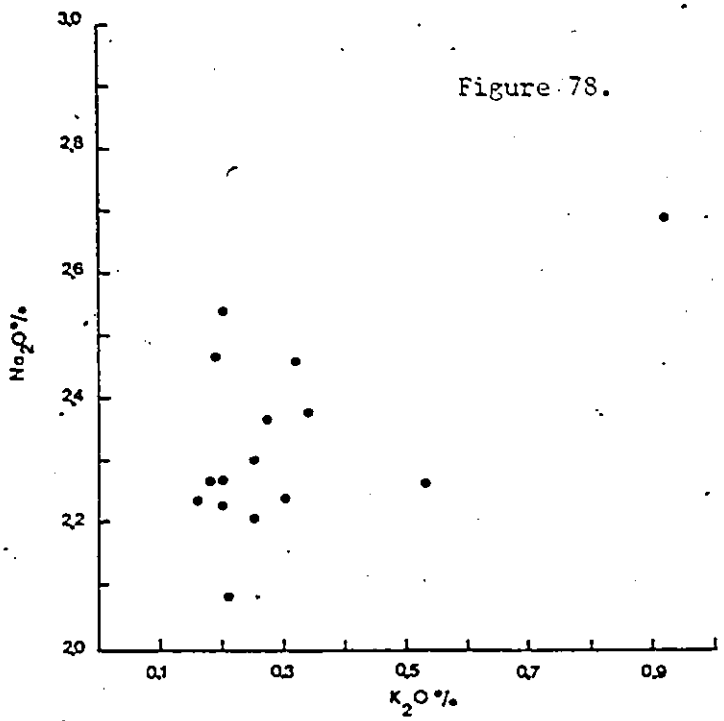

Figure 78.

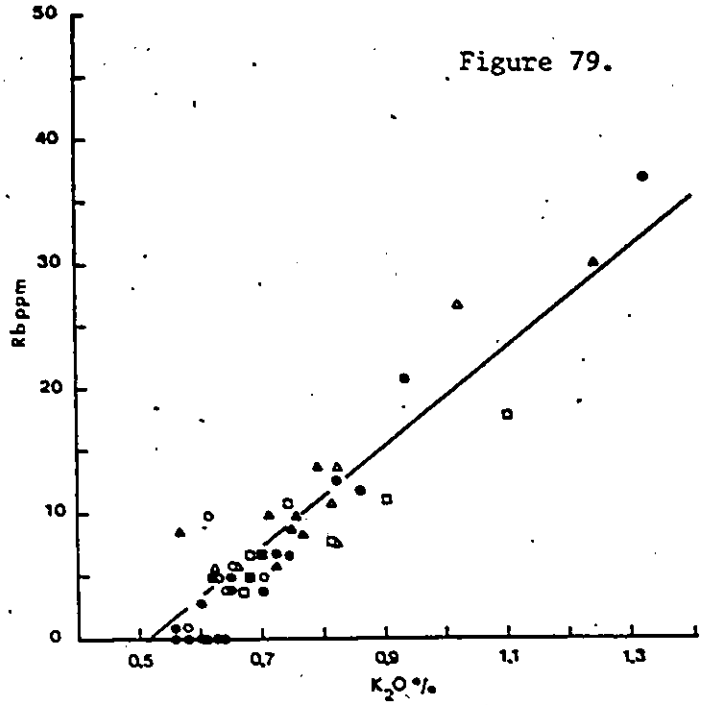

Figure 79.

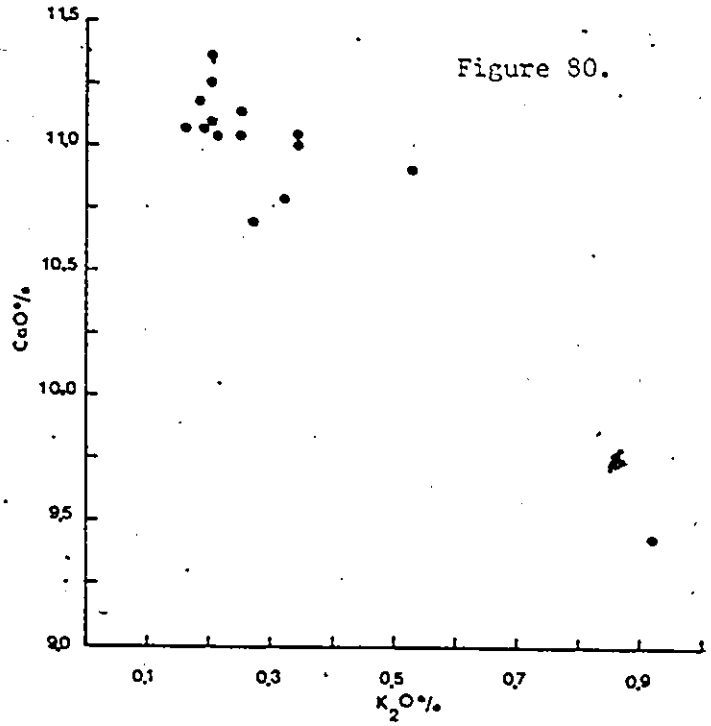

Figure 80.

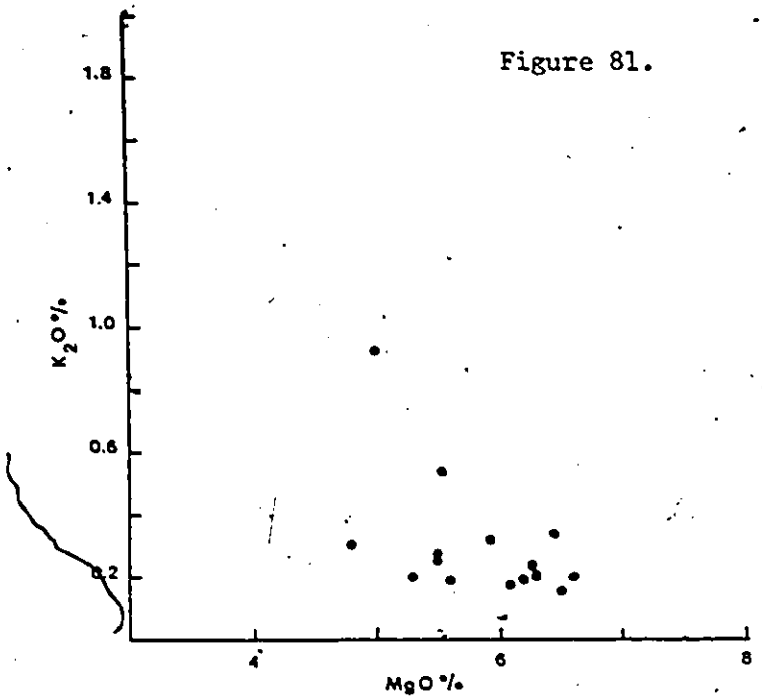

Figure 81.

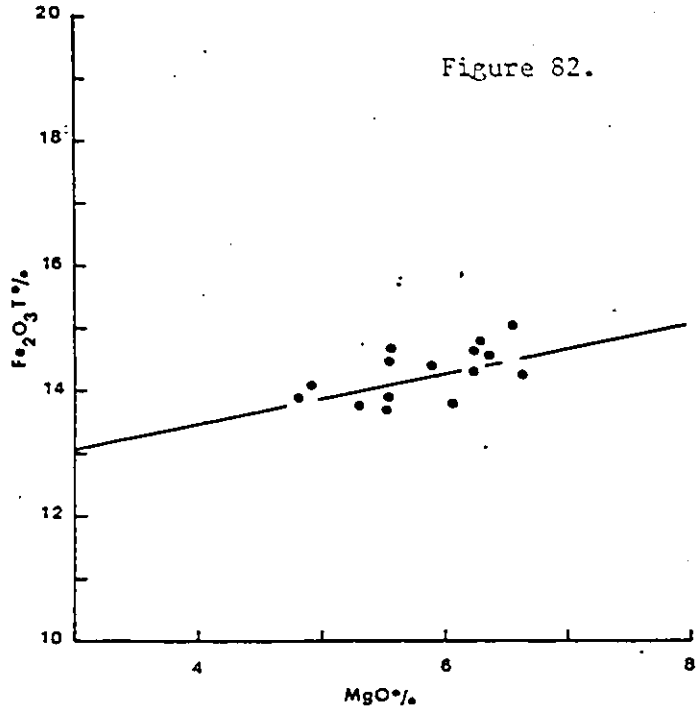

Figure 82.

Figure 83.

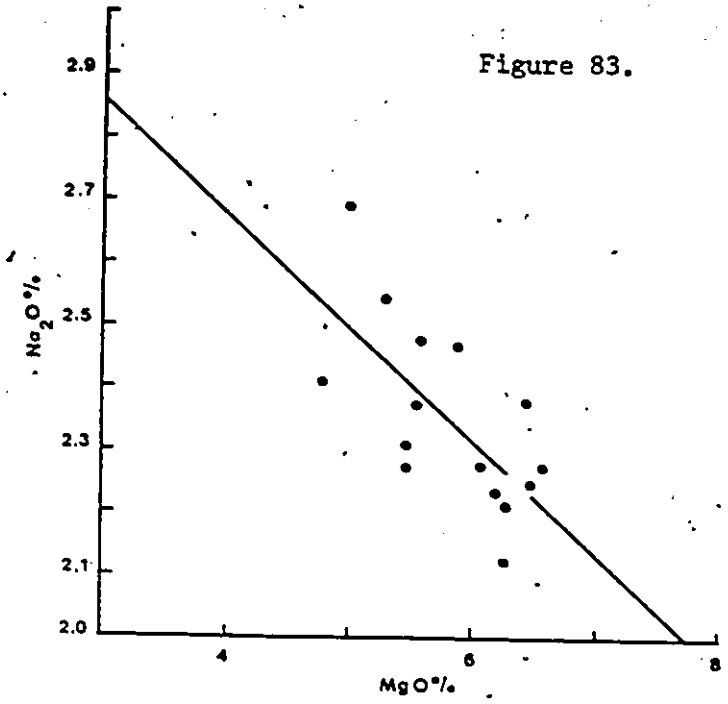

Figure 84.

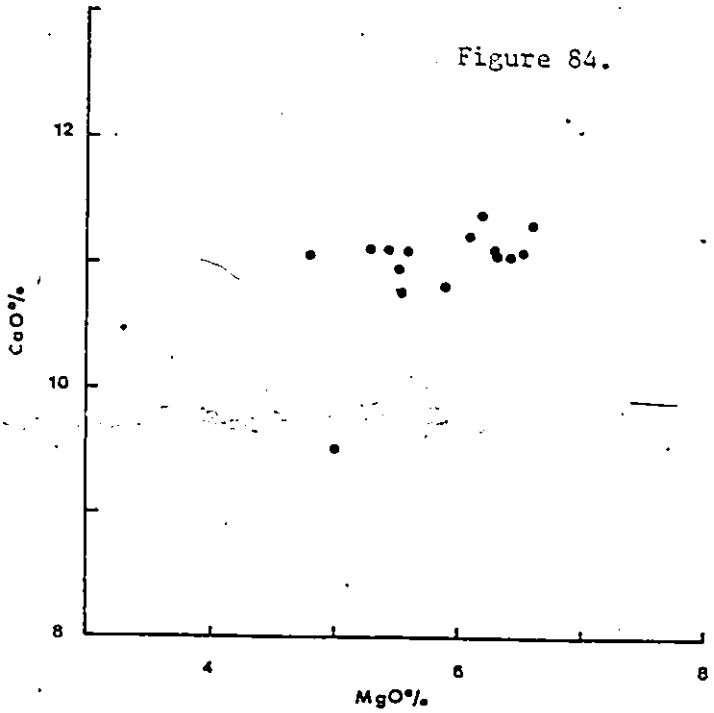

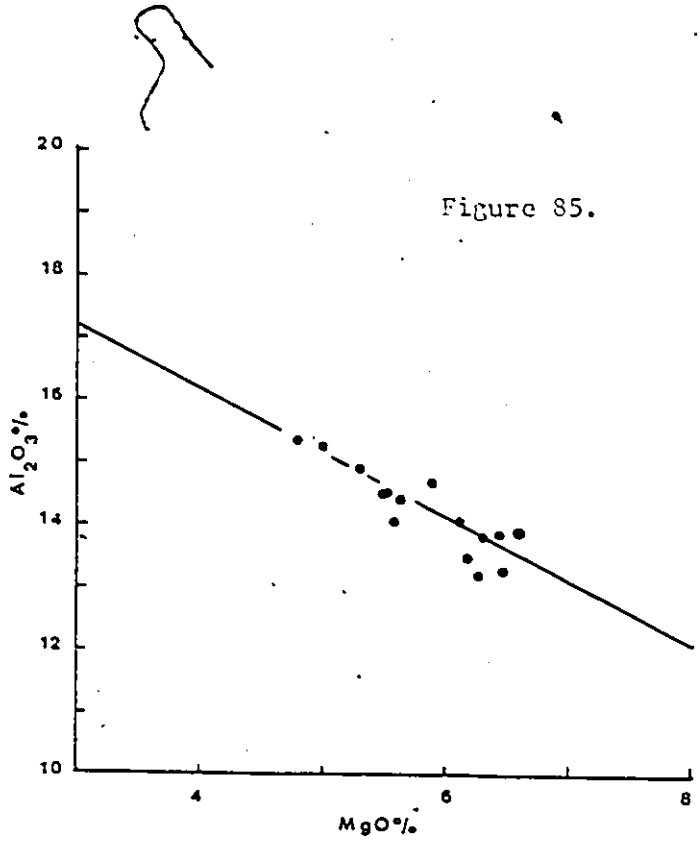

Figure 85.

TABLE 4

X vs Y	r	Equation
Ni vs Zr	0.83	Y=1.76X + 37.66
K_2O vs Sr	0.57	Y=105.6X + 156.2
K_2O vs Rb	0.90	Y=40.41X - 5.00
K_2O vs Na_2O	0.58	Y=0.46X + 2.21
K_2O vs CaO	0.91	Y=-2.08X + 11.58
Y vs Zr	0.80	Y=4.19X + 24.71
Zr vs K_2O	0.73	Y=0.016X + 0.44
Na_2O vs CaO	0.70	Y=18.44X - 3.32
MgO vs K_2O	0.51	Y=-0.17X + 1.32
MgO vs Fe_2O_3T	0.57	Y=0.41X + 11.83
MgO vs Na_2O	0.68	Y=-0.18X + 3.40
MgO vs CaO	0.52	Y=0.41X + 8.55
MgO vs Al_2O_3	0.88	Y=-1.08X + 20.24

Correlation factors "r" and regression equations for element versus element diagrams.

clear cut variations may be attributed to a combination of in situ fractionation, differentiation at the source and possibly magma mixing.

The masking becomes more important for Mg, Al, Fe, Na, K and Ca. When all the samples are plotted on variation diagrams, extremely poor correlations are recorded. For this reason, only samples collected from the portion of the dike corresponding to the largest pulse (pulse three) were plotted, resulting in a dramatic increase in the correlation coefficient.

Although in situ fractionation may account for the element-element variations within each portions of the dike corresponding to different pulses, chemical differences between samples from differeht pulses must be the result of processes active in the source chamber.

Without mineral analyses one can only approximate the true meaning of these variation diagrams. The good positive correlations between K and Zr, and Sr and Rb could indicate that these elements entered the same mineral(s) at the same time during crystallization. Good negative correlations are recorded for K and Ca, and Mg and K. This may indicate that during the course of crystallization one element would have entered one or two specific minerals while the other element would have been excluded from these same minerals, becoming a so called "incompatible element".

If one plots Rb/Sr versus Sr for the total rock, the St-Pierre dike samples follow a Sr depletion trend, that is, although both Rb and Sr increase in content from the contact inward, Rb concentrations increase more rapidly, thus creating a depletion of Sr relative to Rb. Since this is accompanied by a general decrease in Ca and Al, in situ fractionation

of feldspars, especially plagioclase, is thought to have been active between each pulse. As fractionation ensued, both plagioclase and K-feldspar, crystallizing out of the magma pulse, would have gradually contained more K, Sr and Rb, these elements being progressively concentrated in the residual liquids of each pulse.

Let us consider the separation and crystallization of three main minerals: plagioclase (labradorite), augite and pigeonite. The so called "compatible" elements to these minerals would be those that can enter their crystalline structure while "incompatible" elements would be those that do not. Out of the elements that are here considered, those that would be "compatible" are Al, Fe, Ca, Na, Mg, Cr and Ni, while those "incompatible" are K, Zr, Y, Sr and Rb. If the separation of plagioclase and pyroxenes was the process that affected the distribution of these elements, variation diagrams of both compatible versus compatible and incompatible versus incompatible elements should give positive correlations, while diagrams of compatible versus incompatible elements would give negative correlations. This feature is found to be true for most variation diagrams except for Mg versus Na and Mg versus Al which give negative correlations and K versus Na which give a positive correlation. Potassium could, to a certain point, be present in the plagioclase structure, thus explaining the positive correlation between K and Na. The negative correlation observed for Mg versus Na and Mg versus Al could be related to the fact that Na and Al are more readily incorporated in the labradorite structure than Mg. In other words, Mg would be incompatible to labradorite and the separation of the plagioclase could have been the regulating process for the distribution of some of the Na and Al.

DIFFERENTIATION AND CRYSTALLIZATION HISTORY

It was suggested above that both textural and chemical changes could be related to processes active before and during the emplacement of the magma, such processes being in situ fractionation and differentiation at the source accompanied by a multi-pulse mode of emplacement. Although flow differentiation may have been an active process during emplacement, no evidence supporting this process could be recorded. In fact, the occurence of pyroxene and plagioclase phenocrysts at the contact would point otherwise. Bhattacharji (1964) indicated that any evidence supporting flow differentiation was eradicated when pulsating flow conditions occured.

Jaeger (1957) proposed a series of equations and graphics relating temperature, thickness and time of crystallization for dike-like masses (see Fig. 86). Equations relating crystallization temperature and time required to crystallize various portions of a dike approximately 32 m wide, each portion being equal to that of the visible segment of each, were deducted from the same diagram.

Before one can relate any textural or chemical change to time, magmatic differentiation and pulses, basic assumptions must be formulated.

1. The full opening of the fracture (32 m), into which the diabasic magma migrated, occured during the emplacement of the first pulse.
2. The calculated time required to crystallize each visible portion of each pulse is minimum. Each succeeding pulse entering the conduit would encounter increasingly hotter contact rocks (previously crystallized diabasic magma) and would increase the temperature of the central region

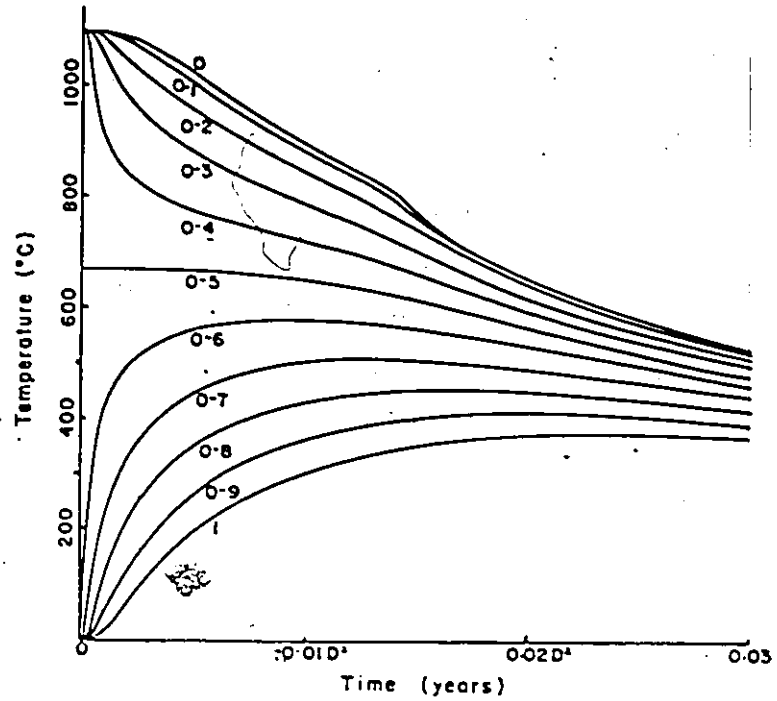

Temperatures T at various points in an intrusive sheet of thickness D metres for which $T_2 = 1100°C$, $T_1 = 800°C$, $L = 100$. The numbers on the curves are distances from the center measured as fractions of the thickness.

Figure 86. Time-Temperature diagram from Jaeger (1957).

of the dike. All these facts would tend to increase the time required for a full crystallization of the dike.

3. Entry temperature of the diabasic magma was approximately 1,100°C.

4. Full crystallization of the magma occurred at 800°C.

Before the emplacement of the first pulse, the magma at the source had only slightly differentiated and contained only a fraction of pyroxene and plagioclase phenocrysts suspended in a large amount of liquid. In fact, at the time and just before the emplacement of the first pulse, the top portion of the magma chamber would have been slightly differentiated while the bottom portion was unchanged. This would explain the ever so slighlty higher differentiation index of Sample D as compared to the following pulse represented by Samples C, B and A.

At time=0, the first pulse would have entered the conduit and the first portion of magma to enter, the highest in the magma chamber, would be represented by material extremely close to the contact. From Jaeger (1957), the time required to crystallize the first pulse would have been 246 days using:

$$T=2.9X10^{-4}\ D^2$$

where T is the time of crystallization in years

and D, the sheet thickness in m.

In fact, we could have had relatively rapid crystallization of the magma leaving both pyroxene and plagioclase phenocrysts embedded in a fine-grained matrix. According to the petrography of the contact zone, the first pulse would have been important enough so as to deplete the section of the magma chamber which contained both pyroxene and feldspar phenocrysts in suspension.

At time=246 days, the second pulse, originating from a now very slightly differentiated magma chamber, would have pushed the uncrystallized portion of the first pulse and implanted a new magma devoid of any phenocrysts. From

$$T=3.33X10^{-3} D^2$$

3.4 years were required for the observable portion of the second pulse to crystallize. The contact would have crystallized relatively rapidly and the rest progressively slower because of decreasing heat loss rates. The 3.4 years would have been enough time for a large portion of the pulse (0.22 m) to crystallize out in the form of pyroxene, plagioclase and opaque crystals, leaving only a few centimetres of material as a fine-grained contact diabase. The gradual appearance of these minerals would account for the chemical variations observed across this portion of the dike. These element variations would then be the result of in situ fractionation.

After 3.4 years, buoyancy pressure in the magma chamber had reached a point where a third pulse occured. Since the differentiation of the magma chamber was an active process throughout the crystallization history of the dike, magma emplaced by succeeding pulses would be slightly more differentiated than the previous ones, the amount of differentiation being directly related to the amount of time between each pulse. This would then cause a general overall increase in the differentiation index toward the centre of the dike.

The third pulse was therefore slightly more differentiated than the previous, although the 3.4 years between each pulse was not enough to create a large difference in differentiation index. According to the

chemistry, 7.28 m of the third pulse magma had time to crystallize before the next pulse. From Jaeger

$$T=1.06X10^{-2}\ D^{2}$$

this 7.28 m would have taken 10.8 years to crystallize. As was the case in previous pulses, plagioclase, pyroxene and opaques would have progressively crystallized out of the emplaced liquid and the whole rock would have contained more K, Fe, Ti, Zr, Sr, Rb and Zn.

A time of 10.8 years would have gone by between the entry of the third pulse and that of the fourth. This period would have been sufficient for the magma chamber to differentiate to the point where the top portions of the latter contained a fairly well differentiated liquid. As in all cases, this top portion of magma would be the first to enter the dike within the fourth pulse and would be represented by Samples X11-25 and X11-26. The fourth pulse would then have tapped progressively deeper levels of the magma chamber, these levels being slightly less differentiated than the top ones. In situ fractional crystallization would then have changed this decrease to a slight increase in differentiation index by selective concentration of K and Fe in residual liquids.

CONCLUSION

The St-Pierre de Wakefield diabase dike dates back to late Precambrian or early Paleozoic. It is part of the Grenville Dike Swarm and intrudes gneisses, quartzites and marbles of the Grenville Supergroup.

The absence of exposure or the extreme fracturing of the contact rocks, associated with vertical fault walls, indicates that the dike intruded along an E-W trending fracture which was subsequently reactivated after the solidification of the magma.

Petrographic studies of the dike indicate the presence of five main minerals: plagioclase, augite, pigeonite, magnetite and ilmenite, and four accessory minerals: chlorite, calcite, quartz and K-feldspar.

Orientation of feldspar laths at the contact, the regional rock protuberances and the mode of pyroxene deposition aroud the latter, indicate a flow direction originating in the lower east and migrating toward the top west.

Textural variations across strike such as the abrupt disappearances and reappearances of pyroxene phenocrysts along with the decreases in feldspar lath sizes, indicate a multi-pulse mode of magma emplacement.

Chemical variations across strike support the multi-pulse mode of emplacement and are thought to be the direct result of processes active before and during the emplacement of the magma. These processes include differentiation at the source progressively creating a zoned magma chamber, and in situ fractionation.

The REE variations also support the multi-pulse mode of emplacement. The decrease in REE contents within each pulse may reflect the emplacement of feldspar, pyroxene and magnetite primocrysts at the beginning of each pulse.

Most chemical variations along strike lie between maximum and minimum values recorded at the natural cross-section. Variations of the kind observed at the natural section may be present along strike but are not fully revealed by the fewer samples obtained.

This work emphasises the importance of detailed sampling and close examination of textural changes when studying diabase dikes. This study also shows that chemical and textural variations of the kind observed in large dikes, such as the Pageland dike, are or could be present in smaller dikes.

Similarities between large and small dikes indicate that processes active during the emplacement are similar throughout regardless of the dike width.

REFERENCES

BARAGAR, W.R.A., 1960. Petrology of basaltic rocks in part of the Labrador Trough. Bulletin Geological Society of America, 71, ppl589-1644.

BLANCHARD, J.P., BAYER, P. & GAGNY, C., 1979. A new criteron for the direction of injection in a dike; the angular relation of minerals near the walls. Tectonophysics, 53, ppl-25.

BHATTACHARJI, S. & SMITH, C.H., 1964. Flowage differentiation. Science, 145, pp 150-153.

BUDDINGTON, A.F., FAHEY, J. & VLISIDES, A., 1955. Thermometric and petrogenetic significance of titaniferous magnetite. American Journal of Science, 253, pp 497-523.

COX, K.G., BELL, J.D. & PANKHURST, R.J., 1979. The interpretation of igneous rocks. London: George Allen & Unwin Ltd, pp 273-282.

JAEGER, J.C., 1957. The temperature in the neighborhood of a cooling intrusive sheet. American Journal of Science. 255, pp306-318.

KERR, P.F., 1977. Optical Mineralogy. New York: McGraw-Hill, pp294-298.

KRETZ, R., 1984. Petrology of the Grenville Swarm of gebbro dikes. Can. J. Earth Sci. (in press).

JEN, L.S., 1973. The determination of iron (II) in silicate rocks and minerals. Anal. Chem. Acta, 66, p315-318.

MARTIGNOLE, J., 1975. Le Precambrien dans le sud de la province tectonique de Grenville (Bouclier Canadien). Ph.D. Thesis, University of Montreal.

MURTHY, G.S., 1971. The paleomagnetism of diabase dike from the Grenville Province. Canadian Journal of Earth Sciences, 8, pp 802-812.

NIXON, C.M., 1977. Petrographic and chemical study of a diabase dike in the Gatineau Park, Quebec. M.Sc. Thesis, University of Ottawa.

RAGLAND, P.C. & WEIGHLAND, P.W., 1970. Geochemistry of Mesozoic dolerite dikes from eastern North America. Contributions to Mineralogy and Petrology, 29, pl95-214.

SCOATES, R.F.J. & MACEK, J.J., 1978. Molson dike swarm. Manitoba Dept. of Mines, Resources and Environm.

STEELE, K.F. & RAGLAND, P.C., 1976. Model for the closed-system Fractionation of a dike formed by two pulses of dolerite magma. Contributions to mineralogy and Petrology, 57, p305-316.

WANLESS, R.K., STEVENS, R.D., LACHANCE, G.R. & DELBIO, R.N., 1972. Age Determinations and geological studies: K-Ar isotopic ages. Report 10, G.S.Canada, paper 71-2.

WILSON, M.E., 1920. Buckingham geological map. Canada Dept. Mines.

WILSON, M.E., 1925. The Grenvile Subprovince. Journal of Geology, 33, pp389.

APPENDIX 1

Individual Thin-section Descriptions.

LEGEND APPENDIX 1

SIZE

1+	0.0 TO 1mm.
2+	1.1 TO 3mm.
3+	3.1 TO 5mm.
4+	5.1 TO —

FORM

S.	SKELETAL
L	LATH
E	EUHEDRAL
A	ANHEDRAL
Z	ZONED
P	PATCHES
EQ	EQUANT

	Magnetite			Augite			Pigeonite			Plagioclase				Chlorite			Qtz+Kfeld			Ilmenite			Calcite		
SECTION	%	SIZE	FORM	%	SIZE	FORM	%	SIZE	FORM	%	SIZE	FORM	An %	%	SIZE	FORM	%	SIZE	FORM	%	SIZE	FORM	%	SIZE	FORM
A1-1	4 0	2 1	S, E	27.8	1 +	A 2	12.4	1+	A,2	54.5	2 +	L,E	5 2	—	—	—	0.4	1 +	A	0.6	1 +	E	0.3	1+	A
A1-2	4.9	1 +	S,E	23.9	2+	A	14.8	2+	A	49.2	2 +	L	5 3	5.1	1 +	P,A	1.8	1 +	A	0.3	1 +	E	—	—	—
A1-3	3.1	2+	A	22.2	2+	A	9.0	2+	A	60.7	1 +	L	5 1	4.3	2 +	A	0.6	1 +	A	0,1	1 +	E	—	—	—
A1-4	4.0	1+	A	29.0	2+	A	17.5	2+	A	42.8	1 +	L	5 3	1.1	1 +	P,A	1.0	1 +	A	0.2	1 +	E	4.4	1+	A
A1-5	2.5	2+	S,E	25.7	2+	Z,A	10.2	2+	Z,A	56.6	1 +	L	4 5	2.2	1 +	P,A	2.1	1 +	A	0.7	1 +	E	—	—	—
A1-6C	3.8	1 +	S,E	30.3	2+	A	4.0	2+	A	55.0	1 +	L	5 3	1.0	1 +	P,A	—	—	—	0.9	1+	E	—	—	—
A2-1	1.2	3+	S,E	30.8	3+	A	13.3	3+	A	52.2	2 +	L	5 4	1.2	3 +	P,A	—	—	—	0.3	1+	E	—	—	—
A2-2	4.6	1+	L,E	33.2	3+	A	3.1	3+	A	51.4	2 +	E,Q	5 4	7.4	2 +	P,A	—	—	—	0.5	1 +	E	—	—	—
A2-3	6.0	2+	S,E	26.0	3+	Z,A	8.2	3+	Z,A	56.4	2 +	L	5 5	1.5	1 +	A	1.1	1 +	A	0.8	1 +	E	—	—	—
A2-4	6.0	1+	A	30.0	2 +	Z,A	10.0	2 +	Z,A	50.0	1 +	E,Q	6 2	3.0	1 +	P,A	—	—	—	1.0	1+	E	—	—	—
A2-5C				6.0	1+	A	3.0	1 +	A	18.0	2+	L	5 4	MA	TRIX	= 73%									
A5-2	5.0	2+	S,E	34.7	2+	A	10.0	2+	A	45.5	2+	L	5 6	3.6	2+	A	—	—	—	1.2	1+	E	SPHENE		
A5-3	4.0	2+	S,E	30.0	2+	A	5.3	2+	A	57.0	2+	L	5 9	2.0	2 +	P,A	1.1	1+	A	0.6	1+	E	%	SIZE	FORM
A5-4	2.6	2+	A	13.5	3+	A	0.8	3+	A	65.6	2+	L	5 8	2.5	2+	A	1.2	1+	A	0.3	1+	E	8.0	2+	S
A6-1	4.6	2+	S,A	29.8	2+	Z,A	10.6	2+	Z,A	52.4	2 +	L	6 8	0.4	1 +	A	1.8	1+	A	0.4	1+	E	—	—	—
A6-2	4.0	2 +	S	26.2	2+	Z,A	17.5	2+	Z,A	47.5	2+	L	5 8	3.0	2+	A	0.06	1+	A	0.2	1+	E	1.0	1+	E
A6-3	1.5	2+	S,E	26.1	3+	A	9.0	3+	A	55.4	1 +	L	5 3	2.7	2+	P,A	1.7	1+	A	0.5	1+	E	3.0	1+	E
A6-4	5.0	3+	S	26.7	3+	A	7.8	3+	A	55.4	2+	L	5 7	3.0	2+	P,A	0.8	1+	A	0.3	1+	E	1.0	1+	E
A6-5	0.3	2+	S	34.0	2+	Z A	8.3	2+	Z,A	54.5	2+	L	5 4	2.9	2+	A	—	—	—	—	—	—	—	—	—
A9-1	2.0	3+	S	23.4	4+	A	6.9	4+	A	63.6	3+	L	5 0	3.4	1+	A	—	—	—	0.7	1+	E	—	—	—
A9-2	4.5	3+	S	22.8	3+	Z,A	4.1	3+	Z,A	64.8	4+	L	5 1	3.2	2+	P,A	—	—	—	0.6	1+	E	—	—	—
A9-3	8.0	2+	S	22.1	2+	Z,A	4.9	2+	Z,A	62.2	2+	L	5 5	2.2	2+	P,A	0.1	1+	A	0.4	1+	E	—	—	—
A9-4	4.5	2+	S	23.4	3+	Z,A	4.6	3+	Z,A	63.4	1 +	L		3.1	1+	P,A	0.4	1+	A	0.6	1+	E	—	—	—
A9-5	10.0	2+	S	27.0	4+	A	1.2	4+	A	53.7	1+	L	5 4	7.3	1+	P, A	—	—	—	0.8	1+	E	—	—	—
A11-3	9.0	2+	S	29.7	2+	A	6.1	2+	A	59.1	1+	L	5 9	1.1	1+	P,A	—	—	—	1.0	1+	E	—	—	—
A11-4	3.0	2+	S	28.3	3+	A	4.4	3+	A	62.0	1+	L	5 3	1.7	1+	P,A	0.2	1+	A	0.4	1+	E	—	—	—
A11-5	3.0	2+	S	39.8	2+	Z,A	3.0	2+	Z,A	48.8	1+	L	5 1	4.5	1+	P,A	0.1	1+	A	1.0	1+	E	—	—	—
A12-1	3.0	2+	S	24.8	2+	Z,A	5.7	2+	Z A	62.2	1+	L	5 0	3.5	1+	P,A	0.4	1+	A	0.4	1+	E	—	—	—
A12-2	1.9	2+	S	33.3	2+	Z,A	7.0	2+	Z,A	53.4	1+	L	5 3	4.0	1+	P,A	0.1	1+	A	0.3	1+	E	—	—	—
A12-3	1.8	2+	S	40.2	2 +	Z,A	—	—	—	57.1	1+	L	4 8	0.7	1+	P,A	—	—	—	0.2	1+	E	—	—	—
A11-2C	4.0	1+	A	30.0	1 +	A	15.0	1+	A	50.0	1 +	L	4 7	—	—	—	—	—	—	1.0	1+	E	—	—	—
A11-6C	3.0	1+	A	25.0	2 +	A	5.0	2+	A	60.0	1 +	L	4 3	6.0	1 +	A	—	—	—	1.0	1+	E	—	—	—
A12-4C	3.0	1+	A	25.0	2 +	A	5.0	2+	A	60.0	1 +	L	4 6	6.0	1 +	A	—	—	—	1.0	1+	E	—	—	—
XII-24	2.0	1+	S	27.0	3 +	A	5.0	2+	A	60.0	1 +	L	5 4	1.9	1 +	P,A	3.7	1 +	A	0.4	1+	E	—	—	—
XII-25	1.0	1+	A	18.0	2 +	A	5.0	2+	A	61.0	1 +	L	5 3	1.7	1+	P,A	13.0	1 +	A	0.3	1+	E	—	—	—
XII-26	2.0	1+	A	24.0	2 +	A	7.0	2+	A	59.0	1+	L	5 0	1.0	1+	P,A	6.0	1 +	A	0.4	1+	E	—	—	—

X11-9

ANALYSIS (WEIGHT PERCENT)							
SIO2	48.32	TIO2	1.74	Q	0.0	DI	12.141
AL2O3	14.02	P2O5	0.01	C	0.0	HE	7.961
FE2O3T	13.94	MNO	0.29	OR	2.319	EN	11.412
FEO		S	0.0	AB	23.187	FS	8.582
MGO	6.66	NIO	0.0	AN	26.255	FO	0.078
CAO	9.91	CR2O3	0.0	LC	0.0	FA	0.065
NA2O	2.65	CO2	0.0	NE	0.0	WO	0.0
K2O	0.33	H2O	0.0	KP	0.0	LN	0.0
				AC	0.0	FL	0.0

X11-10

ANALYSIS (WEIGHT PERCENT)							
SIO2	49.17	TIO2	1.84	Q	2.199	DI	14.089
AL2O3	13.29	P2O5	0.0	C	0.0	HE	10.351
FE2O3T	15.00	MNO	0.23	OR	0.963	EN	9.996
FEO		S	0.07	AB	19.292	FS	8.423
MGO	6.52	NIO	0.0	AN	26.200	FO	0.0
CAO	11.07	CR2O3	0.0	LC	0.0	FA	0.0
NA2O	2.24	CO2	0.0	NE	0.0	WO	0.0
K2O	0.16	H2O	0.0	KP	0.0	LN	0.0
				AC	0.0	FL	0.0

X11-11

ANALYSIS (WEIGHT PERCENT)							
SIO2	48.84	TIO2	1.77	Q	3.111	DI	14.068
AL2O3	13.24	P2O5	0.0	C	0.0	HE	10.262
FE2O3T	14.52	MNO	0.22	OR	1.280	EN	9.699
FEO		S	0.0	AB	18.138	FS	8.114
MGO	6.32	NIO	0.0	AN	26.975	FO	0.0
CAO	11.06	CR2O3	0.0	LC	0.0	FA	0.0
NA2O	2.08	CO2	0.0	NE	0.0	WO	0.0
K2O	0.21	H2O	0.0	KP	0.0	LN	0.0
				AC	0.0	FL	0.0

X11-12

ANALYSIS (WEIGHT PERCENT)							
SIO2	49.01	TIO2	1.76	Q	2.614	DI	13.831
AL2O3	14.14	P2O5	0.0	C	0.0	HE	9.452
FE2O3T	13.77	MNO	0.20	OR	1.092	EN	9.222
FEO		S	0.0	AB	19.701	FS	7.228
MGO	6.12	NIO	0.0	AN	28.583	FO	0.0
CAO	11.19	CR2O3	0.0	LC	0.0	FA	0.0
NA2O	2.27	CO2	0.0	NE	0.0	WO	0.0
K2O	0.18	H2O	0.0	KP	0.0	LN	0.0
				AC	0.0	FL	0.0

X11-13

ANALYSIS (WEIGHT PERCENT)							
SIO2	49.41	TIO2	1.75	Q	2.683	DI	13.006
AL2O3	14.41	P2O5	0.0	C	0.0	HE	9.992
FE2O3T	13.89	MNO	0.21	OR	1.145	EN	8.228
FEO		S	0.0	AB	21.368	FS	7.162
MGO	5.56	NIO	0.0	AN	28.296	FO	0.0
CAO	11.08	CR2O3	0.0	LC	0.0	FA	0.0
NA2O	2.47	CO2	0.0	NE	0.0	WO	0.0
K2O	0.19	H2O	0.0	KP	0.0	LN	0.0
				AC	0.0	FL	0.0

X11-14

ANALYSIS (WEIGHT PERCENT)							
SIO2	49.11	TIO2	1.72	Q	1.495	DI	14.244
AL2O3	13.93	P2O5	0.0	C	0.0	HE	9.651
FE2O3T	14.20	MNO	0.21	OR	1.203	EN	10.189
FEO		S	0.0	AB	19.533	FS	7.918
MGO	6.63	NIO	0.0	AN	27.696	FO	0.0
CAO	11.26	CR2O3	0.0	LC	0.0	FA	0.0
NA2O	2.27	CO2	0.0	NE	0.0	WO	0.0
K2O	0.20	H2O	0.0	KP	0.0	LN	0.0
				AC	0.0	FL	0.0

APPENDIX 2

Major, Trace and REE Analyses

CIPW norm calculations are based on the assumption that no volatiles are present. Total oxides and elements per sample range from 98.7% to 99.8% indicating a very low volitile content. Fe_2O_3T refers to total iron present.

For sample location refer to Figure 25.

Precision of XRF analyses was evaluated using the following "v" values (coefficient of variation) from Kretz (1984)

XRF	v%		
SiO_2	0.9	Cr	10.
Al_2O_3	0.8	Rb	40
TiO_2	0.8	Sr	4
Fe	0.8	Y	20
MnO	4.0	Zr	10
MgO	1.0	Ba	10
CaO	0.8		
Na_2O	2.0		
K_2O	1.2		
P_2O_5	4.0		

X11-15

ANALYSIS (WEIGHT PERCENT):							
SIO2	49.30	TIO2	1.82	Q	1.540	DI	12.068
AL2O3	14.70	P2O5	0.01	C	0.0	HE	9.113
FE2O3T	14.40	MNO	0.21	OR	1.817	EN	9.315
FEO		S	0.0	AB	21.085	FS	8.067
MGO	5.91	NIO	0.0	AN	28.492	FO	0.0
CAO	10.80	CR2O3	0.0	LC	0.0	FA	0.0
NA2O	2.46	CO2	0.0	NE	0.0	WO	0.0
K2O	0.32	H2O	0.0	KP	0.0	LN	0.0
				AC	0.0	RU	0.0

X11-16

ANALYSIS (WEIGHT PERCENT)							
SIO2	49.26	TIO2	1.74	Q	2.286	DI	12.494
AL2O3	14.80	P2O5	0.0	C	0.0	HE	9.838
FE2O3T	13.72	MNO	0.21	OR	1.208	EN	7.746
FEO		S	0.0	AB	21.961	FS	6.995
MGO	5.32	NIO	0.0	AN	29.294	FO	0.0
CAO	11.12	CR2O3	0.0	LC	0.0	FA	0.0
NA2O	2.54	CO2	0.0	NE	0.0	WO	0.0
K2O	0.20	H2O	0.0	KP	0.0	LN	0.0
				AC	0.0	RU	0.0

X11-17

ANALYSIS (WEIGHT PERCENT)							
SIO2	46.71	TIO2	1.84	Q	1.978	DI	14.707
AL2O3	13.46	P2O5	0.0	C	0.0	HE	10.809
FE2O3T	14.64	MNO	0.21	OR	1.212	EN	9.046
FEO		S	0.0	AB	19.324	FS	7.625
MGO	6.22	NIO	0.0	AN	26.761	FO	0.0
CAO	11.37	CR2O3	0.0	LC	0.0	FA	0.0
NA2O	2.23	CO2	0.0	NE	0.0	WO	0.0
K2O	0.20	H2O	0.0	KP	0.0	LN	0.0
				AC	0.0	RU	0.0

X11-18

ANALYSIS (WEIGHT PERCENT)							
SIO2	49.21	TIO2	1.69	Q	1.974	DI	13.324
AL2O3	13.80	P2O5	0.0	C	0.0	HE	10.350
FE2O3T	14.78	MNO	0.21	OR	1.504	EN	9.719
FEO		S	0.0	AB	19.022	FS	8.640
MGO	6.26	NIO	0.0	AN	27.466	FO	0.0
CAO	11.14	CR2O3	0.0	LC	0.0	FA	0.0
NA2O	2.21	CO2	0.0	NE	0.0	WO	0.0
K2O	0.25	H2O	0.0	KP	0.0	LN	0.0
				AC	0.0	RU	0.0

X11-19

ANALYSIS (WEIGHT PERCENT)							
SIO2	49.13	TIO2	1.79	Q	2.784	DI	12.141
AL2O3	14.49	P2O5	0.0	C	0.0	HE	9.945
FE2O3T	14.43	MNO	0.21	OR	1.510	EN	8.410
FEO		S	0.0	AB	19.874	FS	7.904
MGO	5.92	NIO	0.0	AN	29.083	FO	0.0
CAO	11.02	CR2O3	0.0	LC	0.0	FA	0.0
NA2O	2.30	CO2	0.0	NE	0.0	WO	0.0
K2O	0.25	H2O	0.0	KP	0.0	LN	0.0
				AC	0.0	RU	0.0

X11-20

ANALYSIS (WEIGHT PERCENT)							
SIO2	49.16	TIO2	1.74	Q	3.012	DI	10.977
AL2O3	15.40	P2O5	0.0	C	0.0	HE	9.694
FE2O3T	13.85	MNO	0.20	OR	1.515	EN	7.191
FEO		S	0.0	AB	20.774	FS	7.284
MGO	4.82	NIO	0.0	AN	31.065	FO	0.0
CAO	11.04	CR2O3	0.0	LC	0.0	FA	0.0
NA2O	2.40	CO2	0.0	NE	0.0	WO	0.0
K2O	0.30	H2O	0.0	KP	0.0	LN	0.0
				AC	0.0	RU	0.0

X11-21

ANALYSIS (WEIGHT PERCENT)							
SIO2	49.02	TIO2	1.75	Q	0.975	DI	13.942
AL2O3	13.48	P2O5	0.0	C	0.0	HE	9.983
FE2O3T	14.91	MNO	0.22	OR	1.563	EN	10.721
FEO		S	0.0	AB	19.680	FS	8.804
MGO	6.79	NIO	0.0	AN	26.155	FO	0.0
CAO	10.96	CR2O3	0.0	LC	0.0	FA	0.0
NA2O	2.28	CO2	0.0	NE	0.0	WO	0.0
K2O	0.26	H2O	0.0	KP	0.0	LN	0.0
				AC	0.0	RU	0.0

X11-22

ANALYSIS (WEIGHT PERCENT)							
SIO2	49.36	TIO2	1.66	Q	1.146	DI	13.865
AL2O3	13.86	P2O5	0.0	C	0.0	HE	9.993
FE2O3T	14.31	MNO	0.21	OR	2.045	EN	9.878
FEO		S	0.0	AB	20.473	FS	8.166
MGO	6.44	NIO	0.0	AN	26.570	FO	0.0
CAO	11.02	CR2O3	0.0	LC	0.0	FA	0.0
NA2O	2.38	CO2	0.0	NE	0.0	WO	0.0
K2O	0.34	H2O	0.0	KP	0.0	LN	0.0
				AC	0.0	RU	0.0

X11-23

ANALYSIS (WEIGHT PERCENT)							
SIO2	48.32	TIO2	1.86	Q	2.076	DI	12.422
AL2O3	14.02	P2O5	0.0	C	0.0	HE	10.118
FE2O3T	14.63	MNO	0.21	OR	1.651	EN	8.579
FEO		S	0.0	AB	20.727	FS	8.015
MGO	5.57	NIO	0.0	AN	27.725	FO	0.0
CAO	10.73	CR2O3	0.0	LC	0.0	FA	0.0
NA2O	2.37	CO2	0.0	NE	0.0	WO	0.0
K2O	0.27	H2O	0.0	KP	0.0	LN	0.0
				AC	0.0	RU	0.0

X11-24

ANALYSIS (WEIGHT PERCENT)							
SIO2	49.20	TIO2	1.66	Q	2.463	DI	12.486
AL2O3	14.55	P2O5	0.0	C	0.0	HE	9.700
FE2O3T	13.72	MNO	0.22	OR	3.217	EN	8.344
FEO		S	0.01	AB	19.709	FS	7.435
MGO	5.53	NIO	0.0	AN	28.681	FO	0.0
CAO	10.92	CR2O3	0.0	LC	0.0	FA	0.0
NA2O	2.27	CO2	0.0	NE	0.0	WO	0.0
K2O	0.53	H2O	0.04	KP	0.0	LN	0.0
				AC	0.0	RU	0.0

X11-25

ANALYSIS (WEIGHT PERCENT)							
SIO2	48.25	TIO2	1.93	Q	0.0	DI	9.149
AL2O3	15.57	P2O5	0.02	C	0.0	HE	7.432
FE2O3T	13.76	MNO	0.20	OR	11.714	EN	6.484
FEO		S	0.0	AB	20.944	FS	6.041
MGO	4.84	NIO	0.0	AN	26.856	FO	1.196
CAO	9.20	CR2O3	0.0	LC	0.0	FA	1.228
NA2O	2.40	CO2	0.0	NE	0.0	WO	0.0
K2O	1.92	H2O	0.0	KP	0.0	LN	0.0
				AC	0.0	RU	0.0

X11-26

ANALYSIS (WEIGHT PERCENT)							
SIO2	49.49	TIO2	1.89	Q	1.725	DI	6.902
AL2O3	14.80	P2O5	0.04	C	0.0	HE	4.478
FE2O3T	13.50	MNO	0.16	OR	5.167	EN	12.028
FEO		S	0.0	AB	26.396	FS	8.950
MGO	5.86	NIO	0.0	AN	25.413	FO	0.0
CAO	7.67	CR2O3	0.0	LC	0.0	FA	0.0
NA2O	3.00	CO2	0.0	NE	0.0	WO	0.0
K2O	0.84	H2O	0.0	KP	0.0	LN	0.0
				AC	0.0	RU	0.0

X11-28

ANALYSIS (WEIGHT PERCENT)							
SIO2	48.45	TIO2	2.01	Q	2.054	DI	11.753
AL2O3	13.88	P2O5	0.04	C	0.0	HE	10.449
FE2O3T	15.46	MNO	0.24	OR	2.366	EN	8.342
FEO		S	0.01	AB	20.477	FS	8.506
MGO	5.40	NIO	0.0	AN	26.796	FO	0.0
CAO	10.59	CR2O3	0.0	LC	0.0	FA	0.0
NA2O	2.36	CO2	0.0	NE	0.0	WO	0.0
K2O	0.39	H2O	0.0	KP	0.0	LN	0.0
				AC	0.0	RU	0.0

X11-29

ANALYSIS (WEIGHT PERCENT)							
SIO2	48.86	TIO2	2.02	Q	2.751	DI	11.358
AL2O3	13.73	P2O5	0.06	C	0.0	HE	9.928
FE2O3T	15.85	MNO	0.23	OR	1.867	EN	9.292
FEO		S	0.0	AB	19.214	FS	9.315
MGO	5.74	NIO	0.0	AN	27.028	FO	0.0
CAO	10.52	CR2O3	0.0	LC	0.0	FA	0.0
NA2O	2.23	CO2	0.0	NE	0.0	WO	0.0
K2O	0.31	H2O	0.0	KP	0.0	LN	0.0
				AC	0.0	RU	0.0

X11-30

ANALYSIS (WEIGHT PERCENT)							
SIO2	46.41	TIO2	3.05	Q	1.898	DI	14.104
AL2O3	11.12	P2O5	0.02	C	0.0	HE	12.654
FE2O3T	19.39	MNO	0.27	OR	1.091	EN	9.306
FEO		S	0.01	AB	17.163	FS	9.576
MGO	6.21	NIO	0.0	AN	21.438	FO	0.0
CAO	10.60	CR2O3	0.0	LC	0.0	FA	0.0
NA2O	1.98	CO2	0.0	NE	0.0	WO	0.0
K2O	0.18	H2O	0.0	KP	0.0	LN	0.0
				AC	0.0	RU	0.0

X11-31

ANALYSIS (WEIGHT PERCENT)							
SIO2	48.46	TIO2	2.07	Q	1.862	DI	11.200
AL2O3	14.45	P2O5	0.0	C	0.0	HE	9.670
FE2O3T	15.11	MNO	0.22	OR	2.122	EN	8.157
FEO		S	0.0	AB	21.767	FS	8.078
MGO	5.23	NIO	0.0	AN	27.808	FO	0.0
CAO	10.43	CR2O3	0.0	LC	0.0	FA	0.0
NA2O	2.51	CO2	0.0	NE	0.0	WO	0.0
K2O	0.35	H2O	0.0	KP	0.0	LN	0.0
				AC	0.0	RU	0.0

X11-32

ANALYSIS (WEIGHT PERCENT)							
SIO2	48.52	TIO2	2.03	Q	2.309	DI	13.368
AL2O3	14.05	P2O5	0.0	C	0.0	HE	9.660
FE2O3T	14.34	MNO	0.21	OR	2.190	EN	8.424
FEO		S	0.0	AB	19.835	FS	8.982
MGO	5.71	NIO	0.0	AN	27.805	FO	0.0
CAO	10.34	CR2O3	0.0	LC	0.0	FA	0.0
NA2O	2.28	CO2	0.0	NE	0.0	WO	0.0
K2O	0.36	H2O	0.0	KP	0.0	LN	0.0
				AC	0.0	RU	0.0

X11-33

ANALYSIS (WEIGHT PERCENT)							
SIO2	47.88	TIO2	2.11	Q	1.430	DI	12.084
AL2O3	13.85	P2O5	0.0	C	0.0	HE	9.494
FE2O3T	15.31	MNO	0.22	OR	1.951	EN	9.341
FEO		S	0.0	AB	20.761	FS	8.416
MGO	5.82	NIO	0.0	AN	26.976	FO	0.0
CAO	10.39	CR2O3	0.0	LC	0.0	FA	0.0
NA2O	2.38	CO2	0.0	NE	0.0	WO	0.0
K2O	0.32	H2O	0.0	KP	0.0	LN	0.0
				AC	0.0	RU	0.0

X11-34

ANALYSIS (WEIGHT PERCENT)							
SIO2	49.17	TIO2	1.88	Q	1.978	DI	11.656
AL2O3	14.28	P2O5	0.0	C	0.0	HE	9.764
FE2O3 T	15.10	MNO	0.22	OR	2.163	EN	9.041
FEO		S	0.0	AB	20.455	FS	8.687
MGO	5.71	NIO	0.0	AN	27.651	FO	0.0
CAO	10.63	CR2O3	0.0	LC	0.0	FA	0.0
NA2O	2.38	CO2	0.0	NE	0.0	WO	0.0
K2O	0.36	H2O	0.0	KP	0.0	LN	0.0
				AC	0.0	RU	0.0

X11-35

ANALYSIS (WEIGHT PERCENT)							
SIO2	48.69	TIO2	2.22	Q	2.330	DI	13.546
AL2O3	13.51	P2O5	0.0	C	0.0	HE	9.394
FE2O3 T	15.22	MNO	0.22	OR	2.048	EN	9.623
FEO		S	0.01	AB	19.303	FS	7.654
MGO	6.27	NIO	0.0	AN	26.284	FO	0.0
CAO	10.73	CR2O3	0.0	LC	0.0	FA	0.0
NA2O	2.24	CO2	0.0	NE	0.0	WO	0.0
K2O	0.34	H2O	0.0	KP	0.0	LN	0.0
				AC	0.0	RU	0.0

X11-36

ANALYSIS (WEIGHT PERCENT)							
SIO2	48.54	TIO2	1.86	Q	0.290	DI	14.881
AL2O3	12.30	P2O5	0.0	C	0.0	HE	10.977
FE2O3 T	15.96	MNO	0.23	OR	1.328	EN	11.352
FEO		S	0.01	AB	19.949	FS	9.604
MGO	7.18	NIO	0.0	AN	23.012	FO	0.0
CAO	10.75	CR2O3	0.0	LC	0.0	FA	0.0
NA2O	2.31	CO2	0.0	NE	0.0	WO	0.0
K2O	0.22	H2O	0.0	KP	0.0	LN	0.0
				AC	0.0	RU	0.0

X11-37

ANALYSIS (WEIGHT PERCENT)							
SIO2	48.35	TIO2	2.01	Q	0.184	DI	12.052
AL2O3	13.86	P2O5	0.02	C	0.0	HE	10.306
FE2O3 T	15.85	MNO	0.22	OR	1.807	EN	9.275
FEO		S	0.01	AB	22.404	FS	9.096
MGO	5.86	NIO	0.0	AN	25.730	FO	0.0
CAO	10.47	CR2O3	0.0	LC	0.0	FA	0.0
NA2O	2.60	CO2	0.0	NE	0.0	WO	0.0
K2O	0.30	H2O	0.0	KP	0.0	LN	0.0
				AC	0.0	RU	0.0

X11-38

ANALYSIS (WEIGHT PERCENT)							
SIO2	49.34	TIO2	1.62	Q	0.904	DI	12.701
AL2O3	14.79	P2O5	0.0	C	0.0	HE	9.586
FE2O3 T	13.84	MNO	0.21	OR	1.684	EN	8.975
FEO		S	0.0	AB	22.280	FS	7.769
MGO	5.87	NIO	0.0	AN	28.373	FO	0.0
CAO	10.99	CR2O3	0.0	LC	0.0	FA	0.0
NA2O	2.59	CO2	0.0	NE	0.0	WO	0.0
K2O	0.28	H2O	0.0	KP	0.0	LN	0.0
				AC	0.0	RU	0.0

X11-39

ANALYSIS (WEIGHT PERCENT)							
SIO2	46.96	TIO2	2.45	Q	2.554	DI	11.178
AL2O3	12.94	P2O5	0.06	C	0.0	HE	11.626
FE2O3 T	17.16	MNO	0.23	OR	1.661	EN	7.641
FEO		S	0.0	AB	19.979	FS	9.114
MGO	4.95	NIO	0.0	AN	25.303	FO	0.0
CAO	10.29	CR2O3	0.0	LC	0.0	FA	0.0
NA2O	2.27	CO2	0.0	NE	0.0	WO	0.0
K2O	0.27	H2O	0.0	KP	0.0	LN	0.0
				AC	0.0	RU	0.0

X11-40

ANALYSIS (WEIGHT PERCENT)							
SIO2	48.34	TIO2	2.25	Q	2.735	DI	8.725
AL203	14.63	P2O5	0.66	C	0.0	HE	10.135
FE203 T	16.34	MNO	0.22	OR	2.180	EN	6.841
FEO		S	0.0	AB	22.173	FS	9.114
MGO	4.27	NIO	0.0	AN	28.015	FO	0.0
CAO	10.04	CR203	0.0	LC	0.0	FA	0.0
NA2O	2.56	CO2	0.0	NE	0.0	WO	0.0
K2O	0.36	H2O	0.0	KP	0.0	LN	0.0
				AC	0.0	FU	0.0

X11-41

ANALYSIS (WEIGHT PERCENT)							
SIO2	48.37	TIO2	2.36	Q	1.504	DI	9.137
AL203	14.56	P2O5	0.69	C	0.0	HE	9.653
FE203 T	16.09	MNO	0.22	OR	4.230	EN	6.985
FEO		S	0.0	AB	23.513	FS	8.463
MGO	4.41	NIO	0.0	AN	26.005	FO	0.0
CAO	9.70	CR203	0.0	LC	0.0	FA	0.0
NA2O	2.72	CO2	0.0	NE	0.0	WO	0.0
K2O	0.70	H2O	0.0	KP	0.0	LN	0.0
				AC	0.0	FU	0.0

X11-42

ANALYSIS (WEIGHT PERCENT)							
SIO2	48.47	TIO2	2.52	Q	3.396	DI	9.524
AL203	13.72	P2O5	0.12	C	0.0	HE	9.565
FE203 T	16.98	MNO	0.24	OR	1.627	EN	8.097
FEO		S	0.0	AB	21.377	FS	9.337
MGO	4.93	NIO	0.0	AN	25.989	FO	0.0
CAO	9.84	CR203	0.0	LC	0.0	FA	0.0
NA2O	2.48	CO2	0.0	NE	0.0	WO	0.0
K2O	0.27	H2O	0.0	KP	0.0	LN	0.0
				AC	0.0	FU	0.0

X11-43

ANALYSIS (WEIGHT PERCENT)							
SIO2	48.58	TIO2	2.47	Q	4.228	I	7.895
AL203	15.16	P2O5	0.15	C	0.0	HE	9.113
FE203 T	15.89	MNO	0.22	OR	1.753	EN	6.008
FEO		S	0.0	AB	22.847	FS	7.953
MGO	3.80	NIO	0.0	AN	29.374	FO	0.0
CAO	10.01	CR203	0.0	LC	0.0	FA	0.0
NA2O	2.62	CO2	0.0	NE	0.0	WO	0.0
K2O	0.29	H2O	0.0	KP	0.0	LN	0.0
				AC	0.0	FU	0.0

X11-44

ANALYSIS (WEIGHT PERCENT)							
SIO2	49.08	TIO2	2.05	Q	2.688	DI	8.902
AL203	14.24	P2O5	0.11	C	0.0	HE	9.377
FE203 T	16.14	MNO	0.23	OR	3.015	EN	8.260
FEO		S	0.0	AB	21.733	FS	9.979
MGO	4.88	NIO	0.0	AN	26.572	FO	0.0
CAO	9.74	CR203	0.0	LC	0.0	FA	0.0
NA2O	2.52	CO2	0.0	NE	0.0	WO	0.0
K2O	0.50	H2O	0.0	KP	0.0	LN	0.0
				AC	0.0	FU	0.0

X11-45

ANALYSIS (WEIGHT PERCENT)							
SIO2	47.53	TIO2	2.33	Q	1.094	DI	10.690
AL203	13.48	P2O5	0.0	C	0.0	HE	10.048
FE203 T	17.18	MNO	0.24	OR	2.482	EN	9.523
FEO		S	0.0	AB	19.746	FS	10.265
MGO	5.68	NIO	0.0	AN	25.936	FO	0.0
CAO	10.03	CR203	0.0	LC	0.0	FA	0.0
NA2O	2.28	CO2	0.0	NE	0.0	WO	0.0
K2O	0.41	H2O	0.0	KP	0.0	LN	0.0
				AC	0.0	FU	0.0

X11-46

ANALYSIS (WEIGHT PERCENT)							
SIO2	48.67	TIO2	2.11	Q	1.641	DI	10.542
AL2O3	14.05	P2O5	0.05	C	0.0	HE	9.483
FE2O3T	16.19	MNO	0.23	OR	2.461	EN	9.389
FEO		S	0.0	AB	20.517	FS	9.686
MGO	5.65	NIO	0.0	AN	26.786	FO	0.0
CAO	10.19	CR2O3	0.0	LC	0.0	FA	0.0
NA2O	2.39	CO2	0.0	NE	0.0	WO	0.0
K2O	0.41	H2O	0.0	KP	0.0	LN	0.0
				AC	0.0	RU	0.0

X11-47

ANALYSIS (WEIGHT PERCENT)							
SIO2	48.58	TIO2	2.03	Q	0.971	DI	11.054
AL2O3	14.06	P2O5	0.03	C	0.0	HE	9.096
FE2O3T	15.72	MNO	0.23	OR	2.527	EN	10.049
FEO		S	0.0	AB	20.999	FS	9.483
MGO	5.95	NIO	0.0	AN	26.623	FO	0.0
CAO	10.15	CR2O3	0.0	LC	0.0	FA	0.0
NA2O	2.44	CO2	0.0	NE	0.0	WO	0.0
K2O	0.42	H2O	0.0	KP	0.0	LN	0.0
				AC	0.0	RU	0.0

X11-48

ANALYSIS (WEIGHT PERCENT)							
SIO2	49.33	TIO2	1.78	Q	1.816	DI	10.990
AL2O3	14.02	P2O5	0.09	C	0.0	HE	9.599
FE2O3T	15.25	MNO	0.22	OR	2.287	EN	9.452
FEO		S	0.0	AB	21.525	FS	9.468
MGO	5.74	NIO	0.0	AN	26.370	FO	0.0
CAO	10.27	CR2O3	0.0	LC	0.0	FA	0.0
NA2O	2.50	CO2	0.0	NE	0.0	WO	0.0
K2O	0.38	H2O	0.0	KP	0.0	LN	0.0
				AC	0.0	RU	0.0

X11-49

ANALYSIS (WEIGHT PERCENT)							
SIO2	49.17	TIO2	1.77	Q	1.742	DI	13.057
AL2O3	13.84	P2O5	0.0	C	0.0	HE	10.029
FE2O3T	14.88	MNO	0.22	OR	1.203	EN	9.824
FEO		S	0.0	AB	20.131	FS	8.654
MGO	6.27	NIO	0.0	AN	27.121	FO	0.0
CAO	10.93	CR2O3	0.0	LC	0.0	FA	0.0
NA2O	2.34	CO2	0.0	NE	0.0	WO	0.0
K2O	0.20	H2O	0.0	KP	0.0	LN	0.0
				AC	0.0	RU	0.0

X11-50

ANALYSIS (WEIGHT PERCENT)							
SIO2	48.72	TIO2	2.35	Q	4.526	DI	9.803
AL2O3	13.00	P2O5	0.24	C	0.0	HE	9.445
FE2O3T	17.01	MNO	0.24	OR	1.515	EN	9.254
FEO		S	0.0	AB	19.238	FS	10.227
MGO	5.41	NIO	0.0	AN	25.371	FO	0.0
CAO	9.74	CR2O3	0.0	LC	0.0	FA	0.0
NA2O	2.22	CO2	0.0	NE	0.0	WO	0.0
K2O	0.25	H2O	0.0	KP	0.0	LN	0.0
				AC	0.0	RU	0.0

X11-51

ANALYSIS (WEIGHT PERCENT)							
SIO2	49.02	TIO2	1.89	Q	3.157	DI	11.379
AL2O3	13.93	P2O5	0.0	C	0.0	HE	9.578
FE2O3T	15.19	MNO	0.21	OR	1.331	EN	9.456
FEO		S	0.0	AB	19.211	FS	8.970
MGO	5.82	NIO	0.0	AN	28.021	FO	0.0
CAO	10.57	CR2O3	0.0	LC	0.0	FA	0.0
NA2O	2.22	CO2	0.0	NE	0.0	WO	0.0
K2O	0.22	H2O	0.0	KP	0.0	LN	0.0
				AC	0.0	RU	0.0

X11-52

ANALYSIS (WEIGHT PERCENT)							
SIO2	49.41	TIO2	1.78	Q	1.799	DI	11.426
AL2O3	14.67	P2O5	0.0	C	0.0	HE	9.056
FE2O3T	14.60	MNO	0.21	OR	2.099	EN	9.421
FEO		S	0.01	AB	20.929	FS	8.564
MGO	5.83	NIO	0.0	AN	28.431	FO	0.0
CAO	10.59	CR2O3	0.0	LC	0.0	FA	0.0
NA2O	2.44	CO2	0.0	NE	0.0	WO	0.0
K2O	0.35	H2O	0.0	KP	0.0	LN	0.0
				AC	0.0	RU	0.0

X11-53

ANALYSIS (WEIGHT PERCENT)							
SIO2	48.68	TIO2	1.82	Q	2.026	DI	12.498
AL2O3	13.81	P2O5	0.0	C	0.0	HE	9.574
FE2O3T	14.93	MNO	0.22	OR	1.697	EN	10.102
FEO		S	0.0	AB	19.157	FS	8.875
MGO	6.23	NIO	0.0	AN	27.598	FO	0.0
CAO	10.70	CR2O3	0.0	LC	0.0	FA	0.0
NA2O	2.21	CO2	0.0	NE	0.0	WO	0.0
K2O	0.28	H2O	0.0	KP	0.0	LN	0.0
				AC	0.0	RU	0.0

X11-54

ANALYSIS (WEIGHT PERCENT)							
SIO2	49.12	TIO2	1.85	Q	0.860	DI	12.981
AL2O3	13.64	P2O5	0.0	C	0.0	HE	9.739
FE2O3T	15.15	MNO	0.23	OR	2.161	EN	10.360
FEO		S	0.0	AB	20.866	FS	8.914
MGO	6.48	NIO	0.0	AN	25.625	FO	0.0
CAO	10.57	CR2O3	0.0	LC	0.0	FA	0.0
NA2O	2.43	CO2	0.0	NE	0.0	WO	0.0
K2O	0.36	H2O	0.0	KP	0.0	LN	0.0
				AC	0.0	RU	0.0

X11-55

ANALYSIS (WEIGHT PERCENT)							
SIO2	48.65	TIO2	1.91	Q	1.033	DI	14.710
AL2O3	12.08	P2O5	0.0	C	0.0	HE	10.512
FE2O3T	15.96	MNO	0.24	OR	2.116	EN	11.862
FEO		S	0.0	AB	18.415	FS	9.722
MGO	7.34	NIO	0.0	AN	22.862	FO	0.0
CAO	10.56	CR2O3	0.0	LC	0.0	FA	0.0
NA2O	2.13	CO2	0.0	NE	0.0	WO	0.0
K2O	0.35	H2O	0.0	KP	0.0	LN	0.0
				AC	0.0	RU	0.0

X11-56

ANALYSIS (WEIGHT PERCENT)							
SIO2	48.73	TIO2	1.83	Q	0.0	DI	13.538
AL2O3	14.64	P2O5	0.0	C	0.0	HE	9.513
FE2O3T	13.27	MNO	0.22	OR	3.771	EN	8.517
FEO		S	0.0	AB	22.532	FS	6.864
MGO	5.83	NIO	0.0	AN	27.238	FO	0.094
CAO	10.84	CR2O3	0.0	LC	0.0	FA	0.084
NA2O	2.59	CO2	0.0	NE	0.0	WO	0.0
K2O	0.62	H2O	0.0	KP	0.0	LN	0.0
				AC	0.0	RU	0.0

X11-57

ANALYSIS (WEIGHT PERCENT)							
SIO2	49.05	TIO2	1.65	Q	1.989	DI	13.778
AL2O3	14.18	P2O5	0.01	C	0.0	HE	9.662
FE2O3T	13.60	MNO	0.21	OR	2.550	EN	9.105
FEO		S	0.0	AB	19.629	FS	7.323
MGO	6.06	NIO	0.0	AN	28.034	FO	0.0
CAO	11.12	CR2O3	0.0	LC	0.0	FA	0.0
NA2O	2.26	CO2	0.0	NE	0.0	WO	0.0
K2O	0.42	H2O	0.0	KP	0.0	LN	0.0
				AC	0.0	RU	0.0

X11-59

ANALYSIS (WEIGHT PERCENT)							
SIO2	49.45	TIO2	1.69	Q	0.727	DI	14.105
AL203	13.79	P2O5	0.0	C	0.0	HE	10.095
FE203T	14.63	MNO	0.22	OR	1.494	EN	10.289
FEO		S	0.0	AB	20.596	FS	8.446
MGO	6.69	NIO	0.0	AN	26.336	FC	0.0
CAO	11.13	CR203	0.0	LC	0.0	FA	0.0
NA2O	2.41	CO2	0.0	NE	0.0	WC	0.0
K2O	0.25	H2O	0.0	KP	0.0	LN	0.0
				AC	0.0	FL	0.0

X11-60

ANALYSIS (WEIGHT PERCENT)							
SIO2	49.34	TIO2	1.72	Q	2.703	DI	11.683
AL203	14.95	P2O5	0.0	C	0.0	HE	9.534
FE203T	14.05	MNO	0.21	OR	1.808	EN	8.288
FEO		S	0.0	AB	20.175	FS	7.756
MGO	5.40	NIO	0.0	AN	29.965	FC	0.0
CAO	11.01	CR203	0.0	LC	0.0	FA	0.0
NA2O	2.34	CO2	0.0	NE	0.0	WC	0.0
K2O	0.30	H2O	0.0	KP	0.0	LN	0.0
				AC	0.0	FL	0.0

X11-61

ANALYSIS (WEIGHT PERCENT)							
SIO2	48.17	TIO2	1.68	Q	2.695	DI	14.882
AL203	13.47	P2O5	0.0	C	0.0	HE	12.208
FE203T	14.05	MNO	0.23	OR	1.419	EN	7.227
FEO		S	0.01	AB	19.144	FS	6.800
MGO	5.44	NIO	0.0	AN	27.462	FC	0.0
CAO	11.65	CR203	0.0	LC	0.0	FA	0.0
NA2O	2.17	CO2	0.0	NE	0.0	WC	0.0
K2O	0.23	H2O	0.0	KP	0.0	LN	0.0
				AC	0.0	FL	0.0

X11-62

ANALYSIS (WEIGHT PERCENT)							
SIO2	49.29	TIO2	1.73	Q	3.058	DI	14.185
AL203	13.70	P2O5	0.0	C	0.0	HE	10.160
FE203T	14.16	MNO	0.21	OR	1.270	EN	9.267
FEO		S	0.0	AB	18.519	FS	7.613
MGO	6.22	NIO	0.0	AN	27.778	FC	0.0
CAO	11.31	CR203	0.0	LC	0.0	FA	0.0
NA2O	2.14	CO2	0.0	NE	0.0	WC	0.0
K2O	0.21	H2O	0.0	KP	0.0	LN	0.0
				AC	0.0	FL	0.0

X11-63

ANALYSIS (WEIGHT PERCENT)							
SIO2	48.90	TIO2	1.64	Q	0.313	DI	15.456
AL203	13.95	P2O5	0.0	C	0.0	HE	10.254
FE203T	13.36	MNO	0.24	OR	2.185	EN	8.868
FEO		S	0.0	AB	22.229	FS	6.702
MGO	6.25	NIO	0.0	AN	26.183	FC	0.0
CAO	11.30	CR203	0.0	LC	0.0	FA	0.0
NA2O	2.56	CO2	0.0	NE	0.0	WC	0.0
K2O	0.36	H2O	0.0	KP	0.0	LN	0.0
				AC	0.0	FL	0.0

X11-64

ANALYSIS (WEIGHT PERCENT)							
SIO2	49.45	TIO2	1.73	Q	1.663	DI	13.522
AL203	14.10	P2O5	0.0	C	0.0	HE	10.039
FE203T	14.29	MNO	0.22	OR	1.502	EN	9.186
FEO		S	0.0	AB	20.968	FS	7.821
MGO	6.11	NIO	0.0	AN	27.205	FC	0.0
CAO	11.08	CR203	0.0	LC	0.0	FA	0.0
NA2O	2.44	CO2	0.0	NE	0.0	WC	0.0
K2O	0.25	H2O	0.0	KP	0.0	LN	0.0
				AC	0.0	FL	0.0

X11-65

ANALYSIS (WEIGHT PERCENT)							
SIO2	49.23	TIO2	1.77	Q	1.940	DI	13.841
AL2O3	13.75	P2O5	0.0	C	0.0	HE	9.935
FE2O3T	14.58	MNO	0.22	OR	1.143	EN	9.963
FEO		S	0.0	AB	19.525	FS	8.202
MGO	6.47	NIO	0.0	AN	27.214	FO	0.0
CAO	11.13	CR2O3	0.0	LC	0.0	FA	0.0
NA2O	2.27	CO2	0.0	NE	0.0	WO	0.0
K2O	0.19	H2O	0.0	KP	0.0	LN	0.0
				AC	0.0	FO	0.0

X11-66

ANALYSIS (WEIGHT PERCENT)							
SIO2	49.29	TIO2	1.77	Q	2.248	DI	13.568
AL2O3	13.88	P2O5	0.01	C	0.0	HE	10.013
FE2O3T	14.33	MNO	0.22	OR	1.449	EN	5.160
FEO		S	0.01	AB	20.375	FS	7.753
MGO	6.08	NIO	0.0	AN	27.115	FO	0.0
CAO	11.03	CR2O3	0.0	LC	0.0	FA	0.0
NA2O	2.36	CO2	0.0	NE	0.0	WO	0.0
K2O	0.24	H2O	0.0	KP	0.0	LN	0.0
				AC	0.0	FO	0.0

X11-67

ANALYSIS (WEIGHT PERCENT)							
SIO2	49.74	TIO2	1.73	Q	2.705	DI	13.196
AL2O3	13.70	P2O5	0.0	C	0.0	HE	9.529
FE2O3T	14.78	MNO	0.22	OR	1.375	EN	10.676
FEO		S	0.0	AB	18.134	FS	8.841
MGO	6.67	NIO	0.0	AN	27.488	FO	0.0
CAO	10.99	CR2O3	0.0	LC	0.0	FA	0.0
NA2O	2.12	CO2	0.0	NE	0.0	WO	0.0
K2O	0.23	H2O	0.0	KP	0.0	LN	0.0
				AC	0.0	FO	0.0

X11-68

ANALYSIS (WEIGHT PERCENT)							
SIO2	49.62	TIO2	1.77	Q	2.718	DI	12.688
AL2O3	14.14	P2O5	0.0	C	0.0	HE	9.075
FE2O3T	14.40	MNO	0.21	OR	1.440	EN	10.081
FEO		S	0.01	AB	19.309	FS	8.270
MGO	6.32	NIO	0.0	AN	28.173	FO	0.0
CAO	10.86	CR2O3	0.0	LC	0.0	FA	0.0
NA2O	2.25	CO2	0.0	NE	0.0	WO	0.0
K2O	0.24	H2O	0.0	KP	0.0	LN	0.0
				AC	0.0	FO	0.0

X11-69

ANALYSIS (WEIGHT PERCENT)							
SIO2	49.02	TIO2	1.74	Q	2.793	DI	12.896
AL2O3	13.93	P2O5	0.0	C	0.0	HE	9.193
FE2O3T	14.31	MNO	0.21	OR	1.152	EN	10.228
FEO		S	0.0	AB	18.730	FS	8.362
MGO	6.35	NIO	0.0	AN	28.445	FO	0.0
CAO	10.88	CR2O3	0.0	LC	0.0	FA	0.0
NA2O	2.16	CO2	0.0	NE	0.0	WO	0.0
K2O	0.19	H2O	0.0	KP	0.0	LN	0.0
				AC	0.0	FO	0.0

X11-70

ANALYSIS (WEIGHT PERCENT)							
SIO2	49.06	TIO2	1.74	Q	2.906	DI	12.825
AL2O3	13.78	P2O5	0.0	C	0.0	HE	9.645
FE2O3T	14.65	MNO	0.22	OR	1.213	EN	9.730
FEO		S	0.01	AB	18.909	FS	8.566
MGO	6.14	NIO	0.0	AN	27.773	FO	0.0
CAO	10.87	CR2O3	0.0	LC	0.0	FA	0.0
NA2O	2.18	CO2	0.0	NE	0.0	WO	0.0
K2O	0.20	H2O	0.0	KP	0.0	LN	0.0
				AC	0.0	FO	0.0

X11-71C

ANALYSIS (WEIGHT PERCENT)							
SIO2	47.17	TIO2	1.80	Q	0.0	DI	0.0
AL2O3	14.87	P2O5	0.11	C	0.377	HE	0.0
FE2O3T	13.60	MNO	0.17	OR	2.916	EN	20.776
FEO		S	0.01	AB	27.924	FS	11.719
MGO	8.12	NIO	0.0	AN	26.181	FO	0.626
CAO	5.07	CR2O3	0.0	LC	0.0	FA	0.389
NA2O	3.08	CO2	0.0	NE	0.0	WO	0.0
K2O	0.46	H2O	0.0	KP	0.0	LN	0.0
				AC	0.0	RU	0.0

A

ANALYSIS (WEIGHT PERCENT)							
SIO2	48.47	TIO2	1.65	Q	0.510	DI	13.739
AL2O3	13.61	P2O5	0.0	C	0.0	HE	9.364
FE2O3T	14.28	MNO	0.30	OR	3.037	EN	11.150
FEO		S	0.02	AB	18.943	FS	8.716
MGO	6.85	NIO	0.0	AN	26.575	FO	0.0
CAO	10.74	CR2O3	0.0	LC	0.0	FA	0.0
NA2O	2.18	CO2	0.0	NE	0.0	WO	0.0
K2O	0.50	H2O	0.0	KP	0.0	LN	0.0
				AC	0.0	RU	0.0

B

ANALYSIS (WEIGHT PERCENT)							
SIO2	47.54	TIO2	1.66	Q	0.0	DI	13.096
AL2O3	14.14	P2O5	0.0	C	0.0	HE	9.070
FE2O3T	14.17	MNO	0.30	OR	2.447	EN	9.589
FEO		S	0.01	AB	20.304	FS	7.617
MGO	6.65	NIO	0.0	AN	27.917	FO	2.030
CAO	10.70	CR2O3	0.0	LC	0.0	FA	0.901
NA2O	2.32	CO2	0.0	NE	0.0	WO	0.0
K2O	0.40	H2O	0.0	KP	0.0	LN	0.0
				AC	0.0	RU	0.0

C

ANALYSIS (WEIGHT PERCENT)							
SIO2	48.28	TIO2	1.80	Q	1.722	DI	13.372
AL2O3	14.30	P2O5	0.0	C	0.0	HE	9.611
FE2O3T	13.27	MNO	0.32	OR	2.527	EN	7.838
FEO		S	0.02	AB	22.303	FS	6.460
MGO	5.41	NIO	0.0	AN	27.563	FO	0.0
CAO	10.74	CR2O3	0.0	LC	0.0	FA	0.0
NA2O	2.53	CO2	0.0	NE	0.0	WO	0.0
K2O	0.41	H2O	0.0	KP	0.0	LN	0.0
				AC	0.0	RU	0.0

D

ANALYSIS (WEIGHT PERCENT)							
SIO2	46.99	TIO2	1.77	Q	0.0	DI	12.636
AL2O3	14.57	P2O5	0.0	C	0.0	HE	8.819
FE2O3T	13.37	MNO	0.26	OR	2.304	EN	7.806
FEO		S	0.0	AB	23.965	FS	6.248
MGO	5.70	NIO	0.0	AN	27.998	FO	0.899
CAO	10.36	CR2O3	0.0	LC	0.0	FA	0.793
NA2O	2.69	CO2	0.0	NE	0.0	WO	0.0
K2O	0.37	H2O	0.0	KP	0.0	LN	0.0
				AC	0.0	RU	0.0

A1-1

ANALYSIS (WEIGHT PERCENT)							
SIO2	48.87	TIO2	1.74	Q	1.876	DI	14.134
AL2O3	13.71	P2O5	0.0	C	0.0	HE	10.644
FE2O3 T	14.48	MNO	0.21	OR	1.151	EN	9.102
FEO		S	0.0	AB	19.836	FS	7.861
MGO	6.14	NIO	0.0	AN	27.204	FO	0.0
CAO	11.28	CR2O3	0.0	LC	0.0	FA	0.0
NA2O	2.29	CO2	0.0	NE	0.0	WO	0.0
K2O	0.19	H2O	0.0	KP	0.0	LN	0.0
				AC	0.0	FO	0.0

A1-3

ANALYSIS (WEIGHT PERCENT)							
SIO2	48.50	TIO2	1.59	Q	0.894	DI	15.486
AL2O3	13.17	P2O5	0.0	C	0.0	HE	11.074
FE2O3 T	14.52	MNO	0.21	OR	1.154	EN	10.257
FEO		S	0.01	AB	18.452	FS	8.330
MGO	6.78	NIO	0.0	AN	26.324	FO	0.0
CAO	11.51	CR2O3	0.0	LC	0.0	FA	0.0
NA2O	2.17	CO2	0.0	NE	0.0	WO	0.0
K2O	0.19	H2O	0.0	KP	0.0	LN	0.0
				AC	0.0	FO	0.0

A1-5

ANALYSIS (WEIGHT PERCENT)							
SIO2	48.83	TIO2	1.72	Q	1.102	DI	12.936
AL2O3	14.10	P2O5	0.0	C	0.0	HE	9.931
FE2O3 T	14.56	MNO	0.21	OR	1.994	EN	9.573
FEO		S	0.0	AB	20.485	FS	8.429
MGO	6.12	NIO	0.0	AN	27.443	FO	0.0
CAO	10.89	CR2O3	0.0	LC	0.0	FA	0.0
NA2O	2.37	CO2	0.0	NE	0.0	WO	0.0
K2O	0.33	H2O	0.0	KP	0.0	LN	0.0
				AC	0.0	FO	0.0

A2-1

ANALYSIS (WEIGHT PERCENT)							
SIO2	49.24	TIO2	1.67	Q	2.157	DI	13.231
AL2O3	13.38	P2O5	0.0	C	0.0	HE	10.032
FE2O3 T	15.09	MNO	0.22	OR	1.690	EN	10.836
FEO		S	0.0	AB	19.517	FS	9.423
MGO	6.70	NIO	0.0	AN	24.759	FO	0.0
CAO	10.58	CR2O3	0.0	LC	0.0	FA	0.0
NA2O	2.39	CO2	0.0	NE	0.0	WO	0.0
K2O	0.36	H2O	0.0	KP	0.0	LN	0.0
				AC	0.0	FO	0.0

A2-5

ANALYSIS (WEIGHT PERCENT)							
SIO2	47.43	TIO2	1.64	Q	0.703	DI	14.467
AL2O3	13.27	P2O5	0.0	C	0.0	HE	7.391
FE2O3 T	14.24	MNO	0.22	OR	2.166	EN	12.923
FEO		S	0.02	AB	20.567	FS	7.572
MGO	9.02	NIO	0.0	AN	25.142	FO	2.393
CAO	10.68	CR2O3	0.0	LC	0.0	FA	1.346
NA2O	1.94	CO2	0.0	NE	0.0	WO	0.0
K2O	0.24	H2O	0.0	KP	0.0	LN	0.0
				AC	0.0	FO	0.0

A5-5

ANALYSIS (WEIGHT PERCENT)							
SIO2	48.81	TIO2	2.00	Q	0.0	DI	12.992
AL2O3	12.91	P2O5	0.05	C	0.0	HE	10.609
FE2O3 T	15.95	MNO	0.23	OR	1.456	EN	9.864
FEO		S	0.0	AB	16.840	FS	9.237
MGO	6.25	NIO	0.0	AN	27.483	FO	0.0
CAO	10.60	CR2O3	0.0	LC	0.0	FA	0.0
NA2O	2.26	CO2	0.0	NE	0.0	WO	0.0
K2O	0.28	H2O	0.0	KP	0.0	LN	0.0
				AC	0.0	FO	0.0

A6-1

ANALYSIS (WEIGHT PERCENT)							
SIO2	49.58	TIO2	1.75	Q	3.094	DI	13.982
AL2O3	13.64	P2O5	0.0	C	0.0	HE	9.929
FE2O3 T	14.43	MNO	0.22	OR	1.622	EN	9.862
FEO		S	0.0	AB	17.707	FS	8.032
MGO	6.46	NIO	0.0	AN	27.609	FO	0.0
CAO	11.25	CR2O3	0.0	LC	0.0	FA	0.0
NA2O	2.06	CO2	0.0	NE	0.0	WO	0.0
K2O	0.27	H2O	0.0	KP	0.0	LN	0.0
				AC	0.0	RU	0.0

A6-3

ANALYSIS (WEIGHT PERCENT)							
SIO2	48.60	TIO2	2.01	Q	2.630	DI	9.419
AL2O3	14.94	P2O5	0.04	C	0.0	HE	9.713
FE2O3 T	15.55	MNO	0.20	OR	1.632	EN	7.544
FEO		S	0.01	AB	21.443	FS	8.923
MGO	4.68	NIO	0.0	AN	29.471	FO	0.0
CAO	10.40	CR2O3	0.0	LC	0.0	FA	0.0
NA2O	2.48	CO2	0.0	NE	0.0	WO	0.0
K2O	0.27	H2O	0.0	KP	0.0	LN	0.0
				AC	0.0	RU	0.0

A6-5

ANALYSIS (WEIGHT PERCENT)							
SIO2	49.44	TIO2	1.61	Q	2.073	DI	13.683
AL2O3	13.80	P2O5	0.0	C	0.0	HE	9.552
FE2O3 T	14.54	MNO	0.22	OR	1.377	EN	11.172
FEO		S	0.0	AB	17.296	FS	8.945
MGO	6.95	NIO	0.0	AN	28.245	FO	0.0
CAO	11.26	CR2O3	0.0	LC	0.0	FA	0.0
NA2O	2.02	CO2	0.0	NE	0.0	WO	0.0
K2O	0.23	H2O	0.0	KP	0.0	LN	0.0
				AC	0.0	RU	0.0

A9-1

ANALYSIS (WEIGHT PERCENT)							
SIO2	48.98	TIO2	2.41	Q	4.662	DI	7.920
AL2O3	14.45	P2O5	0.10	C	0.0	HE	10.012
FE2O3 T	16.53	MNO	0.23	OR	1.996	EN	6.029
FEO		S	0.02	AB	22.490	FS	8.740
MGO	3.81	NIO	0.0	AN	27.384	FO	0.0
CAO	9.75	CR2O3	0.0	LC	0.0	FA	0.0
NA2O	2.60	CO2	0.0	NE	0.0	WO	0.0
K2O	0.33	H2O	0.0	KP	0.0	LN	0.0
				AC	0.0	RU	0.0

A9-3

ANALYSIS (WEIGHT PERCENT)							
SIO2	48.85	TIO2	2.33	Q	4.087	DI	7.240
AL2O3	15.34	P2O5	0.16	C	0.0	HE	10.587
FE2O3 T	16.01	MNO	0.21	OR	2.415	EN	4.700
FEO		S	0.01	AB	23.400	FS	7.882
MGO	3.17	NIO	0.0	AN	29.099	FO	0.0
CAO	10.14	CR2O3	0.0	LC	0.0	FA	0.0
NA2O	2.71	CO2	0.0	NE	0.0	WO	0.0
K2O	0.40	H2O	0.0	KP	0.0	LN	0.0
				AC	0.0	RU	0.0

A9-5

ANALYSIS (WEIGHT PERCENT)							
SIO2	47.12	TIO2	2.88	Q	1.536	DI	5.947
AL2O3	13.73	P2O5	0.10	C	0.0	HE	10.560
FE2O3 T	17.98	MNO	0.24	OR	2.548	EN	6.682
FEO		S	0.0	AB	23.778	FS	9.046
MGO	4.24	NIO	0.0	AN	24.541	FO	0.0
CAO	9.54	CR2O3	0.0	LC	0.0	FA	0.0
NA2O	2.74	CO2	0.0	NE	0.0	WO	0.0
K2O	0.42	H2O	0.0	KP	0.0	LN	0.0
				AC	0.0	RU	0.0

A12-1

ANALYSIS (WEIGHT PERCENT)							
SIO2	48.94	TIO2	1.77	Q	1.272	DI	12.776
AL2O3	14.68	P2O5	0.0	C	0.0	HE	9.198
FE2O3T	13.67	MNO	0.20	OR	3.695	EN	8.842
FEO		S	0.0	AB	20.884	FS	7.134
MGO	5.71	NIO	0.0	AN	28.102	FO	0.0
CAO	10.79	CR2O3	0.0	LC	0.0	FA	0.0
NA2O	2.41	CO2	0.0	NE	0.0	WO	0.0
K2O	0.61	H2O	0.0	KP	0.0	LN	0.0
				AC	0.0	RU	0.0

A12-3

ANALYSIS (WEIGHT PERCENT)							
SIO2	49.58	TIO2	1.85	Q	3.126	DI	15.097
AL2O3	14.82	P2O5	0.0	C	0.0	HE	4.284
FE2O3T	13.55	MNO	0.20	OR	1.745	EN	7.902
FEO		S	0.0	AB	20.311	FS	8.475
MGO	5.54	NIO	0.0	AN	29.489	FO	0.0
CAO	11.24	CR2O3	0.0	LC	0.0	FA	0.0
NA2O	2.36	CO2	0.0	NE	0.0	WO	0.0
K2O	0.29	H2O	0.0	KP	0.0	LN	0.0
				AC	0.0	RU	0.0

	FeO%
X11-12	8.14
X11-13	8.96
X11-14	9.45
X11-15	9.97
X11-16	9.07
X11-17	8.99
X11-18	10.26
X11-19	9.43
X11-20	8.35
X11-21	8.85
X11-22	8.51
X11-23	6.43
X11-24	9.14
X11-25	9.29
X11-26	9.86
X11-28	9.54
X11-29	9.36
X11-30	9.70
X11-31	9.16
X11-32	8.96

FeO% values of samples from the St-Pierre dike determined by titration.

	FeO%
X11-33	10.02
X11-34	10.09
X11-35	9.80
X11-36	11.42
X11-37	10.68
X11-38	10.13
X11-39	9.34
X11-40	10.13
X11-41	10.70
X11-42	10.56
X11-43	12.23
X11-44	10.13
X11-45	9.77
X11-46	9.88
X11-47	9.93
X11-48	9.70
X11-49	7.90
X11-50	9.70
X11-51	11.29
X11-52	10.58

FeO% values of samples from the St-Pierre dike determined by titration.

	FeO%
X11-53	8.22
X11-54	8.37
X11-55	11.76
X11-56	8.13
X11-57	8.35
X11-59	9.30
X11-60	8.85
X11-61	8.17
X11-62	8.33
X11-63	8.04
X11-64	8.87
X11-65	9.08
X11-66	8.82
X11-67	9.66
X11-68	8.35
X11-69	8.67
X11-70	8.55
X11-71c	8.40

FeO% values of samples from the St-Pierre dike determined by titration.

X11-22	40.	150.	90.	192.	7.	27.	3.	80.	71.				
X11-21	18.	169.	83.	187.	8.	28.	3.	105.	77.				
X11-20	51.	90.	68.	205.	4.	27.	2.	95.	29.				
X11-19	97.	131.	85.	164.	4.	24.	4.	96.	64.				
X11-18	9.	166.	75.	178.	5.	25.	0.	104.	65.				
X11-17	26.	170.	84.	159.	0.	26.	3.	93.	63.				
X11-16	39.	120.	85.	178.	3.	26.	4.	90.	45.				
X11-15	137.	135.	87.	169.	7.	27.	3.	92.	60.				
X11-14	65.	169.	84.	169.	0.	28.	5.	81.	70.				
X11-13	82.	130.	84.	175.	1.	27.	1.	82.	49.				
X11-12	108.	159.	81.	173.	1.	26.	3.	95.	60.				
X11-11	50.	169.	82.	165.	0.	28.	0.	107.	68.				
X11-10	45.	164.	84.	163.	0.	26.	3.	114.	61.				
X11-9	126.	167.	81.	160.	12.	29.	0.	87.	70.				
	BA	CF	2F	5G	RE	Y	NB	ZA	NI				

X11-38	34.	130.	92.	5.	28.	3.	90.	88.															
X11-37	56.	196.	82.	5.	27.	0.	89.	79.															
X11-36	64.	141.	92.	11.	27.	0.	105.	88.															
X11-35	15.	130.	92.	0.	27.	1.	106.	82.															
X11-34	14.	124.	83.	8.	26.	3.	96.	51.															
X11-33	27.	131.	85.	9.	26.	3.	80.	58.															
X11-32	21.	117.	93.	9.	27.	3.	92.	49.															
X11-31	0.	155.	102.	9.	29.	7.	133.	59.															
X11-30	34.	122.	102.	10.	30.	0.	129.	51.															
X11-28	99.	120.	103.	14.	26.	1.	96.	51.															
X11-26	137.	141.	86.	30.	28.	0.	66.	53.															
X11-25	266.	70.	92.	46.	27.	3.	79.	29.															
X11-24	66.	143.	73.	21.	24.	0.	102.	45.															
X11-23	143.	87.	177.	28.	1.	88.	65.																
	BA	CR	ZR	SR	RB	Y	NB	ZA	NI														

	X11-52	X11-51	X11-50	X11-49	X11-48	X11-47	X11-46	X11-45	X11-44	X11-43	X11-42	X11-41	X11-40	X11-39
BA	28.	6.	0.	24.	30.	0.	0.	3.	49.	0.	21.	28.	18.	0.
CE	126.	120.	114.	82.	117.	109.	129.	116.	87.	60.	96.	90.	108.	106.
ZR	91.	160.	132.	115.	100.	95.	97.	86.	114.	125.	119.	111.	93.	107.
SE	208.	177.	170.	221.	224.	250.	246.	299.	259.	216.	167.	292.	198.	181.
FE	10.	6.	6.	8.	9.	8.	11.	8.	11.	7.	4.	18.	4.	4.
Y	26.	29.	35.	31.	31.	26.	27.	25.	33.	35.	30.	28.	27.	30.
NE	3.	5.	6.	4.	5.	3.	1.	0.	4.	5.	4.	5.	0.	3.
ZA	108.	105.	117.	122.	102.	107.	112.	138.	112.	115.	126.	120.	109.	122.
NI	58.	48.	57.	31.	62.	50.	55.	54.	53.	19.	38.	33.	47.	36.

	X11-67	X11-66	X11-65	X11-64	X11-63	X11-62	X11-61	X11-60	X11-59	X11-57	X11-56	X11-55	X11-54	X11-53
BA	13.	0.	0.	8.	8.	0.	13.	24.	0.	58.	63.	13.	46.	25.
CR	167.	135.	167.	140.	155.	167.	135.	113.	170.	177.	146.	194.	151.	143.
ZR	82.	88.	84.	81.	75.	80.	79.	83.	77.	81.	82.	87.	88.	86.
SR	188.	171.	164.	171.	170.	160.	165.	185.	168.	181.	233.	193.	263.	184.
RB	5.	1.	1.	6.	9.	10.	1.	5.	4.	14.	27.	10.	9.	6.
Y	26.	27.	26.	26.	27.	24.	26.	26.	26.	27.	27.	27.	27.	25.
NE	5.	1.	1.	0.	3.	2.	3.	0.	0.	5.	2.	6.	1.	5.
ZN	100.	101.	112.	81.	74.	131.	106.	101.	108.	99.	93.	117.	103.	96.
NI	100.	84.	81.	58.	60.	57.	59.	26.	66.	63.	61.	78.	63.	63.

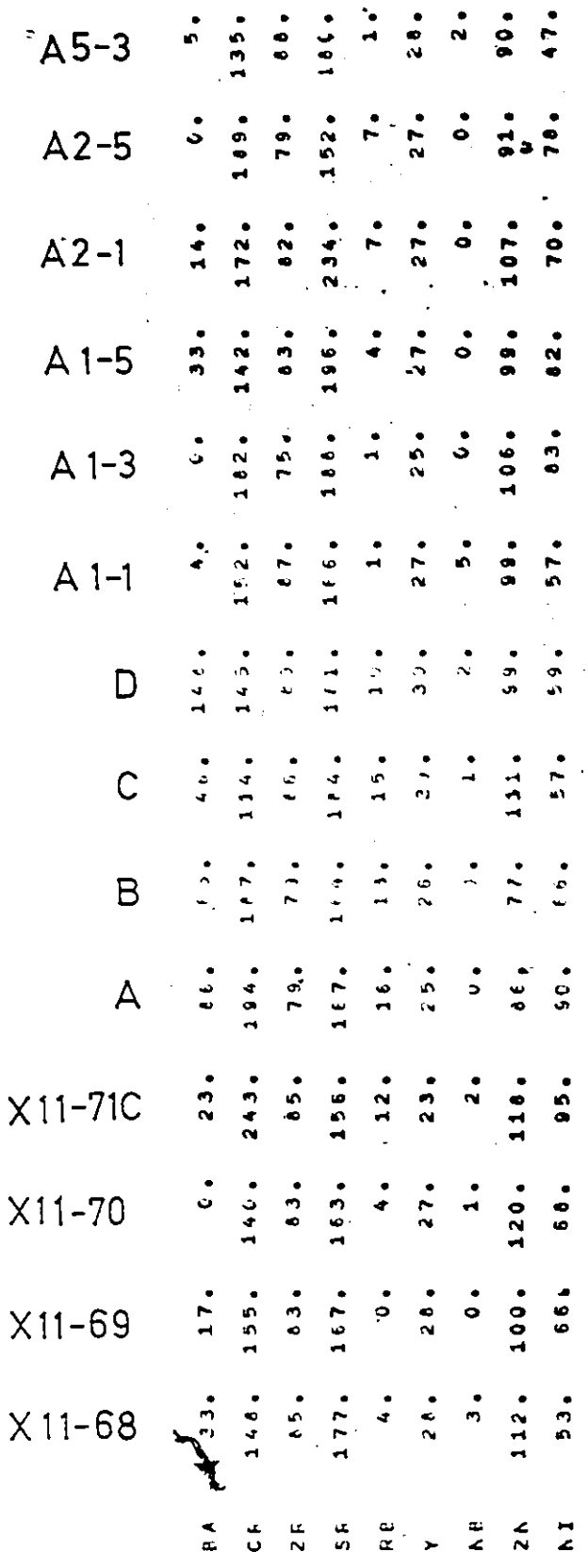
A5-3
A2-5
A2-1
A1-5
A1-3
A1-1
D
C
B
A
X11-71C
X11-70
X11-69
X11-68
BA
CR
ZR
SR
RB
Y
AB
ZA
AI

	A5-5	A6-1	A6-3	A6-5	A9-1	A9-3	A9-5	A11-5	A12-1	A12-3
BA	0.	21.	0.	0.	8.	11.	0.	67.	35.	0.
CR	135.	170.	94.	184.	70.	54.	82.	183.	127.	86.
ZR	94.	85.	106.	68.	139.	133.	114.	83.	89.	93.
SR	158.	189.	198.	162.	203.	211.	249.	211.	339.	227.
RB	1.	1.	1.	22.	1.	10.	5.	41.	12.	23.
Y	31.	28.	30.	23.	35.	33.	30.	27.	26.	28.
NB	4.	3.	3.	0.	4.	3.	3.	1.	5.	3.
ZN	120.	121.	149.	100.	124.	126.	177.	120.	95.	85.
NI	61.	63.	43.	87.	30.	16.	32.	78.	54.	33.

	La	Ce	Pr	Nd	Sm	Eu	Gd	Tb	Dy	Ho	Yb
X11-9	9.61	18.90	-	9.52	2.02	0.71	2.52	-	2.40	0.56	1.25
X11-10	5.86	8.79	-	2.54	0.43	0.09	0.54	-	0.90	0.21	0.69
X11-13	10.70	25.60	-	9.63	2.58	0.79	3.35	-	3.72	0.65	1.55
X11-16	8.00	18.80	-	8.81	2.09	0.60	2.76	-	3.32	0.60	1.62
X11-19	6.74	17.50	-	8.06	2.20	0.63	2.91	-	3.34	0.60	1.42
X11-25	8.80	24.20	-	11.80	3.07	0.96	3.99	-	4.55	0.77	1.98
X11-28	6.21	10.60	-	4.53	0.91	0.32	1.43	-	1.40	0.32	0.83
X11-31	5.24	8.06	-	3.29	0.77	0.15	0.87	-	1.10	0.24	0.64

REE values (ppm) for eight samples from the St-Pierre diabase dike.

APPENDIX 3

Analytical Techniques.

ANALYTICAL TECHNIQUES

Sampling

The dike was initially sampled at 5 m intervals across its width, at 500 m intervals along its lenght for a total of thirty eight samples. Over seventy additional samples were collected at a natural section indicated by X11 on Figure 1. The samples were spaced at 30 cm intervals along a line extending from wall to wall. At the southern contact three oriented samples, two perpendicular and one parallel to the southern contact, were also collected. All samples measured approximately 3,500 cm^3 so as to ensure good representation.

Crushing

Fresh 1,000 cm^3 portions of the original samples were initially crushed to 1 cm^3 fragments with the combination of a jaw and plate crusher. The samples were quartered and visually inspected so as to remove all altered fragments. The samples were then powdered with a Shatterbox.

Point Counting

Modal contents of the initial thirty eight samples were obtained by point counting procedures. A total of two thousand points per thin-section were recorded.

XRF Analyses

1.5 g of fresh whole rock powders are first weighed in a platinum crucible. 4.5 g of $Li_2B_4O_7$ and 0.5 gr of Li_2CO_3 powders are then added,

thoroughly mixed with the rock powder to ensure homogeneity and the subsequent complete dissolution of the samples. The flux mixtures are then heated until molten, poured into platinum dishes and left to solidify. Analyses are then performed using a Philips PW 1410 spectrometer.

Titration Analyses

FeO% values were determined following the titration method described in Jen, L.S.(1973) and using a "Dosimat" E-535 automatic titrator.

APPENDIX 4

REE Analytical Technique.

INTRODUCTION

In the past few years REE contents of either whole rocks or minerals, have been determined with relatively high cost using Neutron Activation. The advent of Inductively Coupled Plasma (I.C.P.)and Direct Current Plasma (D.C.P.) instruments have made it possible for a variety of elements to be analysed via wet geochemistry. Inter-element interferences being the most cumbersome problem encountered during REE analyses, a reliable and inexpensive separation method had to be devised and tested. This Appendix deals with such a method in full detail.

Sample Digestion

A multitude of acid digestions and fusion methods were investigated and the following was found to be the most suitable for this type of analysis.

From 2 to 3 g of powdered sample are accurately weighed in teflon beakers and 3 ml of concentrated HCl along with 1 ml of concentrated HNO_3 are added and the solution heated on a hot plate for half an hour. When the solutions are evaporated by half, 10 ml of HF are added and the slurry returned to the hot plate and dried. An additional 10 ml of HF along with 4 ml of $HClO_4$ are added, heated and dried. The digested sample is taken into solution by the addition of 6 ml of hot 8N HNO_3 and brought to a 50 ml volume with distilled deionized water. Should apatite or zircon be present they would only be slightly affected by the acid digestion and would be detected as small particles in the final sample solution. Since REE can be concentrated in such minerals, complete sample digestion must be assured. The undissolved portion are filtered

out, ashed and the residue mixed with Lithium Metaborate. The mixture is transfered to graphite crucibles and fused in a furnace at 1,000 °C for half an hour. The molten sample is added directly to the sample solution and left to dissolve. This will assure a complete decomposition of resistant minerals.

Standard Solution Preparation

All standards are prepared with Johnson Matthey Specpure rare earth oxide powders with the exception of Ce which is prepared with Ceric Ammonium Nitrate. Pre-weighed standard powders are dissolved in 6.5 ml of concentrated HNO_3. These solutions are heated until full dissolution, cooled and brought up to 0.1N.

Column Preparation

Bio-Rad AG50W-X8 cation exchange resin, 100 to 200 mesh hydrogen form, is used for the separation procedure. The resin is first washed with deionized water and introduced into the separation column as a water-resin slurry up to a bedded height of 25 cm. Care must be taken so as not to create voids in the resin column since they decrease column effectiveness.

Separation Procedure

In order to assure a clean resin, 100 ml of distilled deionized water are first passed through the column. The resin is then activated by the passage of 100 ml of 1N HNO_3 at a flow rate of 1 ml per minute. During the passage of the last 20 ml of 1N HNO_3, the sample solution is

gradually introduced in the column resulting in a gradation of concentration assuring the full use of the resin. The liquid level in the column is left to decrease to the top of the resin.

Major and trace elements are then eluated from the resin by passing 100 ml of 2N HNO_3. The eluates can then be analysed for major and trace element contents. Again the liquid level is left to decrease to the resin top. REE are the last to be eluated by passing 50 ml of 2N HNO_3, 50 ml of 6N HNO and 50 ml of 8N HNO_3. If extreme REE concentrations are expected, an additional 50 ml of 8N HNO_3 are passed to assure complete removal of all REE. The REE eluates are dried under heat lamps, brought to volume with a 0.1N HNO_3 solution and analized on the D.C.P.. The use of heat lamps prohibits the formation of Ce oxide which is undissolvable in HNO_3.

Precision and Accuracy of REE Analyses

Precision of analytical methods is best evaluated by the magnitude of the standard deviation "s", where

$$S = \frac{\sqrt{(X-\bar{X})^2}}{N-1}$$

The standard deviation may be expressed as a fraction of $\bar{X}$, (the coefficient of variation):

$$v = s/\bar{X}$$

where $\bar{X}$=mean concentration

Three standards BCR-1, RHY-1 and SY-2, and two doubles 725 and X11-13

were analysed four, four, six, two and two times respectively. BCR-1 is a basalt, RHY-1 a rhyolite, SY-2 a syenite, 725 an apatite-rich carbonatite and X11-13 a diabase sample from the St-Pierre dike. Means of observed values are presented in Table 5 along with corresponding s, v and vx100 values. From these values it is then evident the lower the element concentration, the lower the precision or the higher the "v" values.

Accuracy was also evaluated with the above samples and the mean of the results compared with published values. In this case accuracy was taken as the numerical difference between the two values and evaluated as the E%.

$$E=O-A$$

where E=error

O=observed values

A=accepted values

$$E\%=Ex100/A$$

The relative errors on each sample are also presented in Table 5 but care must be taken on evaluating these errors. Observed values are compared to published values, themselves the result of Neutron Activation, accurate to within 10%. This degree of uncertainty is expressed as ?. In conclusion, accuracy and precision decrease with the lowering of concentrations.

More work must be performed on this and similar REE analysis methods so as to determine the true accuracy and precision.

	La	Ce	Pr	Nd	Sm	Eu	Gd	Tb	Dy	Ho	Er	Yb
BCR-1												
Mean O	29.2	55.1	-	20.9	5.3	1.6	9.3	-	4.5	-	2.1	-
A	27.0	53.0	-	26.0 ?	6.5 ?	2.0 ?	6.6 ?	-	7.0 ?	1.2 ?	3.5 ?	3.4
s	1.3	7.6	-	5.7	-	1.8	0.9	-	-	-	-	-
v%	4.4	13.4	-	27.3	12.5	19.4	20.0	-	-	-	-	-
E%	8.1	4.0	-	19.7 ?	18.7 ?	20.0 ?	41.0 ?	-	36.4 ?	-	40.0 ?	-
RHY-1												
Mean O	22.1	46.6	-	18.5	4.2	0.7	3.8	-	2.7	0.5	2.4	2.2
A	18.5	41.9	-	20.7	5.5	1.0	-	-	-	-	-	5.6
s	1.0	3.1	-	2.1	0.2	0.1	0.2	-	0.3	0.1	0.1	0.1
v%	4.6	8.1	-	11.0	4.7	15.7	5.2	-	11.1	10.0	5.2	2.3
E%	19.6	11.3	-	10.5	23.6	35.0	-	-	-	-	-	-

Table 5. Rare earth values for various standards and double.

Mean O: Mean of observed values
A: accepted "published" values
s: standard deveation
v %: coefficent of variation
E %: percent error

	La	Ce	Pr	Nd	Sm	Eu	Gd	Tb	Dy	Ho	Er	Yb
SY-2												
Mean 0	85.0	182.2	-	70.3	12.3	1.80	14.8	-	16.9	3.3	13.5	12.3
A	88.0	210 ?	-	71.0	15.0 ?	2.4 ?	?	-	20.0 ?	?	12.0 ?	17.0 ?
s	3.5	7.6	-	7.1	1.3	0.2	1.3	-	1.3	0.2	0.7	1.0
v%	4.1	4.1	-	10.0	10.5	11.1	8.7	-	7.7	6.0	5.2	8.1
E %	3.4	13.2 ?	-	0.9	18.0 ?	27.1 ?	?	-	15.0 ?	?	12.5 ?	30.0 ?

Table 5 cont.

	La	Ce	Pr	Nd	Sm	Eu	Gd	Tb	Dy	Ho	Er	Yb
BCR-1												
-	27.3	74.5	-	-	6.8	2.6	12.1	-	5.0	-	-	-
-	29.7	54.0	-	28.5	-	1.3	8.8	-	-	-	-	-
-	30.0	44.0	-	12.3	-	1.6	7.0	-	2.9	-	1.5	-
-	27.8	50.0	-	21.8	3.8	0.6	-	-	5.3	-	2.7	-
RHY-1												
-	22.7	42.2	-	15.0	3.4	0.5	3.2	-	2.6	0.5	2.3	2.3
-	23.0	45.6	-	20.3	5.3	0.8	3.9	-	3.0	0.5	2.3	2.3
-	23.3	54.4	-	22.9	5.0	0.8	3.8	-	3.0	0.6	2.7	2.3
-	19.5	44.3	-	15.9	3.2	0.5	3.0	-	2.1	0.4	2.2	1.8
SY-2												
-	87.2	153	-	53.7	8.8	1.1	9.7	-	14.6	3.4	12.7	12.7
-	88.7	173	-	54.9	9.8	1.4	13.9	-	13.9	2.9	11.9	10.1
-	92.3	202	-	60.6	10.7	1.4	15.2	-	14.8	2.7	12.7	10.0
-	66.1	186	-	88.3	16.1	2.4	18.1	-	20.8	3.2	13.1	13.4
-	90.1	190	-	77.7	13.3	1.9	15.7	-	17.7	3.3	14.1	11.5
-	85.8	189	-	86.7	14.8	2.3	16.1	-	19.8	4.1	16.5	15.8
725												
	679	1268	-	532	71.3	14.6	-	-	12.7	-	-	9.2
-	654	1283	-	517	72.0	15.4	-	-	11.3	-	-	7.0
X11-13												
-	10.7	75.6	-	9.6	-	2.6	0.8	-	0.9	0.7	2.70	1.6
-	12.8	28.6	-	7.1	-	3.6	1.1	-	-	0.8	-	2.1

Table 6. Rare earth values for standards.

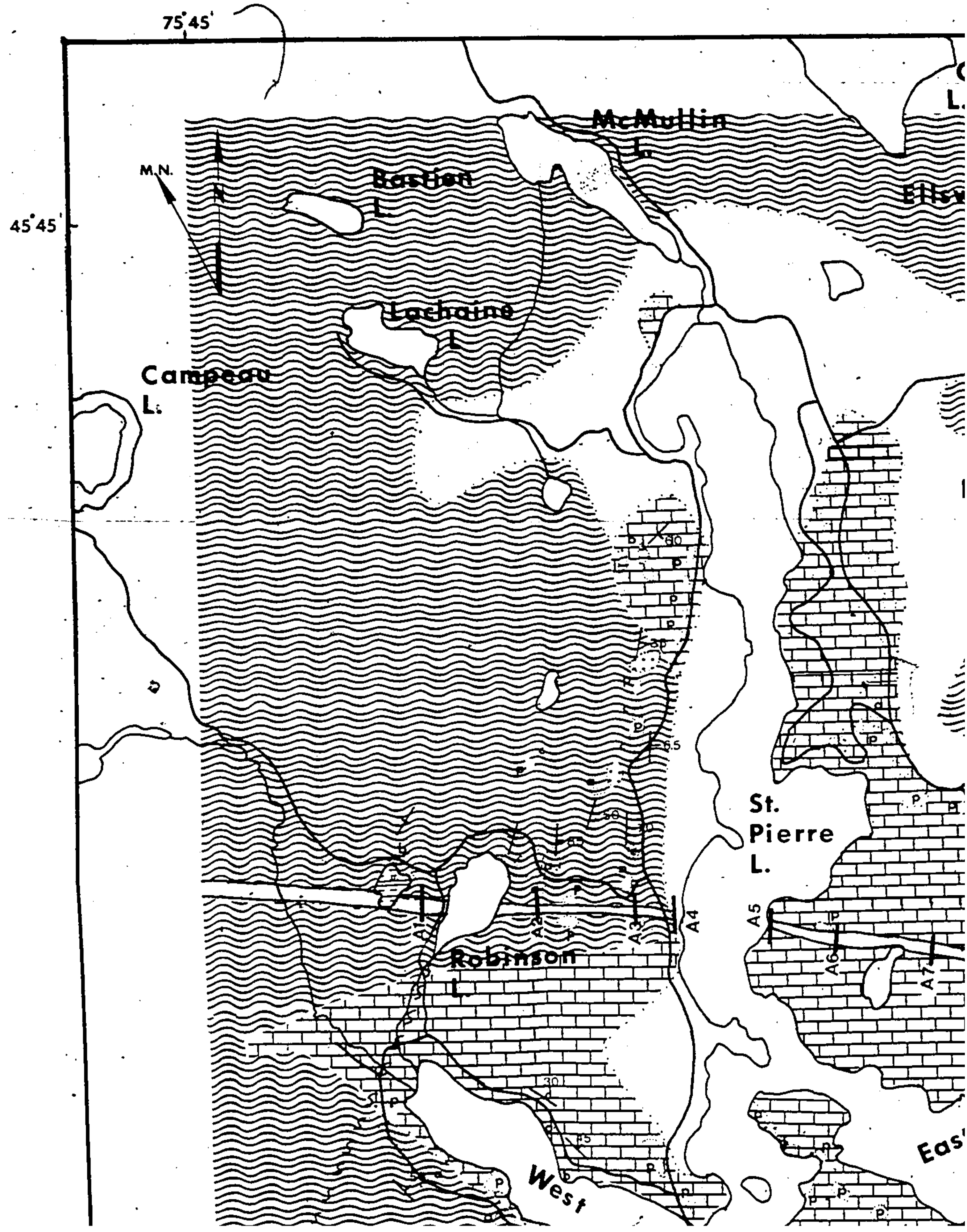
75°45'
45°45'
M.N.
N
McMullin
L.
Bastien
L.
Ellsw
Lachaine
L.
Campeau
L.
St.
Pierre
L.
Robinson
L.
West
Eas
A1
A2
A3
A4
A5
A6
A7

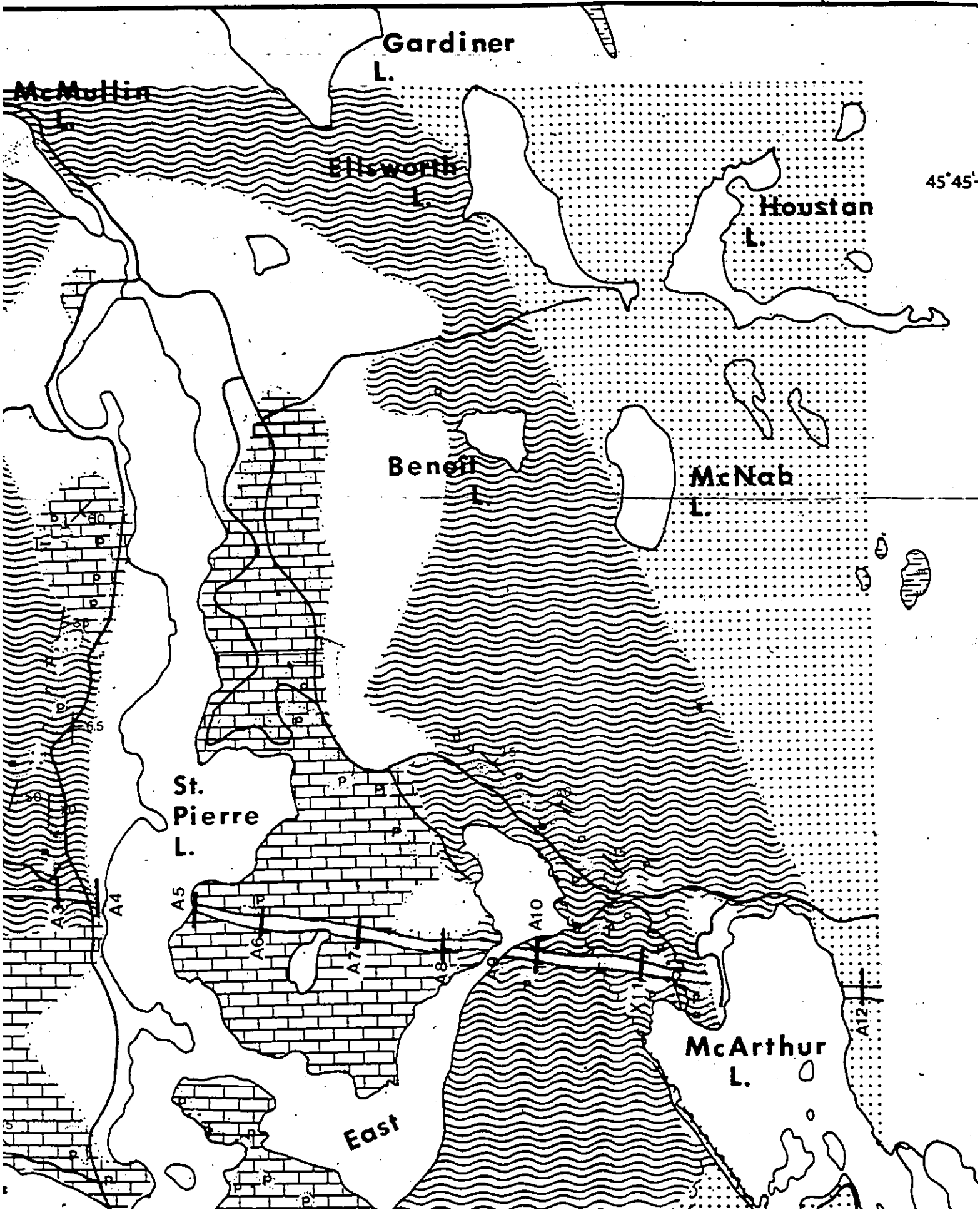
75°40'
45°45'
Gardiner L.
McMullin L.
Ellsworth L.
Houston L.
Benoit L.
McNab L.
St. Pierre L.
East
McArthur L.
A3
A4
A5
A6
A7
A8
A10
A12
X11

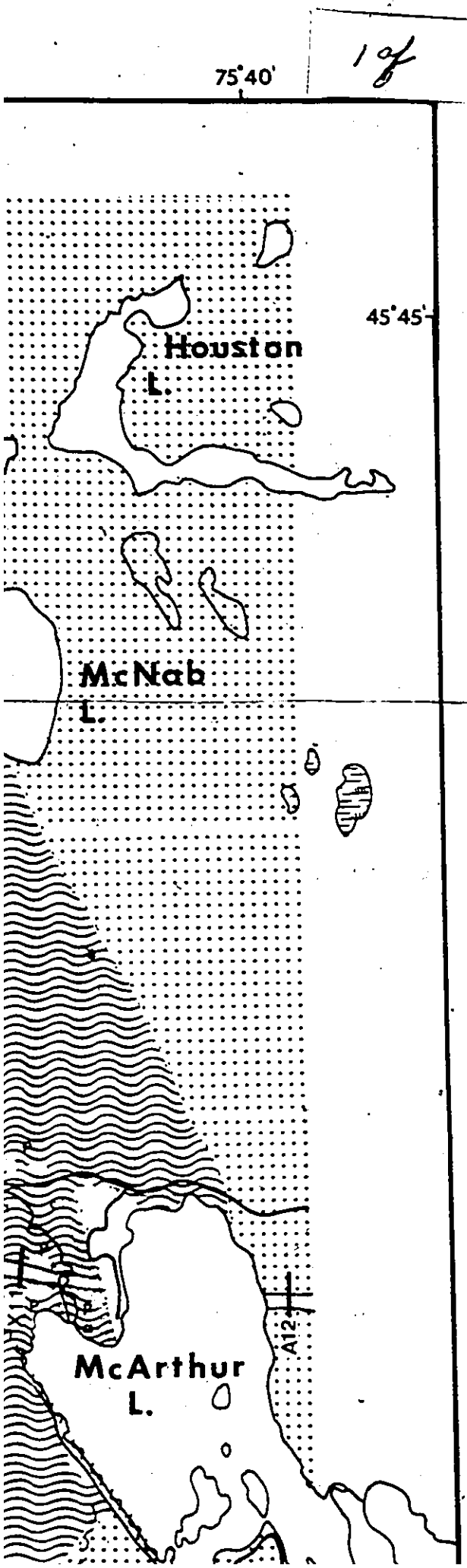

LEGEND

QUATERNARY

Sand, gravel and clay

HADRINIAN

Diabase

P — Pegmatite

PROTEROZOIC

Gneiss, undifferentiated except where stated (minor quartzite, pegmatite and marble)

a — Quartz feldspar gneiss

b — Biotite garnet gneiss

c — Hornblende gneiss

d — Biotite gneiss

PROTEROZOIC OR OLDER

Quartzite

Crystalline limestone

SYMBOLS

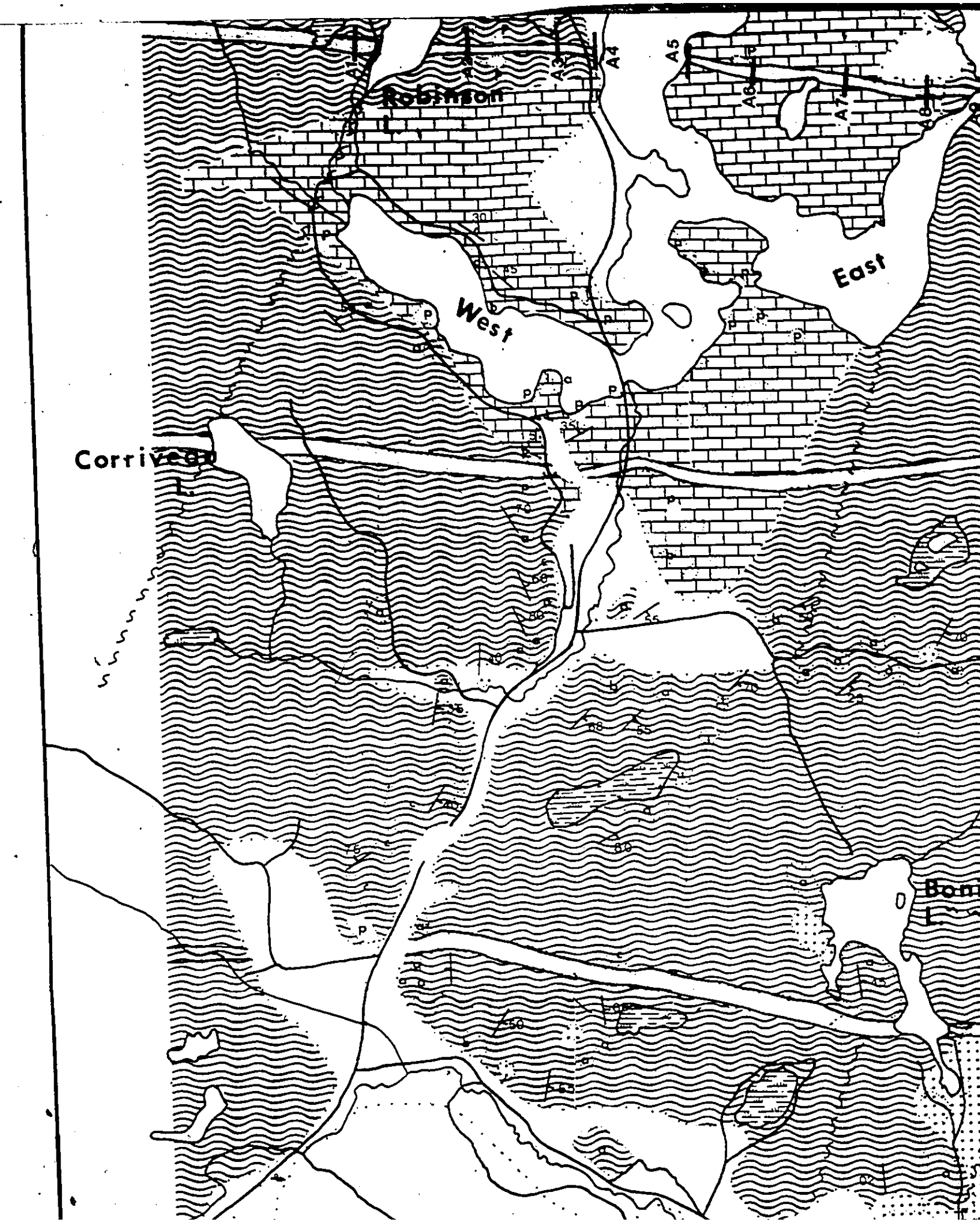
A1
A2
A3
A4
A5
A6
A7
Robinson
L.
West
East
Corriveau
L.
Bon
L.

A4
A5
A6
A7
A8
A10
A11
A12
McArthur
L.
East
Bonin
L.
Grand
L.
PROTEROZOIC OR
OLDER

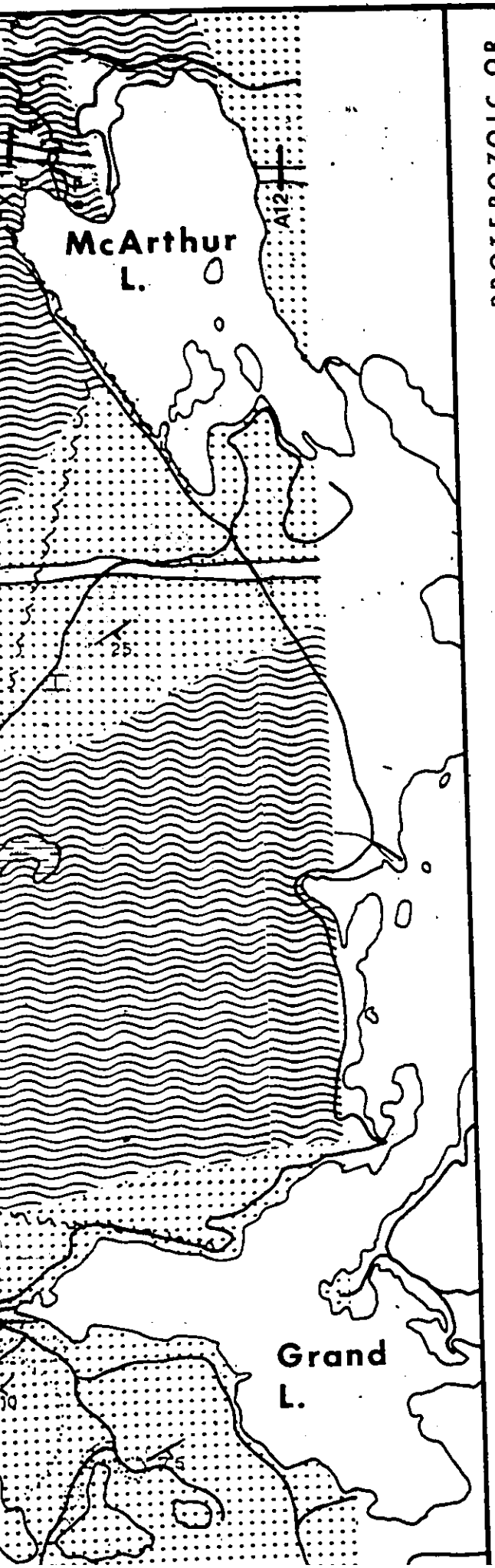

PROTEROZOIC OR OLDER

Quartzite

Crystalline limestone

SYMBOLS

Stike and dip of foliation and gneissosity

Vertical foliation and gneissosity

Geological boundary

Boundary of visited outcrop

Possible fault

March

A10 — Section Locations

In the studied district, the various rock types are highly variable and because of this, areas

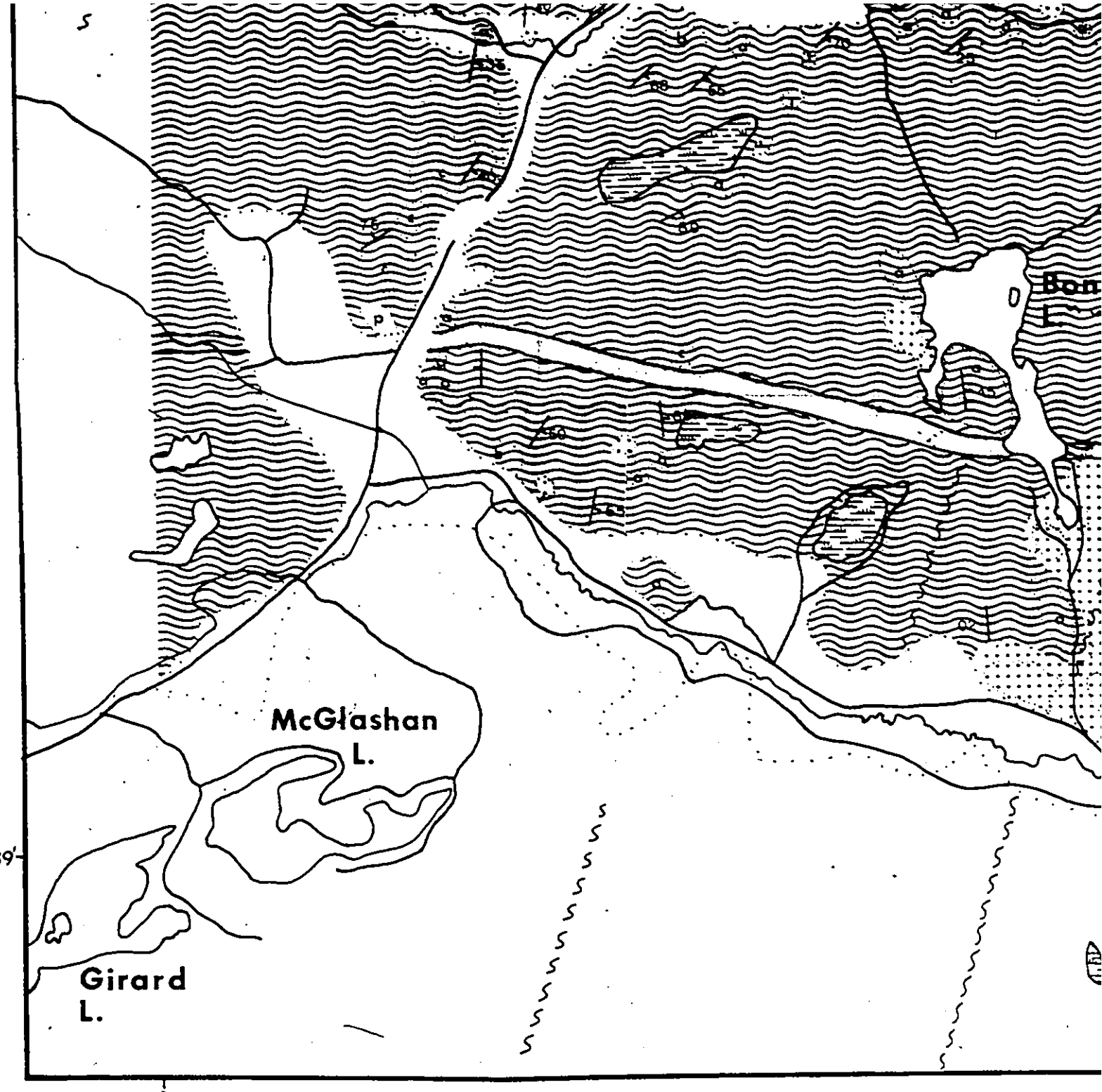

ST-PIERRE DE WAKEF

QUEBEC

Scale 1:25,000

0 500 1000 1500 2000

FIGURE 1

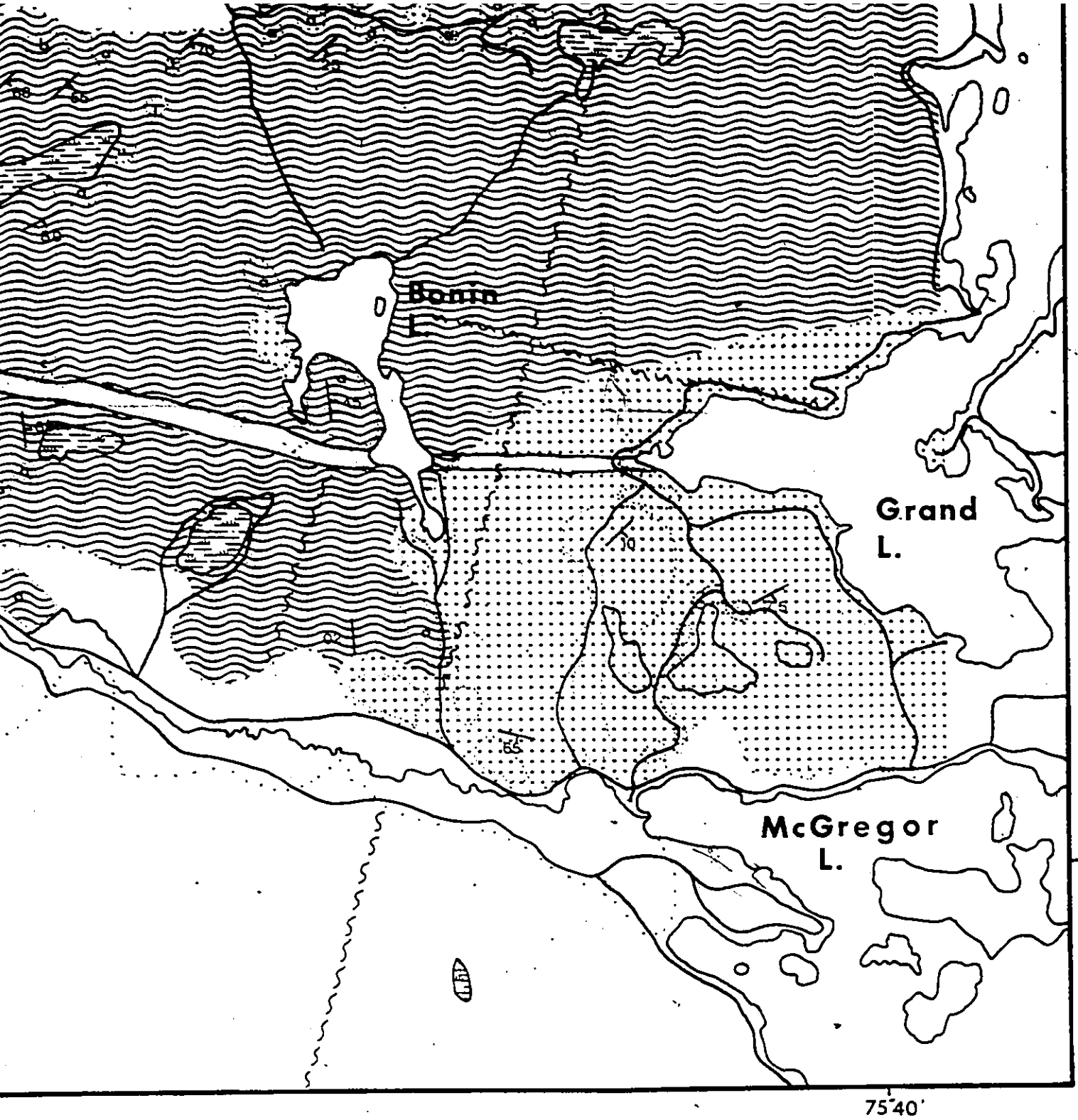

PIERRE DE WAKEFIELD

QUEBEC

Scale 1:25,000

500 1000 1500 2000 2500 meters

FIGURE 1

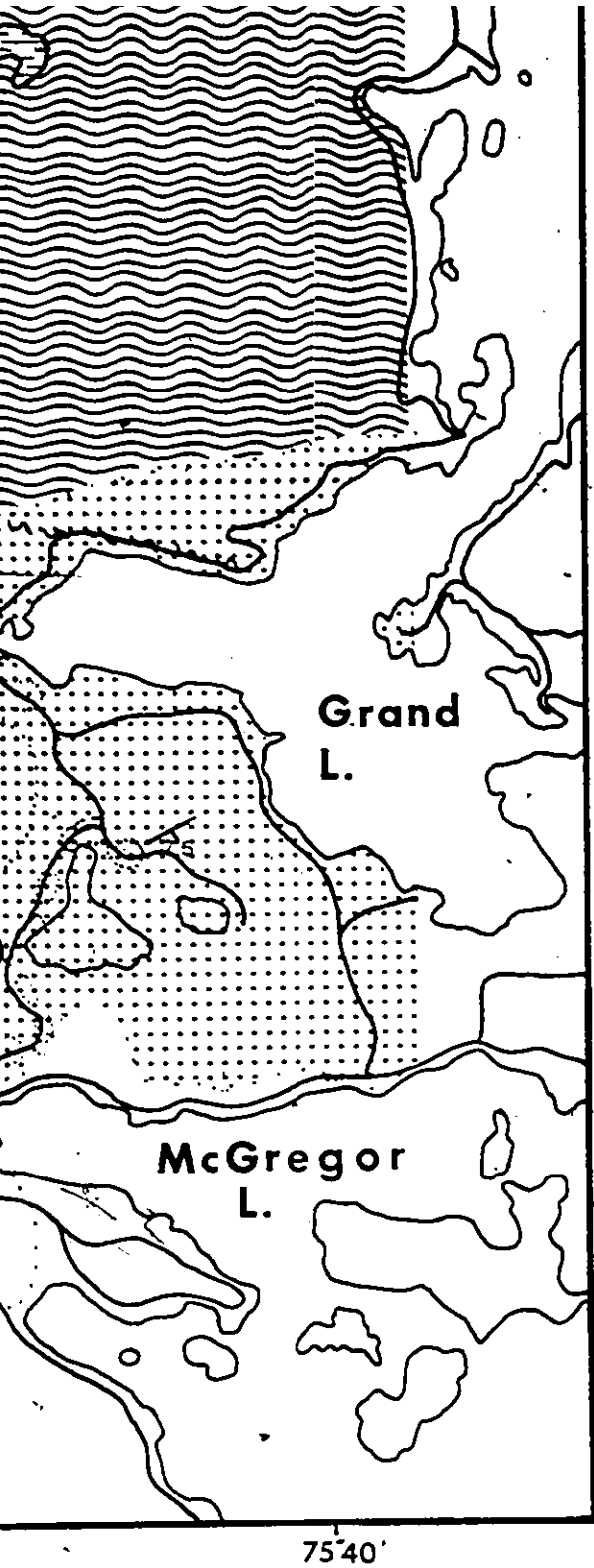

Boundary of visited outcrop

Possible fault

March

A10 — Section Locations

In the studied district, the various rock types are highly variable and because of this, areas of uninterrupted same rock over a few hundred square meters are uncommon. It was then necessary to omit detail and to indicate general areas where a certain rock type predominates (except were stated).

General geology based on M.E. Wilson (1920) and updated by Gilles Reny (1982)

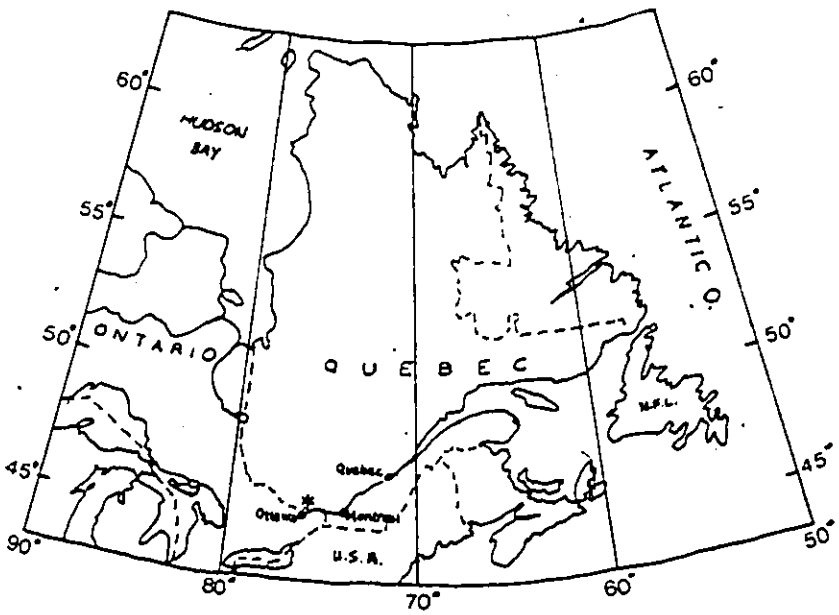

Location Map